DESIGN, FABRICATION, AND CHARACTERIZATION OF COMPLEX, MULTILAYER HETEROSTRUCTURES OF CONJUGATED AND NON-CONJUGATED POLYMERS VIA MOLECULAR SELF-ASSEMBLY

by

Augustine Che-Tsung Fou

Submitted to The Electronic Materials Panel of
The Department of Materials Science and Engineering
in Partial Fulfillment of the Requirements for the Degree of

Doctor of Philosophy

at the
Massachusetts Institute of Technology
July 1995.

Signature of Author _____
Department of Materials Science and Engineering
August 11, 1995.

Certified by _____
Prof. Michael F. Rubner, Thesis Supervisor
TDK Professor of Polymer Physics

Accepted by _____
Prof. Carl V. Thompson II
Professor of Electronic Materials
Chair, Departmental Committee on Graduate Students

DESIGN, FABRICATION, AND CHARACTERIZATION OF COMPLEX, MULTILAYER HETEROSTRUCTURES OF CONJUGATED AND NON-CONJUGATED POLYMERS VIA MOLECULAR SELF-ASSEMBLY

by

Augustine Che-Tsung Fou

Submitted to the Department of Materials Science and Engineering on August 11, 1995 in partial fulfillment of the requirements for the degree of Doctor of Philosophy in The Electronic Materials Panel.

ABSTRACT

In this thesis, we will present the development of molecular self-assembly as a powerful and versatile processing technique for handling ultrathin films of electroactive polymers. It will be demonstrated that self-assembly provides a unique ability to manipulate an arsenal of electroactive polymers with technologically useful electrical and optical properties into ultrathin multilayer films with molecular level control. The supermolecular architecture of these multilayer assemblies of polymers may be tailored such that the whole assembly will exhibit novel characteristics that cannot be achieved by the components individually. The intermolecular interactions between the various components contained in these multilayer heterostructures ultimately determine the macroscopic characteristics and performance of organic thin film devices such as light-emitting diodes. Therefore a deeper understanding of these interactions will allow us to design and fabricate complex, multilayer thin film devices with specific, desired properties.

There are two particular emphases in this thesis. The first part consists of the development of the self-assembly process to handle the underivatized forms of highly conductive, air-stable, and commercially significant polymers such as polypyrrole and polyaniline. We will demonstrate the use of self-assembly to deposit extremely uniform films of

polypyrrole between 30 Å and 500 Å thick with conductivities as high as 300 S/cm, comparable to that of the bulk material. The second section will concentrate on the development of the self-assembly procedure for fabricating thin film light-emitting diodes from poly(p-phenylene vinylene), the associated procedures of device characterization, and the elucidation of possible mechanisms of device operation. We will present for the first time, successful light-emitting diodes based on self-assembled films with thicknesses from as little as 80 Å up to 1000 Å; this is particularly significant as it attests to the quality and uniformity of the multilayer films fabricated by molecular self-assembly. Finally, it will be shown that the manipulation of single layers of material, on the order of 5 Å to 15 Å, allows us to alter the macroscopic properties of the thin film devices.

In this way, molecular self-assembly will be shown to be a significant thin film processing technique that is vital to the realization and optimization of molecular-scale, all-organic devices.

Thesis Supervsor: Prof. Michael F. Rubner

Title: TDK Professor of Polymer Physics

Acknowledgements

As I am about to finish another significant "stepping stone" in the course of my life, I'd like to take a moment to thank those people whose lives have touched mine.

I'd like first to acknowledge God's abundant blessings in my life that have allowed me to be where I am today. I thank my sister, Adora Ann, my mother, Mary, and my father, Joseph for their constant love and support. It is by their tangible guidance, encouragement, and example that I have been able to strive on in good times and trying times.

I'd like to express my sincere thanks and appreciation to Prof. Michael Rubner, my advisor, whose deep concern and care for myself, as well as other students, have imparted lessons and experience in far more than science alone. These were truly edifying and memorable years.

I'd like to thank the other members of my thesis committee, Prof. Kirk D. Kolenbrander, Prof. Harry L. Tuller, and Prof. Moungi G. Bawendi for their keen eye and constructive critique of my work.

And now to my colleagues and friends, whose lives and friendships have provided the inspiration to strive harder and a foundation of stability both inside and outside of school, my thanks for the wonderful memories and those yet to be made. My very special thanks to Osamu Onitsuka and Mary-Silvia Ferreira; I couldn't have done it without you. And thanks to the other members of the Rubner Research Group: Ken "The Juggler" Zemach, Bill "The Radio Man" Stockton, Jeff "Dad" Baur, Dong-Sik You, Sandy Schaefer-Ung, Bashir Dabbousi, Douglas Howie, Debra Spence, Mike Durstock, Erika Abbas, Erik Handy, Pascal Besson, Anand Raghunathan, and Michael Whitney.

Acknowledgements

And warmest regards to Tracey Burr, whose friendship is cherished, and to Peter Ragone, whose expertise and insight are valued.

And thanks to all the other friends and acquaintances whose lives have enriched mine. I will not forget you.

Augustine Fou
July 18, 1995.

DESIGN, FABRICATION, AND CHARACTERIZATION OF COMPLEX, MULTILAYER HETEROSTRUCTURES OF CONJUGATED AND NON-CONJUGATED POLYMERS VIA MOLECULAR SELF-ASSEMBLY

by

Augustine Che-Tsung Fou

B.Sc. Chemistry, University of Dallas, May, 1991.

Submitted to the Electronic Materials Panel of
The Department of Materials Science and Engineering
in Partial Fulfillment of the Requirements for the Degree of

Doctor of Philosophy

at the

Massachusetts Institute of Technology
July 1995.

DESIGN, FABRICATION, AND CHARACTERIZATION OF COMPLEX, MULTILAYER HETEROSTRUCTURES OF CONJUGATED AND NON-CONJUGATED POLYMERS VIA MOLECULAR SELF-ASSEMBLY

TABLE OF CONTENTS

LIST OF FIGURES

Pages

Chapter 1

Chapter 2

Chapter 3

Chapter 1

General Introduction and Background

1.1 General Introduction

Tremendous progress has been made in every facet of the relatively young field of electroactive polymers since its advent in the late 1970s with the discovery of highly conductive, doped polyacetylene [1.1 - 1.3]. Since that time, not only have many new materials been designed and synthesized, but also new applications, never before possible, have been conceived and realized through the novel use of these materials. Owing to the ability to design and synthesize organic materials with desired properties, this field has seen the application of electroactive polymers blossom into as diverse areas as biology, aerospace, and microelectronics, to name a few. Indeed, electroactive polymers have already been used as the active elements at the heart of novel electronic, optical, and chemical devices such as flexible light-emitting devices [1.4], lightweight, thin-film batteries [1.5], chemical sensors [1.6], thin-film supercapacitors [1.7], photovoltaic devices [1.8],

and many, many others [1.9]. The synthesis of new organic materials and the improvements in the properties of existing materials have resulted in such a wide variety of applications and devices which can take advantage of the customizable properties of these electroactive organic materials.

However, in order to manipulate these materials into useful forms, such as thin films, handling, processing, and fabrication techniques must also be developed concomitantly. This is no simple task since these materials, especially the electroactive polymers, exhibit poor processibility and may be intractable, infusible, and insoluble in common organic solvents. But despite these limitations, the electroactive properties that they possess, such as conductivity, light-emission, sensitivity to chemical environments, non-linear optical properties, and many more, make them highly desirable to be used in novel applications. Adding to the urgency of developing simpler, more versatile, and more facile processing techniques is the need to use processing as a way to optimize the performance of these materials in applications; that is, in some cases, the intrinsic properties of the materials have already been exploited to their fullest extent and further improvements can only be achieved by improvements in the processing and fabrication of the desired device or application. For example, doped polyaniline exhibits a bulk conductivity of 1 to 10 S/cm while polyaniline, oriented by additional processing steps such that the polymer chains are preferentially aligned parallel to each other, exhibits

anisotropic conductivities with over a 100-fold enhancement [1.10] in the direction parallel to the polymer chains. Therefore, processing and handling have become crucial to the fabrication and optimization of novel applications based on these electroactive polymers. Finally, despite the non-trivial task of developing suitable processing and handling techniques to be able to make use of these materials, the use of these materials, especially in novel electronic applications, eliminates the need for elaborate and costly fabrication facilities required by the traditional semiconductor materials. Also, since the variety of organic polymers have now been shown to span the spectrum of conductivity, from the most insulating to the most conductive, and simultaneously provide sundry other unique and useful properties, electroactive polymers have become an extremely important class of materials from the standpoints of cost, abundance, versatility, and customizability, and thus have been widely studied and applied.

Many of the advanced applications proposed for electroactive polymers, such as microelectronic devices, chemical and biochemical sensors, electrochromic displays, and transparent anti-static coatings require uniform thin films of these materials. Precise control over the film thickness and molecular organizations is also necessary to realize some of these applications. There exist well known processing techniques such as spin-coating, electrochemical deposition, and Langmuir-Blodgett thin film transfer for the processing of electroactive polymers into thin films. These techniques have all been utilized to

varying degrees of success in the manipulation of polymers into thin films. However, as it will be demonstrated in this thesis, none of the above techniques are as versatile, powerful ,and technologically useful as molecular self-assembly.

Molecular self-assembly is an aqueous-solution based, thin film processing technique which offers the unique ability to manipulate polymers into ultrathin films with molecular level control over the deposition of single layers of polymer and control over the supermolecular architecture of a multilayer thin film. This technique involves the spontaneous adsorption of organic molecules or macromolecules in a layer-by-layer manner onto suitable substrates; the adsorption process takes advantage of intermolecular interactions such as electrostatic attraction between ionized functional groups and is not limited to the deposition of only one monolayer onto the surface of a substrate. Additional monolayers can simply be stacked on top of each other to form a multilayer, heterostructure thin film. A wide variety of derivatized [1.11 - 1.12], conjugated [1.13 - 1.14], and underivatized polymers [1.15 - 1.16], and organic dye molecules [1.17] have been successfully manipulated into multilayer heterostructures by molecular self-assembly. Complex, multicomponent superlattices can be made simply and quickly by self-assembling the desired materials into the heterostructures. With this ability, it is possible to fabricate devices which exhibit novel properties not exhibited by the components individually; that is, it is possible to conceive and realize

multicomponent, multifunctional thin films in which each component serves a particular function and the interactions among the components give rise to new properties not present in the individual components. Furthermore, as a dip-coating process, self-assembly can deposit uniform films onto all surfaces of substrates with irregular geometries, insulating properties, or surface treatments; such substrates are typically inaccessible to one or more of the other techniques for thin film deposition. Thus, self-assembly uniquely provides simplicity, versatility, and the molecular-level control needed to fabricate the ever more complex thin film heterostructures required to exploit new materials properties in novel electrical and chemical devices.

1.2 Background and Significance

In this section, we describe the other thin film processing techniques in more detail and the development of the self-assembly technique and compare and contrast the advantages and limitations of each technique. Then we will present examples of the use of molecular self-assembly in a variety of thin film systems studied by our group.

Figure 1.1 provides schematic representations of each of the techniques discussed below.

1. Spin Coating

limitations:

- flat substrate
- limited size
- soluble polymers
- difficult multilayer deposition

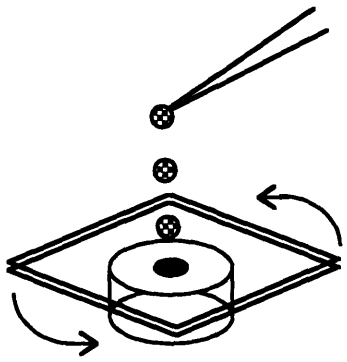

2. Electrochemical Deposition

limitations:

- conductive substrate
- restricted geometry
- difficult multilayer deposition

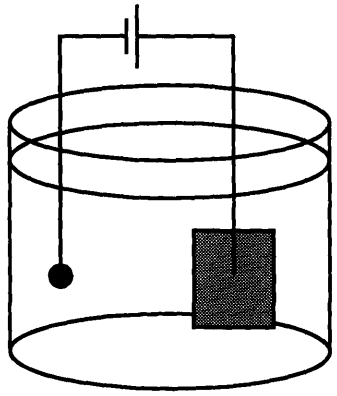

3. Langmuir-Blodgett Technique

limitations:

- hydrophobic substr.
- flat, small substrate
- mix surface active agent with polymer
- extremely slow

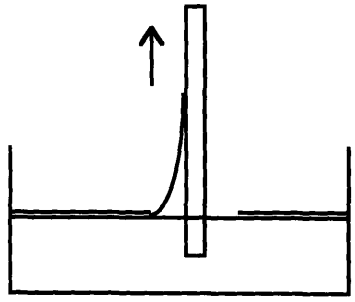

Figure 1.1 Standard techniques of thin film deposition.

The traditional spin coating technique involves dissolving a pre-formed polymer in a suitable volatile organic solvent, dripping this solution onto a rapidly spinning substrate, and allowing the solvent to evaporate leaving a film of the desired material on the substrate. The spinning motion allows the solution to spread and cover the entire surface of the substrate and also facilitates the rapid evaporation of the solvent. The advantage of this process is its speed in depositing a thin film onto substrates. But this technique, although simple, offers limited control over the film thickness and uniformity. The thickness is typically controlled by parameters such as the solution concentration, the solvent rate of evaporation, and the spin rate of the substrate during deposition. Although refinements in the technique have allowed control of film thicknesses down to the range of 500 Å total thickness, the precision of this thickness control is typically no better than 100 Å. In addition, the uniformity and roughness of the surface of the film is uncontrollable. In fact, prevalent problems with the technique are the appearance of rainbow interference patterns due to surface "ripples" and pin-hole defects caused by incomplete coverage of the surface by the thin film. When thin film uniformity and surface smoothness are of importance, especially in thin film microelectronic devices such as light-emitting diodes, this technique has its limitations. This technique is further limited to spinning substrates of small sizes and substrates with surfaces that are flat. It is difficult to cover large areas with uniform thin films of sufficient quality for microelectronic applications.

Further this technique requires the desired polymers to be soluble in a suitable solvent. It is well known that conductive, conjugated polymers are difficult to solubilize. However, some of these polymers have been made water and solvent-soluble by means of functionalization or derivatization; that is, by attaching enough soluble side groups to the main polymer backbone, the entire macromolecule itself is rendered soluble in the same solvents. The cure of one problem, however, has led to another problem since it is well documented, for example, that the functionalized form of conjugated polymers typically show conductivities one to several orders of magnitude lower than the unfunctionalized form of the same polymer [1.18 - 1.19]. Therefore, whenever possible, it is desirable to use the more conductive, unfunctionalized form of the conjugated polymers.

Also, when using spin coating, it is difficult to build multilayer structures because when spinning another material onto the surface of an existing film, the solvent partially or completely redissolves the material of the previous layer. Even if a suitable, mutually insoluble polymer/solvent system were used, the surface and interface morphology of the resulting film are difficult to control.

Self-assembly, on the other hand, provides molecular level control over the deposition of organic macromolecules; by controlling the solution chemistry and the deposition conditions, it is possible to adjust thicknesses with a precision of 5 - 10 Å. And, it is a simple

matter to build up thicker films by stacking more layers on top of each other. The solution chemistries and dipping conditions were developed for aqueous solutions since water is the solvent of choice to replace toxic and hazardous organic solvents in sundry, commonly used processing techniques. Furthermore, extremely sophisticated control over multilayer heterostructure is provided without the sacrifice of simplicity; that is, with self-assembly, a complex film of tens or hundreds of layers can be built up simply by dipping substrates into various aqueous solutions containing the electroactive materials in the desired sequence. In this way, self-assembly makes the fabrication of multiple component heterostructure films routine. And finally, self-assembly can be used to manipulate materials such as unfunctionalized, conductive p-doped conjugated polymers such as polypyrrole, a technologically important conducting polymer notorious for its intractability and insolubility.

Other techniques have been developed to alleviate some of these difficulties in the processing of electroactive polymers. For example, electrochemical deposition has been used to polymerize pyrrole monomer and form conducting thin films of polypyrrole on gold substrates [1.20]; such films can either be peeled off the electrode as stand-alone conductive films or can be used simply to modify the surface characteristics of the electrode. However, this technique is difficult to apply to substrates which are electrically insulating, although some successful attempts have been reported [1.21]. Electrochemical

deposition thus provides a relatively good level of control over the thickness of the deposited film; but little control is afforded over the deposition at the molecular level. Other chemical oxidative polymerization techniques have also been used to deposit conductive polypyrrole onto such things as fabric fibers [1.22], within pre-formed structural polymer matrices [1.23], via "template synthesis" in microtubules [1.24], and within Langmuir-Blodgett films [1.25]. These chemical routes provide little or no control over the deposition of the polypyrrole. In some cases, the in-situ chemical reaction produces black, insoluble polypyrrole which precipitates and physisorbs onto all surfaces, resulting in films of poor uniformity and adhesion. As will be shown later, self-assembly of polypyrrole, as developed in this study, exploits the attractive interactions of p-doped polypyrrole and a negatively charged polyelectrolyte (polyanion) to form extremely uniform thin films over large areas. These films are of optical quality (uniform optical density over large areas) and strongly adherent to the surface of the substrate.

Finally, relative to the aforementioned thin film processing techniques, the Langmuir-Blodgett thin film transfer technique has been used to manipulate electroactive polymers into thin films with the highest degree of control. In our group, work was done to apply this technique specifically to a variety of conducting polymers [1.14], including polypyrrole [1.25a,b]. Although significant advances in this technique were made in our lab to provide control over monolayers of

polypyrrole, this technique still involves the lengthy process of forming a monolayer film at the air-water interface of a special dipping trough and the extremely slow physical transfer of this film onto a flat, clean, hydrophobic surface. It also requires the polypyrrole to be mixed with a surface-active agent (typically an amphiphile such as 3-octadecanoyl-pyrrole), which is incorporated into the film at the expense of the overall conductivity. And, even the most sophisticated two-trough LB systems permit multilayer architectures containing only two components at a time. Finally, owing to the extremely slow steps involved, the LB technique has not become technologically useful; that is, it will remain only a useful laboratory technique, with limited application in large-scale fabrication processes.

Enter molecular self-assembly; this process provides a simple, aqueous-solution based technique to manipulate an ever expanding arsenal of electroactive organic materials into uniform thin films. With the angstrom-level control over the deposition of molecules, self-assembly provides the unique ability to fabricate complex, multicomponent, multilayer films quickly and simply.

1.3 Advent of Molecular Self-Assembly

Molecular self-assembly was developed by exploiting the well known phenomenon of polyelectrolyte adsorption; the deposition of polyelectrolytes onto surfaces is controlled by solution parameters such as concentration, pH, and ionic strength. These parameters determine the degree of coiling of the polymer and therefore the thickness and orientation of the polymer as it deposits onto the surface. In the deposition of polymer electrolytes from aqueous solution onto solid substrates, we can vary the thickness of the layers that are deposited by varying the solution parameters. It is well known from polymer solution chemistry that the configuration of the polymer in solution can be changed by such parameters as concentration and ionic strength. For example, in the extremes, a long chain polymer can adopt a highly coiled configuration or it can be spread out into an extended chain configuration (see Figure 1.2). In high ionic strength solutions, there are free ions such as sodium or chloride ions in solution which can help to shield the electrostatic charge repulsion between adjacent functional groups on the polymer backbone, allowing for closer approach of these groups to each other. This allows the polymer to coil together more tightly. The polymer can be thought of as a ball of yarn. On the other extreme, for example, in low ionic strength solutions, the charge repulsion between adjacent ionized functional groups will give the polymer an extended chain configuration, because the functional groups must stay as far apart from each other as possible. If the polymer

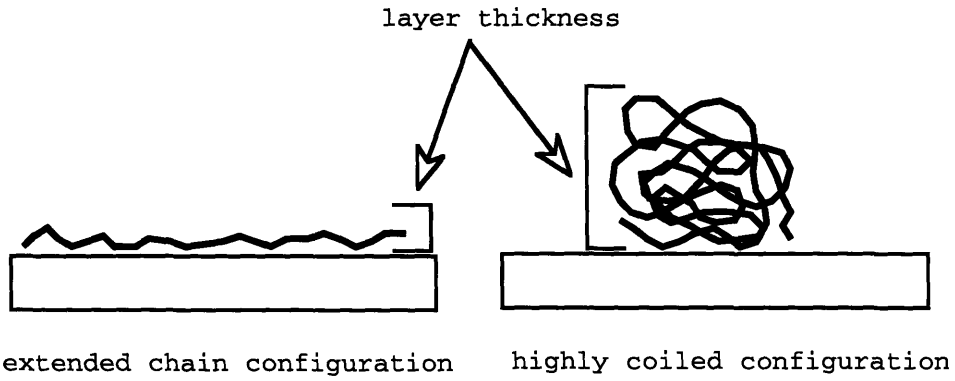

Figure 1.2 Polymer Polyelectrolyte Adsorption

deposits onto the surface in the former, highly coiled configuration and the surface is completely covered, the thickness imparted by this single layer would be thicker than if the polymer chains were laid down in the extended chain configuration..

The ability to control how macromolecular polyelectrolytes deposit onto the surface had to be taken one step further, however, because a monolayer of material on the surface of a substrate serves little purpose and will most likely not exhibit the desirable properties present in the bulk form. Therefore it was necessary to develop a process to deposit films of sufficient thickness to exhibit the desirable bulk properties, but a process that would still provide molecular level control over the deposition and result in extremely uniform films. Decher and coworkers first demonstrated molecular self-assembly for functionalized polyelectrolytes, polymers fitted with functional groups

pendant to the main polymer backbone, e.g. sulfonated polystyrene and polyallylamine [1.11]. The basis of this multilayer self-assembly process is the ionic attraction between the ionized functional groups of the polycations and polyanions. Figure 1.3 shows the chemical structures of several polymer polyelectrolytes used in molecular self-assembly.

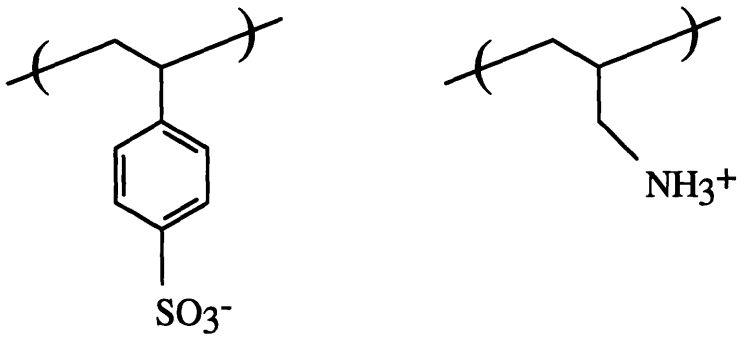

sulfonated polystyrene polyallylamine

Figure 1.3 Chemical Structures of Polymer Polyelectrolytes

Figure 1.4 illustrates the self-assembly process using these polymers. As a substrate is dipped into a dilute aqueous solution containing a polyelectrolyte (e.g. polyanion) a single layer of the polymer deposits onto the surface. (Typically the substrate is pre-treated to anchor charges covalently to the surface. This process amino-silanizes the surface. In slightly acidic solution, the amine group is protonated and positive and thus able to attract negatively charged polyanions. The details of amino-silanizing the surface is described in the appropriate

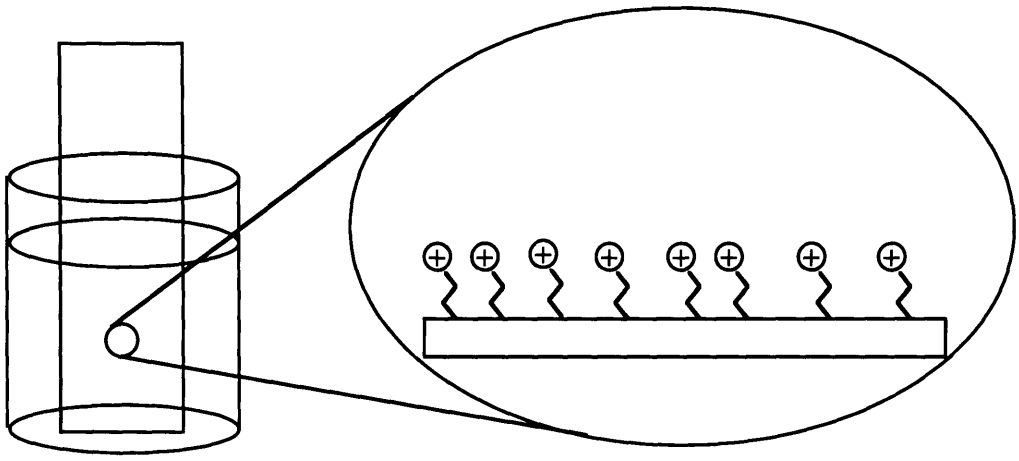

substrate surface silanization

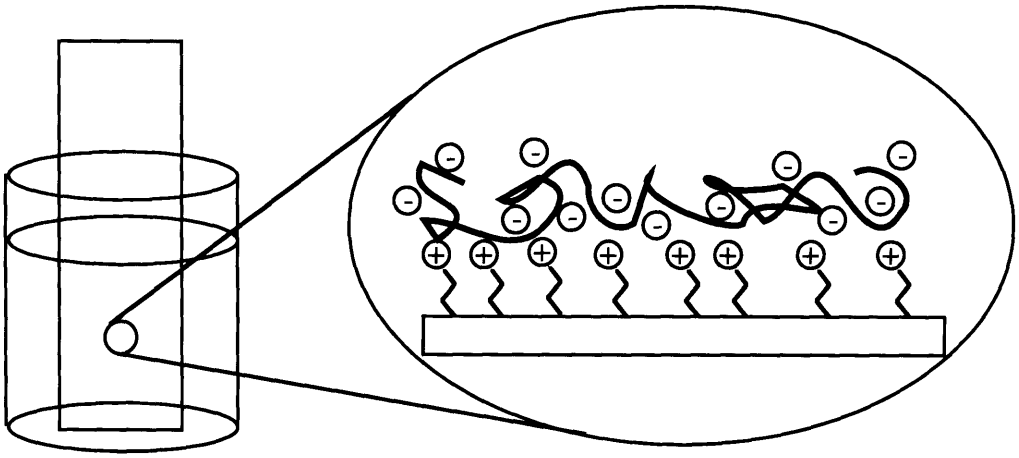

deposition of polyanion

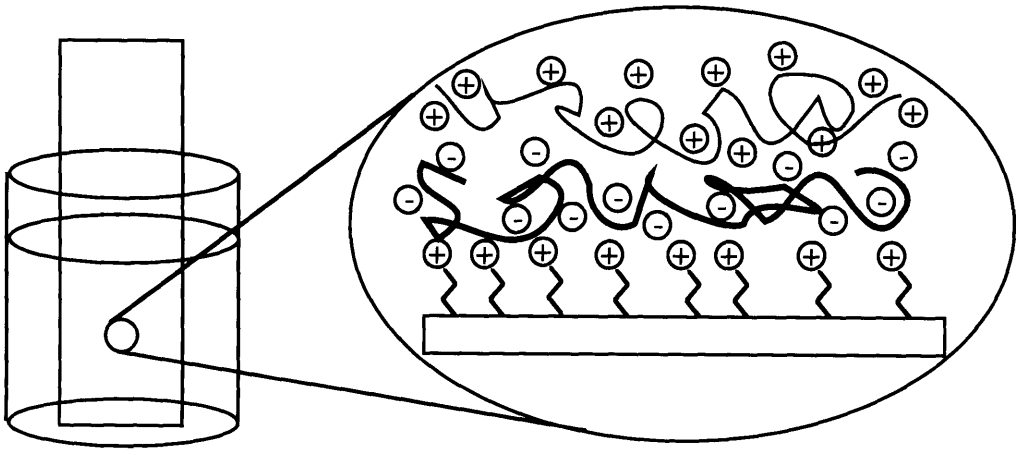

deposition of polycation

Figure 1.4 Schematic of Self-Assembly Procedure

experimental sections below.) After a given amount of time, referred to as the "dip time," the substrate is removed and vigorously rinsed with a stream of ultrapure water; this rinses off any loosely bound material. Then the substrate is dried off with a stream of compressed air to eliminate any excess rinse water that may dilute or contaminate the other solutions. With each dip, a single layer of the polyelectrolyte is adsorbed by electrostatic attraction; some of the functional groups are ionically bound to the previous layer while the rest are left dangling. These "dangling" functional groups then serve to attract the next layer of the complementary polyelectrolyte. Next, the substrate is dipped into a solution containing an oppositely charged polyelectrolyte (e.g. polycation). Again, a single layer of polymer is attracted to the surface by electrostatic attraction. The rinse and dry steps are repeated. Thus by alternately dipping a substrate into a solution containing the pre-formed polycation and another solution containing the polyanion, a multilayer film can be built up. As mentioned before, the thickness of each deposited layer is dictated by the solution chemistry and the dip time; that is, the concentration, pH, ionic strength, and the time the substrate is immersed in the dipping solution may all be adjusted to give the desired thickness per layer. The resultant multilayer films are highly coherent and uniform.

Work in our group quickly demonstrated that functionalized, conducting polymers such as sulfonated polyaniline or poly(thiophene-3-acetic acid) could also be self-assembled into highly conductive,

ultrathin films in a similar manner [1.13 - 1.14]. Figure 1.5 shows the chemical structures of some of these functionalized conducting polymers.

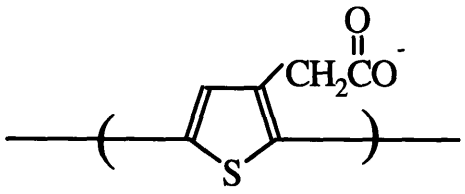

poly(thiophene-3-acetic acid)

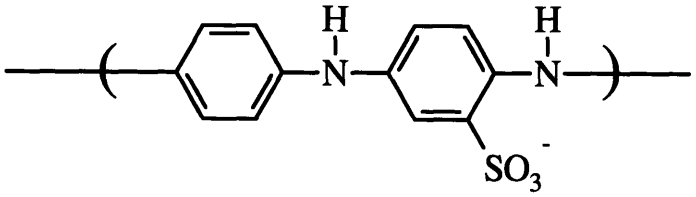

sulfonated polyaniline

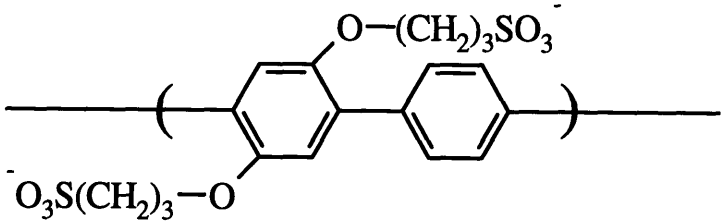

sulfonated polyphenylene

Figure 1.5 Functionalized Conducting Polymers

But, as mentioned before, the functionalized form of conducting polymers exhibited one to several orders of magnitude lower conductivities than the unfunctionalized form. Therefore, we went on to investigate the use of self-assembly to process and deposit the unfunctionalized form of such commercially important and relatively air-stable conducting polymers as polypyrrole and polyaniline. This was no simple task as these polymers are completely insoluble in organic solvents or water; despite this challenge, we wanted to develop an aqueous solution based technique to manipulate these polymers into uniform films of high quality with the same molecular-level control afforded by self-assembly in the case of the functionalized conducting polymers. The first main section of this thesis will describe in detail the self-assembly of unfunctionalized and highly conductive polypyrrole.

In addition to the self-assembly of conducting polymers, our group has shown the utility of molecular self-assembly in handling many other types of polymers and organic materials into uniform, ultrathin films. For example, we have demonstrated that self-assembly may be achieved not only with ionically functionalized polyelectrolytes; it can also be achieved through secondary forces such as hydrogen bonding interactions between polymers. Figure 1.6 shows the structure of some of these hydrogen bonding polymers. Also, organic molecules such as functionalized laser dyes can be self-assembled in a highly controlled manner. Figure 1.7 shows a few examples of other organic molecules used in the work of our group.

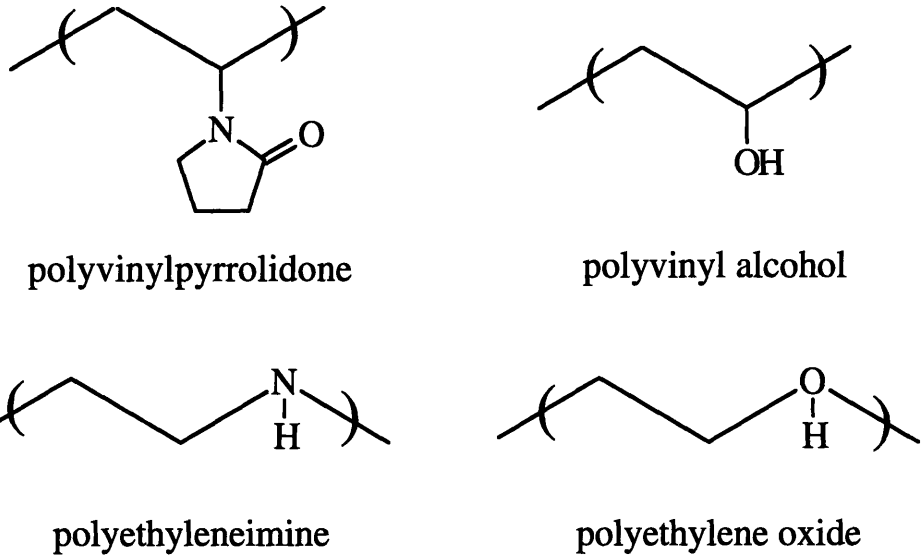

polyvinylpyrrolidone polyvinyl alcohol

polyethyleneimine polyethylene oxide

Figure 1.6 Hydrogen Bonding Polymers for Self-Assembly

An important characteristic of the self-assembly of all of these materials is the linear deposition with respect to the number of layers deposited. That is, if a figure of merit such as the thickness or absorbance of the film were monitored during the buildup of multilayers by the self-assembly process, there would be a linear relationship with the number of layers. This implies that by keeping the solution conditions and the dip times constant, a highly reproducible amount of material is deposited with each dip. Another hallmark of this technique is the ability to controllably deposit coherent and dense layers of material. An elegant demonstration of coherence of each self-assembled layer comes from the contact angle work by Dongsik You of

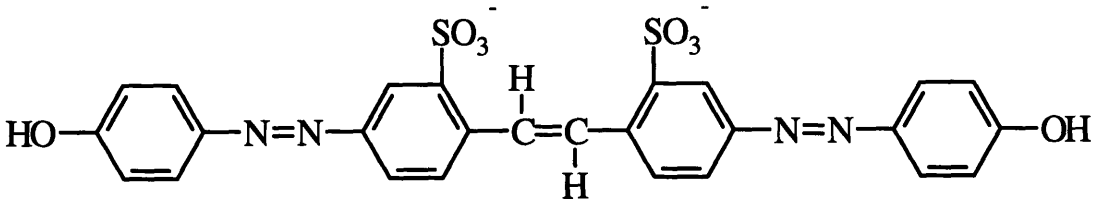

brilliant yellow (dye)

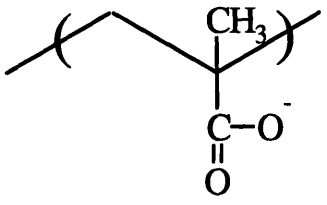

polymethacrylic acid

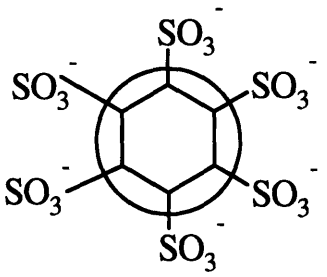

sulfonated fullerenes

Figure 1.7 Other Organic Molecules for Self-Assembly

our group [1.26]. In this experiment, the contact angle was measured on the self-assembled films after each layer was deposited. Depending on the system of polymers used to fabricate the film, the contact angle could be reproducibly adjusted between two values in the range of 10 degrees to 60 degrees by the deposition of just a single layer. This implies that each self-assembled layer is completely coherent and dense allowing it to modify the macroscopic surface characteristics.

There is further evidence from our photoluminescence work on poly(p-phenylene vinylene) of the layered structure of the self-assembled film. As will be mentioned in more detail later, we can use self-assembly to manipulate single layers of polymers in the range of thicknesses between 10 Å and 100 Å each. This has allowed us to tailor and adjust the macroscopic luminescence properties of the film by adjusting the multilayer architecture at the molecular level. The layer-by-layer architecture and the intermolecular interactions between the various components in adjacent layers give rise to the observed properties. Remarkably, this layer-by-layer heterostructure remains intact after thermal treatments for up to 12 hours at temperatures up to 290 °C; the components in the film are not homogenized [1.27].

Another example of the ability to design and fabricate complex multilayer heterostructures comes from the work of Diane L. Ellis in our group [1.28]. Using the self-assembly techniques developed in the work of this thesis, heterostructures containing conducting polypyrrole and insulating poly(thiophene-3-acetic acid) were designed and fabricated. The architecture of these films consisted of conducting "slabs" (multiple bilayers) of polypyrrole sandwiched between insulating "slabs" of polythiophene (undoped). This architecture was designed to exhibit highly anisotropic properties. The in-plane conductivity would be on the order of the conductivity of the polypyrrole slabs which lie in the plane of the film; the transverse conductivity, measured normal to the plane of the film, would be

extremely low due to the isolation of the conducting polypyrrole slabs by the insulating polythiophene slabs. Indeed our results bear this out and further comments will be given below in Chapter 2.

1.4 Purpose and Overview

Having touched upon the general advantages of molecular self-assembly over other thin film processing techniques, given examples of the novel supermolecular architectures that can be easily fabricated via self-assembly, and mentioned the wide variety of materials that can be manipulated by self-assembly, we begin the scientific journey of this thesis. In this thesis, we will first concentrate on the development of the self-assembly procedures to handle the unfunctionalized form of conducting polymers, specifically polypyrrole. We will describe the unique advantages of using self-assembly as opposed to other thin film processing techniques and give an example of a thin film device application made possible by self-assembly. We will then turn our attention to the application of self-assembly in the extremely active field of thin film organic light-emitting diodes. We first characterize the solid state properties of the self-assembled films (absorbance, photoluminescence, and thickness) and then apply these films in simple light-emitting device configurations. Then we will turn to investigate the influence of the supermolecular architecture of these multilayer

films on the overall characteristics of the thin film device, such as light output, efficiency, and stability. As will be seen, remarkably, single layers of material have pronounced effects on the performance of these ultrathin light-emitting devices.

Our work provides mounting evidence that this technique offers distinct advantages over other thin film fabrication techniques in the realization and optimization of all-organic microelectronic devices such as light-emitting diodes. The molecular-level control and the ability to easily manipulate electroactive polymers into ultrathin films makes self-assembly ideally suited for the fabrication of organic microelectronic devices which have stringent requirements on the quality of the thin films. Furthermore, self-assembly has allowed us, through processing, to achieve significant enhancements of device properties such as light output efficiency simply by modifying the supermolecular architecture of the thin film. Not only is it significant that using self-assembly, we have been able to show that single layers of material, on the order of 5 Å to 15 Å, influence the external, macroscopic properties of these thin film devices; but self-assembly has also allowed us to access a thickness regime, from 100 Å to 500 Å, not easily achieved by techniques such as spin-coating. Finally, the ability to form uniform films over large areas with a high degree of precision and reproducibility is crucial to bridging the gap between organic thin film devices remaining a laboratory curiosity and their being applied in technologically useful ways.

In each of the experimental sections, where appropriate, specific comments will be made to explain the experimental or theoretical bases for adopting a particular technique or protocol. In the results and discussion sections, overarching topics, interpretations of the gathered data, and conclusions from the experimental data will be presented.

1.5 Chapter 1 References

1.1 H. Shirakawa, E.J. Louis, A.G. MacDiarmid, C.K. Chiang, A.J. Heeger, *J. Chem. Soc. Chem. Comm.* **1977**, 578.

1.2 C.K. Chiang, M.A. Druy, S.C. Gau, A.J. Heeger, E.J. Louis, A.G. MacDiarmid, Y.W. Park, H. Shirakawa, *J. Amer. Chem. Soc.* **1978**, (100), 1013.

1.3 C.K. Chiang, C.R. Fincher, Y.W. Park, A.J. Heeger, H. Shirakawa, E.J. Louis, S.C. Gau, A.G. MacDiarmid, *Phys. Rev. Lett.* **1977**, (39), 1098.

1.4 a) J.H. Burroughes, D.D.C. Bradley, A.R. Brown, R.N. Marks, K. MacKay, R.H.Friend, P.L.Burn, A.B.Holmes, *Nature*, **347**, 539 (1990).

b)G. Gustafsson. Y. Cao, G.M. Treacy, F. Klavetter, N. Colaneri, A.J. Heeger, *Nature*, **357**, 477 (1992).

1.5 Jow, et al. *J. Electrochem. Soc.*, **136**, 1, 1989.

1.6 a) T.M. Swager, et al., *MRS Proc.* **328**, 263 (1994).

b) D.L.Ellis, PhD Thesis, Dept. of Chemistry, Harvard University, 1993.

1.7 S. Roth, et al. *Synth. Metals*, **57**, 3623 (1993).

1.8 S. Glenis, G. Horowitz, G. Tourillon, F. Garnier. *Thin Solid Films*, **111** (1984), 93-103.

1.9 a) *Science and Applications of Conducting Polymers*, A.G. MacDiarmid and A.J. Epstein, IOP Publ Ltd. 1990.

b) *Advanced Organic Solid State Materials*, L.Y. Chiang, P. Chaikin, D. Cowan, Eds. (1990).

1.10 a) Y. Min, A.G. MacDiarmid, A.J. Epstein, *Polymer Preprints,* Vol.35, No.1, March 1994, p. 231, and references therein.

b) A.G. MacDiarmid, J.K. Avlyanov, Z. Huang, Y-G. Min, A.J. Epstein, *ACS Spring 1995 Meeting Proceedings, Symposium "Polymeric Materials Science and Engineering (PMSE),* p. 395.

1.11 a) Y. Lvov, G. Decher, H. Mohwald. *Langmuir* 1993, **9**, 481.

b) G. Decher, J.D. Hong, *Ber. Bunsenges. Phys. Chem.* 1991, **95**, 1430.

c) G. Decher, J.D. Hong, *Makromol. Chem., Macromol. Symp.* 1991, **46**, 321.

d) G. Decher, J.D. Hong, *European Patent*, application number 91 113 464.1.

e) G. Decher, J.D. Hong, J. Schmitt, *Thin Solid Films*, 1992, **210/211**, 831.

f) G. Decher, J. Schmitt, *J. Progr. Coll. Poly. Sci.*, 1992, **89**, 160.

1.12 E.M. Genies, A. Boyle, M. Lapkowski, C. Tsintavis, *Synthetic Metals*, 1990, **36**, 139.

1.13 M. Ferreira, J.H. Cheung, M.F. Rubner, *SPE Proceedings*, New Orleans, LA, USA (1993).

1.14 J.H. Cheung, Sc.D. Thesis, Dept. Mat'l Sci. and Engr., MIT, June 1993. and references therein.

1.15 A.C. Fou, D.L. Ellis, M.F. Rubner, *MRS Symp Q Proc.*, 1993, **328**, 113.

1.16 W.B. Stockton, M.F. Rubner, to be published.

1.17 D.S. You and M.F. Rubner, SPE Spring 1995 Meeting Proceedings

1.18 J. Yue, A.J. Epstein, *J.Amer.Chem.Soc.*, **112**, 2800 (1990).

1.19 M. Angelopoulos, A. Ray, A.G. MacDiarmid, A.J. Epstein, *Synthetic Metals*, **21** (1987), 21.

1.20 T. Shimidzu, T. Iyoda, H. Segawa, M. Fujitsuka, *Polymer Preprints*, **1994**, *35*, 1, 236. and references therein.

1.21 A.F. Diaz, J.A. Logan, *J.Electroanal.Chem.*, **111** (1980), 111.

1.22 a) Gregory, R.V.; Kimbrell, W.C.; Kuhn, H.H. *Synthetic Metals*, **1989**, *28*, C823.

b) Gregory, R.V.; Kimbrell, W.C.; Kuhn, H.H. *Journal of Coated Fabrics*, **1991**, *20*.

1.23 a) Pron, A.; Fabianowski, W.; Budrowski, C. *Synthetic Metals*, **1987**, *18*, 49.

b) Dubitsky, Y.A.; Zhubanov, B.A. *Synthetic Metals*, **1993**, *53*, 303.

c) Pouzet, S.; Bolay, N.E.; Richard, A.; Jousse, F. *Synthetic Metals*, **1993**, *55-57*, 1079-1084.

1.24 a) Liang, W.; Lei, J.; Martin, C.R. *Synthetic Metals*, **1992**, *52*, 227-239, and references therein.

b) Martin, C.R. *Adv. Mater.*, **1991**, *3*, 457-459

c) Cai, Z. and Martin, C.R. *J. Amer. Chem. Soc.*, **1989**, *111*, 4138.

1.25 a) R.B. Rosner and M.F. Rubner *Chemistry of Materials* **1994**,

6, 581-586.

b) Hong, K.; Rosner, R.B.; Rubner, M.F. *Chemistry of Materials* **1990**, *2*, 82-88.

c) Shimidzu, T.; Iyoda, T.; Ando, M.; Ohtani, A.; Kaneko, T.; Honda, K. *Thin Solid Films* **1988**, *160*, 67.

1.26 D.S. You and M.F. Rubner, to be published.

1.27 M.S. Ferreira, PhD Thesis, 1994.

1.28 D.L. Ellis, PhD Thesis, Harvard University, Dept. of Chemistry, 1993.

Chapter 2

Ultrathin Films of P-Doped Conducting Polymers via Molecular Self-Assembly

2.1 Introduction and Background

In this chapter, we discuss the manipulation of technologically important conducting polymers such as polypyrrole and polyaniline. Because of the unique properties of electrical conductivity and optical activity, conjugated polymeric systems have been widely studied. The following section puts forth a very simple picture of the physics behind these properties.

Polymers whose backbone is made up of aromatic groups or double bonds possess the π-orbitals necessary for the delocalization of electrons over the space of several atoms (see Figure 2.1) The extent of delocalization varies depending on the degree of twisting or bending of

the backbone which affect how much overlap exists between the π-orbitals on adjacent atoms. The greater the overlap, the larger the extent of delocalization. In their undoped state, the polymer can be thought of as having a relatively wide energy gap, similar to insulators or semiconductors, between the valence band and the conduction band.

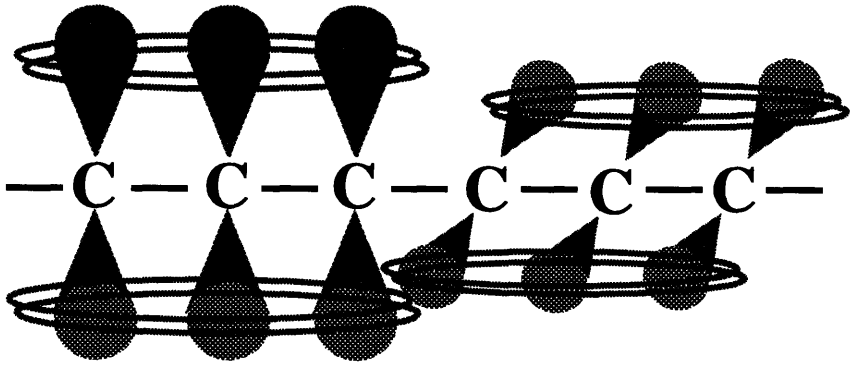

Figure 2.1 Schematic of π-orbital Overlap

However, these organic conjugated chains can be rendered conductive by oxidation (p-type doping) or reduction (n-type doping). During doping, electrons are either stripped away from their states in the valence band or are added to states in the conduction band. Most stable conducting polymers are p-type doped; that is, electrons have been removed from the backbone by means of a strong oxidizing agent. The resulting positive charge is delocalized along the conjugated backbone; the positive charge, of course, is balanced by negative counterions

derived from the doping agent. These counterions are associated with but not necessarily bound to the positive defect. Thus, the electrically conductive forms of conjugated polymers can be described as p-type doped polymeric charge transfer salts.

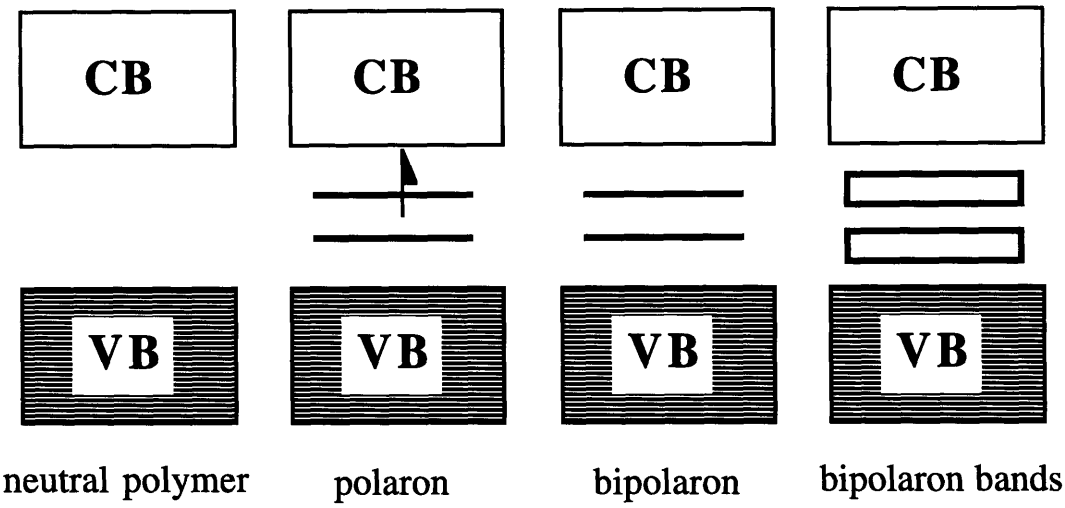

Figure 2.2 Schematic Band Diagrams of Neutral and Doped Conjugated Polymers

Schematic band diagrams can be used to visualize the doping process (Figure 2.2). The process of doping can be thought of as creating polaron (coupled radical cations) and bipolaron (coupled dications) states in the energy gap of a previously insulating polymer [2.1, 2.2]. The existence of these new electronic states are clearly evident by the new absorption behavior of the material upon doping; that is, typically, the undoped polymer exhibits a certain broad

absorption in the visible region due to the high energy transitions between the valence band and the conduction band. Upon doping and the formation of these intergap states, the absorption spectra exhibit new, broad bands at lower energies. The band gaps of conjugated polymers such as polypyrrole, polythiophene, and polyaniline are between 1 eV and 3.5 eV, so they absorb strongly in the visible region. In polyaniline, for example, the undoped state is deep blue in color and the doped state is green to the eye. The process of p-type doping can be thought of as removal of electrons from the valence band; once free states are left behind in the valence band by doping, electronic conduction can occur under the influence of an applied electric field. N-type doping introduces electrons into the conduction band. When a conjugated polymer is exposed to such doping agents, the conductivity increases rapidly to a maximum conductivity characteristic to the particular polymer-dopant system.

Using the schematic band diagrams to visualize the doping process might imply that the conduction in conducting polymers occurs by the movement of free unpaired electrons, created upon doping, under the influence of an applied electric field, similar to traditional inorganic semiconductors. There is evidence that this is not the case. For example, the number of free spins present in conducting polymers is too low to account for the observed levels of conductivity [2.3]. Although several possible conduction mechanisms have been proposed [2.4], a widely accepted model for conduction in polymers is called variable range

hopping. In this model, radical cation defects (polarons) or dication defects (bipolarons) are created along the polymer backbone by doping. These positively charged defects "hop" from one atom to another along the chain by the rearrangement of single and double bonds. This model is consistent with the physically observed anisotropies in the conductivity along the polymer backbone versus perpendicular to it; that is, in films with the polymer chains preferentially oriented in one direction, the conductivity in the direction of the chains is higher than the conductivity perpendicular to the direction of the chains. The intrachain hopping of charged defects is easier than interchain hopping [2.5a].

With an arsenal of electrically and optically active polymers with properties that can be exploited in sundry applications, we go on to describe molecular self-assembly as a unique handling technique which provides significant advantages over other techniques of thin film processing.

2.2 Self-Assembly of P-doped Conducting Polymers

The following section describes the development of the solution conditions and experimental protocols for the molecular self-assembly

of commercially significant conducting polymers, specifically polypyrrole. Figure 2.3 shows the chemical structures of a few such polymers.

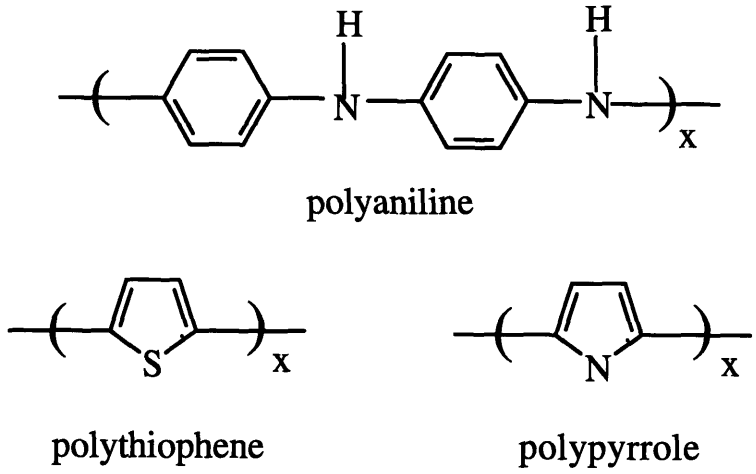

polyaniline

polythiophene

polypyrrole

Figure 2.3 Unfunctionalized P-Doped Conducting Polymers for Self-Assembly

As mentioned before, the chemistry for producing highly conductive polypyrrole is well known. However, the solution chemistry and experimental procedures necessary to achieve molecular self-assembly for chemically produced polypyrrole were not known and were first developed in this work. With self-assembly we could achieve the deposition of extremely uniform, highly conductive, ultrathin films of polypyrrole. A deposition technique, referred to here as "free growth" deposition represents the adsorption of polypyrrole onto the

surface of a substrate left immersed in a solution containing extremely dilute concentrations of the chemical "ingredients" reacting to oxidatively polymerize conductive polypyrrole. The thickness of the layer that was deposited was simply dependent on the amount of time the substrate was dipped in the solution. "Free growth" deposition was thus useful for quickly covering surfaces with a conductive film. However, like the other chemical techniques, the deposition was not controlled on the molecular level. The films produced by this method may serve well in "low-tech" applications such as simple anti-static coatings, but is most likely not of high enough quality microscopically to be used in thin film microelectronic devices such as organic light-emitting diodes. Therefore, self-assembly had to be developed to produce "device quality" films.

Exploiting the fact that the nascent polypyrrole chains in their p-doped state had delocalized positive charges along the backbone, we self-assembled multilayers of polypyrrole by alternately dipping it with the polyanion, sulfonated polystyrene, similar to the self-assembly of pre-formed polycations and polyanions. However, in this case, since polypyrrole is insoluble in organic solvents and water, it could not be formed beforehand and redissolved. It could only be produced in-situ; that is, it had to be formed in the dipping solution during the self-assembly process and deposited onto the substrate as it was formed. This requirement demanded that new solution conditions be found that would allow the polypyrrole to be produced in solution at a slow rate just as it

is needed. This is contrasted to the other chemical techniques in which the polypyrrole is formed in solution and precipitates in the form of macro-aggregates, not useful in the formation of thin films which must be uniform on the microscopic level. In addition to the ability to control the reaction to form polypyrrole in solution, we have also found that the surface chemistry that is exposed to the active solution strongly influences the adsorption behavior of the polypyrrole to the surface. We have exploited these differences in a process that allows us to selectively deposit conductive polypyrrole onto certain areas of a substrate by patterning the substrate surface with appropriate charges. The following sections describe each of the above procedures in detail.

For unfunctionalized, conducting polymers such as polypyrrole, polyaniline, and polythiophene the process of oxidative doping by a strong oxidizing agent produces positive charges along the main backbone of the polymer. This p-doped, conducting state of conjugated polymers involves the delocalization of the positive charges (polarons and bipolarons) along the conjugated backbone (Figure 2.4). It is this partial positive character of the conducting polymer which enable them to be self-assembled with suitable polyanions. And since the conductive form of many conjugated polymers are insoluble in water, the polymer cannot be pre-formed and redissolved; it must be oxidatively polymerized in the dipping solution during the dipping of the substrate. Using an in-situ polymerization/oxidation chemistry is advantageous because it eliminates the separate steps of pre-forming, doping,

solubilizing, and depositing, as required by the other self-assembly processes. As the polymer is being formed in the aqueous solution, it is

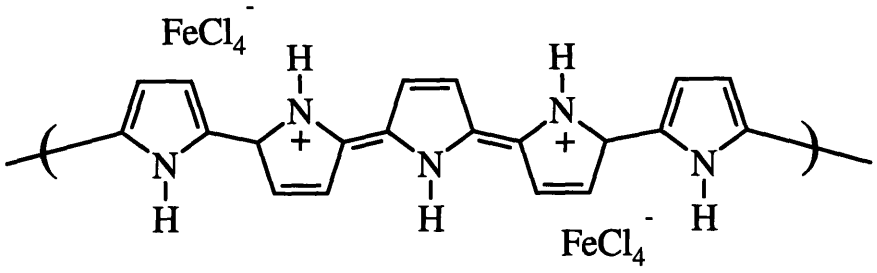

doped polypyrrole

Figure 2.4 Positive Character of P-Doped Polypyrrole

attracted to the surface covered with polyanionic charges; this deposition occurs to form layers, the thickness of which can be precisely controlled by solution parameters and dip times, similar to the self-assembly of other polymers. However, unlike the adsorption of pre-formed polyelectrolytes which is a self-limiting process, the adsorption of in-situ polymerized polypyrrole is a continuous process until the reactants are exhausted. With this technique, we have successfully deposited ultrathin films of 100 Å to 1000 Å which exhibit conductivities comparable to the best bulk samples prepared by standard chemical or electrochemical means. In this way, self-assembly has provided a method to handle and manipulate insoluble, intractable, and unfunctionalized polymers into extremely uniform thin films. In the

sections to follow, we describe the experimental details of each of the steps necessary achieve molecular self-assembly of p-doped conducting polymers.

2.2.1 Substrate Surface Treatment

Since it was realized from previous self-assembly work in our group that the surface chemistry of the substrate strongly influences the deposition of polyelectrolytes, substrates with four types of surfaces were created and used to study the deposition characteristics of polypyrrole [2.5d,e]. The substrates were ordinary glass microscope slides treated with one of the following procedures to render their surfaces hydrophilic, hydrophobic, negatively charged, or positively charged. All of the substrates were first cleaned with a 7:3 concentrated sulfuric acid/hydrogen peroxide solution and a 1:1:5 ammonium hydroxide/hydrogen peroxide/water solution for one hour each, followed by vigorous rinsing with ultrapure water. This rendered the surface hydrophilic. These slides can then be stored under ultrapure water to maintain their hydrophilicity for up to 4 weeks.

Some of these cleaned slides were dried in a stream of air and then exposed to 1,1,1,3,3,3-hexamethyldisilazane (98%, Aldrich) in a dessicator under static vacuum of 200 mTorr for 36 hours to render the surface hydrophobic. The liquid disilazane was placed into a small

evaporating dish and placed inside a vacuum dessicator. The chamber was subjected to vacuum in order to vaporize the liquid disilazane at room temperature. Once 200 mTorr was reached, the chamber was sealed and a static vacuum was maintained. After 36 hours, the slides were removed and stored in air. The resulting surface was hydrophobic with contact angles around 60 degrees.

Other slides were subjected to the following treatments to covalently anchor charges onto the surface. The cleaned slides were placed in polyethylene slide holders and immersed for 15 minutes each into the following solvents: methanol (HPLC grade, Mallinckrodt), 1:1 methanol/toluene, and toluene (analytic reagent grade, Mallinckrodt), without rinsing between the steps. Then they were exposed to a 5 vol% solution of N-2-aminoethyl-3-aminopropyl-trimethoxysilane (Huls America, Inc.) in toluene for 12 hours. It was observed that if this time were exceeded, the silane tended to crosslink and polymerize to form an insoluble white precipitate that could not be rinsed from the surface of the glass slides. Therefore it is critical that the slides be removed at 12 hours. After silanization, the slides were immersed in fresh boiling toluene for one hour. This must be done by transferring the slides from the polyethylene trays into glass staining dishes. (The polyethylene trays are swelled and gradually dissolved by the boiling toluene.) The slides are then boiled in the toluene for 1 hour in a 2000 ml beaker on a standard hot plate. The temperature should be adjusted so that the toluene is boiling slowly. Extreme caution should be used when

handling boiling toluene, as it is above its flash point at that boiling temperature. Aluminum foil may be used to lightly cover the mouth of the beaker to slow the loss of volume due to evaporation; but additional toluene may need to be added to compensate for evaporation and keep the slides submerged. Then the slides were removed from the boiling toluene and transferred back to the polyethylene trays and immersed for 15 minutes each in toluene, 1:1 methanol/toluene, and methanol. This sequence of immersions is critical in conditioning the surface and ensuring clear, uniform silanization of the glass slides. After this surface conditioning sequence the slides are thoroughly rinsed with Millipore® (ultrapure) water. If the surface is still slightly cloudy after water rinsing, immersion in water overnight typically remedies the problem. This silanization process produces a surface with covalently anchored amine functionalities; these amine groups are protonated and thus positively charged in the slightly acidic solutions used in this study.

To produce a negative surface, these slides were immediately dipped into a solution of 0.001 M sodium poly(styrene-4-sulfonate) with the pH adjusted to unity by HCl. It was found that these slides are also best stored under ultrapure water prior to use. When stored this way, the surface characteristics change very little over the course of up to 4 weeks. If similar slides are stored in air, the hydrophilicity of the surface decreases and the subsequent deposition is less uniform and adherent.

2.2.2 Free Growth Deposition of Polypyrrole

Once the substrates are ready, the dipping solutions for the self-assembly of polypyrrole are prepared. The dipping solutions were prepared in the following manner. The solution of the negative polyelectrolyte, sulfonated polystyrene, was made by dissolving (SPS, 99% sodium poly(styrene-4-sulfonate), Aldrich) in Millipore® water to the concentration of 0.001 M; the pH adjusted to unity by hydrochloric acid. The pH was monitored by a calibrated pH meter and enough hydrochloric acid was added to the solution to give a pH of unity. The active dipping solutions of the p-doped, conducting polymer were made by dissolving an oxidizing agent, ferric chloride (>98% anhydrous $FeCl_3$, Fluka Chemika) in Millipore® water and then adjusting the pH to unity by adding HCl. A sulfonic acid such as p-toluene sulfonic acid (PTS, 99%, Aldrich) or anthraquinone-2-sulfonic acid (ASA, 97%, Aldrich) was then dissolved in the solution, followed by the addition of the pyrrole monomer (99% pyrrole, Aldrich). The specific concentrations utilized are discussed later in the text since each was varied to control the layer thickness and conductivity. However, a typical dipping solution contained 0.006 M $FeCl_3$, 0.026 M PTS or 0.005 M ASA, and 0.02 M pyrrole monomer. As will become apparent, these extremely dilute concentrations (typically one order of magnitude more dilute than other chemical techniques) are required to achieve self-assembly; much higher concentrations lead to the uncontrolled precipitation of polypyrrole. After the addition of the pyrrole

monomer, the solutions were allowed to stir for 15 minutes when PTS was used and for 2 minutes if ASA was used. These conditions were chosen because the reaction kinetics of the PPY-ASA solution are faster than that of the PPY-PTS; therefore the solution is ready for dipping after a shorter "induction period." All active solutions were filtered through a 0.45 micron syringe filter just before dipping.

In this process which we designate as "free growth," the substrate is simply immersed into a solution containing the "active ingredients" of pyrrole monomer, the oxidant/dopant ferric chloride, and a reaction rate enhancement agent, and left immersed for a specified amount of time. The polypyrrole deposits onto the surface as it is formed in solution. Since the doped and conductive form of polypyrrole is insoluble in water, it eventually precipitates out onto the substrate and all surfaces exposed to the solution. Using the solution concentrations specified above, this does not occur until nearly 3 hours. Thus, by keeping the dip times well below this "useful lifetime" limit, relatively uniform films can be deposited onto the surface of the substrate. It should be noted though, that this is still an uncontrolled process like the other chemical deposition techniques mentioned before.

2.2.3 Self-Assembly of Polypyrrole

Obviously, the "free growth" process does not provide the necessary control over the deposition nor results in films of sufficiently high quality. Therefore molecular self-assembly was invoked to address and solve some of these issues. The basic layer-by-layer self-assembly of conductive polypyrrole involves the deposition of polypyrrole onto a substrate pre-treated to cover the surface with negative charges. Figure 2.5 shows an aminosilanized surface which is dipped into a solution of sulfonated polystyrene to render it negatively charged. The substrate is then simply dipped into an extremely dilute solution containing the active ingredients for the chemical oxidative polymerization of conducting polypyrrole. As the polypyrrole is formed, the delocalized positive charge on the backbone is electrostatically attracted to the negative functional groups on the surface of the substrate. The substrate is left immersed in the solution for a given amount of time, removed, and rinsed vigorously with ultrapure water. The dip times are kept to between 5 and 10 minutes such that the thickness of each layer deposited is in the range of 20 Å to 60 Å depending on the solution chemistry. A single such layer serves little purpose and does not exhibit bulk conductivities. Therefore the process is continued in a manner similar to the other self-assembly process. The substrate is then dipped for 10 minutes into a solution of the polyanion, sulfonated polystyrene. Again,

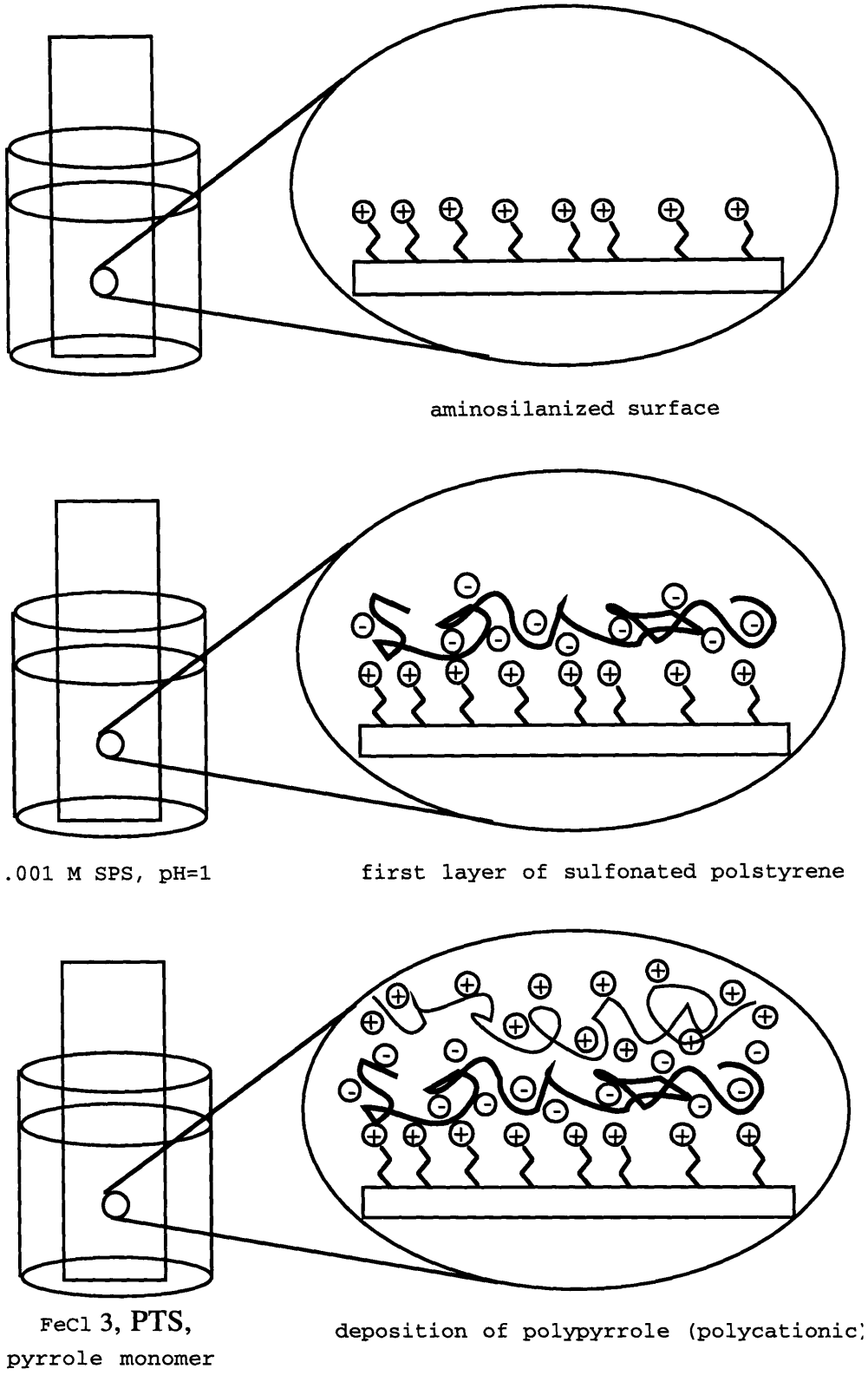

Figure 2.5 Schematic of Self-Assembly of Polypyrrole

a single layer is adsorbed. Due to the complex configuration of the polymer, some of the charges are "bound" to the previous layer while the rest are left exposed, changing the surface charge again to negative. The surface is now ready to attract the next layer of polypyrrole when it is immersed in the active polypyrrole solution again. The alternating dipping sequence between polypyrrole and polystyrene is repeated as necessary to build up multilayers. The active polypyrrole solution is useful for about three hours before the polymerization results in visible aggregates of insoluble, black polypyrrole which litters any and all surfaces exposed to the solution by physisorption of clumps of material.

In order to demonstrate the utility of this process for another technologically important conductive polymer, self-assembly was applied to polyaniline. Although this system was not the focus of this study, the basic parameters necessary to achieve self-assembly are presented briefly here. In-situ polymerized polyaniline was self-assembled in a similar manner. The polyaniline active solutions contained 0.004 M ammonium peroxysulfate (99%, Aldrich) in Millipore water with the pH adjusted to unity by hydrochloric acid. P-toluene sulfonic acid was added to give 0.026 M PTS and aniline monomer (99%, Aldrich) was added to a concentration of 0.02 M. The solution was allowed to stir for 30 minutes and then filtered through 0.45 micron syringe filters. Typical 10 bilayer sample films are built up with 5 minute dips in the active polyaniline solution and 10 minute dips into the SPS solution.

2.2.4 Self-Assembled Heterostructure

With the level of control over monolayers of material afforded by molecular self-assembly it is possible to conceive of more complex heterostructures which can be designed specifically to exhibit certain properties. As a demonstration of the successful use of self-assembly in the realization of novel heterostructure architectures very difficult to achieve by any other thin film deposition techniques, we designed a thin film architecture which sandwiched conductive "slabs" (multilayers) of polypyrrole between insulating "slabs" of undoped poly(thiophene-3-acetic acid). This structure, shown in Figure 2.6 would theoretically show highly anisotropic properties. For example, the in-plane conductivity is expected to be much larger than the transverse conductivity since the conductive slabs lie in the plane of the substrate and are not interconnected with each other in the transverse direction. The experimental details are presented in the following paragraphs. The experiments were carried out by another member of our group, Diane Ellis [2.5a].

Since self-assembly is a layer-by-layer deposition process, it gives us the freedom to build complex, multicomponent films simply by alternating between dipping solutions of a wide variety of different conjugated and non-conjugated polymer polyelectrolytes. As long as the substrate is alternately dipped into a solution containing a polycation and

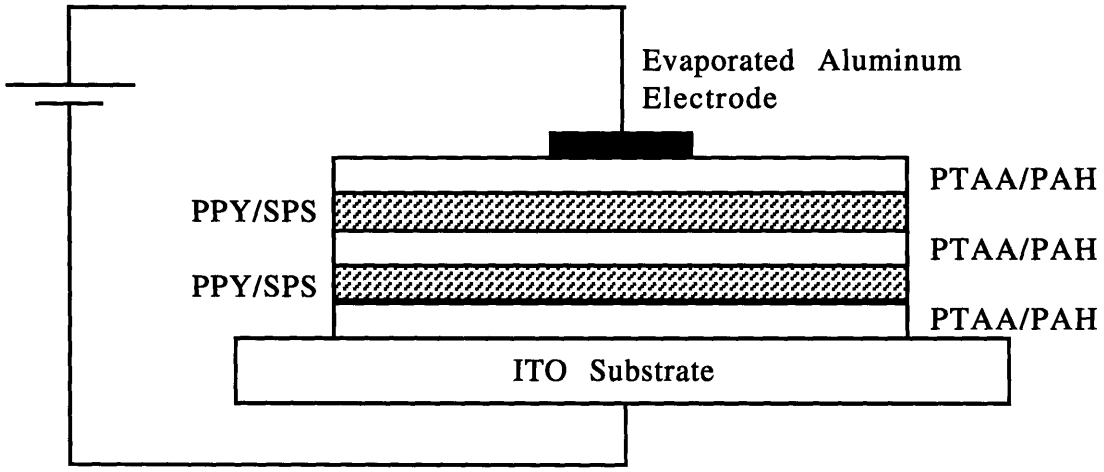

Figure 2.6 Schematic Architecture of Self-Assembled Heterostructure Film (PPY/SPS and PTAA/PAH blocks are 150 Å each)

a solution containing a polyanion, it is possible to fabricate multilayer heterostructures in which layers of different materials are positioned within the multilayer film to create specific electrical and optical effects. The heterostructure proposed above contains blocks (multiple bilayers) of electrically conductive polypyrrole (PPY)/sulfonated polystyrene (SPS) alternating with blocks of insulating poly(thiophene-3-acetic acid) (PTAA)/polyallylamine (PAH) [2.5a]. As can already be seen, this structure contains four components easily manipulated into a heterostructure by molecular self-assembly.

The insulating blocks were created by self-assembling poly(thiophene-3-acetic acid) (PTAA) and polyallylamine (PAH). The PTAA solution was 0.001 M and was made by dissolving the PTAA

powder in pH = 10 solution of water and sodium hydroxide. This produced the salt form of the carboxylic acid. Additional sodium chloride (NaCl) was added to a concentration of 0.5 M. The pH was subsequently adjusted to 4.8 by the addition of enough hydrochloric acid. A pH of 4.8 was found to give the optimal deposition, such as uniformity and thickness, and the best solution stability; solutions held at other pHs tended to turn cloudy and show precipitation. The polyallylamine solution was 0.001 M with no pH adjustment. The dip times into each of these solutions were 10 minutes each. From previous studies [2.5c, 2.5d] this combination of PTAA/PAH produced bilayers that were 17 - 20 Å each in thickness. The conductive blocks were self-assembled using the solution chemistries described above for the polypyrrole (PPY)/sulfonated polystyrene (SPS) system. Briefly, these were 0.001 M SPS in water, with the pH adjusted to unity by hydrochloric acid (HCl), and 0.02 M pyrrole monomer in water, with 0.03 M p-toluene sulfonic acid and 0.006 M ferric chloride at pH = 1. In this study, however, the polypyrrole was self-assembled using 30 minute dips into the active polypyrrole solution and 10 minute dips into the SPS solution, giving a bilayer thickness of 150 Å. This was done to reduce the number of rinsing and drying steps in between each dip; since the growth of polypyrrole onto polyanions (in this case, the SPS) is linear up to 60 minutes, dip times of 30 minutes produced the desirable results. Finally, between each conductive and insulating blocks, 2 bilayers of SPS/PAH were self-assembled; this was found to promote the adhesion of the film and adhesion of the blocks.

The in-plane conductivity was measured with the standard van der Pauw technique, mentioned above. The transverse conductivity measurements posed a greater challenge. The heterostructure films to be used in the transverse conductivity measurements had to be self-assembled onto glass substrates coated with conducting, transparent ITO. After the films were built up onto these substrates, they were allowed to dry in a dessicator for at least 48 hours. Then, circular aluminum top electrodes were evaporated to provide a top contact. The rate of deposition was roughly 3 - 5 Å per second. The aluminum top electrodes were between 750 - 1000 Å thick. The bottom contact was made to the ITO underneath the film; the aluminum electrodes on top were contacted by touching a loop of gold wire onto each electrode. The transverse conductivity was calculated from the measured resistance across the film, the known top electrode area, and the film thickness. Our analyses of the heterostructure films show that they indeed behave as expected according to their design. The films with 150 Å blocks, for example, exhibited in-plane conductivities ($\sigma_{=}$) of 1-10 S/cm and transverse conductivities ($\sigma_{\perp}$) of about 10^{-10} S/cm, giving conductivity anisotropies ($\sigma_{=}/\sigma_{\perp}$) on the order of 10^{10}. It was also demonstrated that the dielectric properties of these heterostructure films could be altered by changing the volume fractions of the PPY and PTAA blocks or by increasing the number of interfaces between the conducting and insulating blocks [2.5b, c].

Thus far, we have delineated the reasons for using self-assembly to handle and deposit conjugated conducting polymers out of aqueous solution and presented the experimental conditions required to achieve self-assembly of p-doped conducting polymers. We now move on to describe other techniques used in the characterization of the buildup process and the resulting thin film.

2.3 Conductive Thin Film Characterization

2.3.1 Thickness by Dektak Profilometry

The thickness of sample films was determined by profilometry using a Sloan Dektak 8000. Several parallel scratches in the film were scribed by a razor blade and a stylus with a pressure of 12 milligrams was traced perpendicularly across the series of scratches. An average step height was calculated and taken as the thickness of the film.

2.3.2 Ultraviolet-visible Absorption Spectroscopy

The deposition of doped polypyrrole was monitored by visible absorption spectroscopy since polypyrrole is strongly absorbing in this region of the spectrum. A circular area of one centimeter in diameter was scanned with polychromatic light from 400 to 870 nm using an Oriel Instaspec 250. In order to quickly estimate total film thicknesses, visible absorption data were directly correlated with the thickness of the film obtained by Dektak profilometry. The resulting linear correspondence between absorbance and thickness allows an accurate estimate of the thickness of the films simply by measuring the absorbance. It was found, however, that this method of estimating thickness was not completely universal for all polypyrrole thin films. Specifically, when substantially higher ferric chloride concentrations were used, the films showed greater absorbance per unit thickness. Therefore, it was necessary to generate new absorbance versus thickness plots for films made with solution chemistries containing different ferric chloride concentrations. Otherwise, the above method provided a quick and simple way of determining the thicknesses of these ultrathin films. Finally, it should be noted that the SPS accounts for about 15 Å of the thickness of each bilayer; this thickness contribution was determined by comparing the thickness of a self-assembled film of 10 bilayers with that of a film made by free growth with a dip time of 50 minutes, equivalent to 10 dips of 5 minutes each into the active polypyrrole solution. Since the sulfonated polystyrene is non-colored

and does not absorb in this region, the increase in absorption of the film is due solely to the deposition of polypyrrole. Finally, this self-assembly system of polypyrrole and sulfonated polystyrene exhibits the characteristic linear deposition; the absorbance increases linearly with the number of layers of polypyrrole deposited.

2.3.3 Conductivity by van der Pauw Technique

To measure the in-plane conductivity of the films created by self-assembly, we use the standard four-point, van der Pauw technique on a square area of 1 cm x 1 cm. The original film on the glass slide was scraped down with a razor blade to leave the square centimeter area. Thin gold wire leads were contacted at each of the four corners with graphite electrodag or silver paste. Voltages were measured with a Keithley model 614 electrometer and the current was generated by a Keithley model 224 current source. The applied currents were adjusted such that the maximum current that could be supported by the film was used (typically 1-10 mA). The resulting voltage readings and a set of voltages using currents one order of magnitude smaller were averaged and used in the van der Pauw calculations. This particular method was used because it is applicable to films of any geometry (the four probes can be contacted at any four points at the edge of the film) as long as the thickness is uniform across the area measured.

Current was passed through two adjacent leads of the four leads attached to the corners of the 1 square centimeter film area. The voltage drop was detected by the opposite two leads. The current values were varied at least two orders of magnitude and the polarity changed for each value. This yielded resistance values that could be averaged, resulting in R_1 for this geometry. Then the leads were change such that one of the original current leads was exchanged with one of the voltage leads giving geometry 2. Again, several current values were used and both polarities of each value were scanned. Calculations with these numbers gave resistance R_2 for this geometry. Then the resistivity of the sample was calculated with the following equation:

$$\rho = \frac{\pi d}{\ln 2} \cdot \frac{R_1 + R_2}{2} \, f(R_1 / R_2)$$

where d is the thickness of the film in centimeters, and f is a constant determined by iteration of the following equation:

$$\frac{R_1 + R_2}{R_1 - R_2} = f \, \frac{\arccos(\exp(\ln 2/f))}{2}$$

2.4 Results and Discussion

Now we present the results and interpretations of the data on the self-assembly of polypyrrole.

2.4.1 Free Growth Deposition and Surface Effects

The chemical oxidative polymerization of polypyrrole has previously been used to create a wide variety of electrically conductive coatings and composites. The polymerization of polypyrrole, for example, has been successfully carried out onto fabric fibers [2.6], within per-formed polymer matrixes [2.7], via "template synthesis" in microtubules [2.8], and within LB films [2.9]. Thin films of polypyrrole can also be prepared by electrochemical polymerization onto a conducting substrate [2.10]. Although this approach has been used to deposit thin films, to date, an understanding of the factors required to provide molecular-level control over the deposition process has not been developed. In the sections to follow, we will present our understanding of the deposition of polypyrrole based on the observations and results of our development of the self-assembly process for p-doped conducting polymers.

As will become apparent shortly, we have found that the key to molecular level control over the deposition of in-situ polymerized conducting polymers lies in the nature of the surface onto which the deposition occurs. Figure 2.7 compares the time-dependent growth of in-situ polymerized polypyrrole onto surfaces with four different characteristics. The growth of polypyrrole was monitored by taking visible absorption spectra and reading the absorbance at 550 nm. The wavelength 550 nm was chosen for monitoring growth since it is away from the bipolaron bands at longer wavelengths and will thus be least affected by the levels of doping. In this way, the increase in the absorbance at this wavelength monitors only the amount of polypyrrole

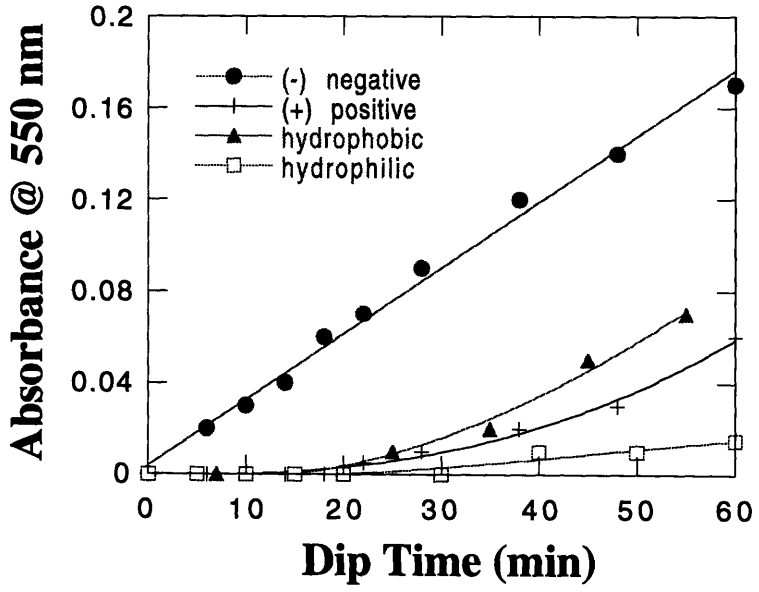

Figure 2.7 Time Dependent Growth of PPY onto Various Surfaces

deposited without convolution with the level of doping. In this experiment, the samples were made by immersing multiple substrates with the various surface treatments into a polypyrrole dipping solution. A substrate of each kind was removed after the indicated amount of time, rinsed, and dried. The absorbance spectra was taken immediately thereafter; as mentioned before, the increase in absorption traces the deposition of polypyrrole. The single-dip process used here is the "free growth" of polypyrrole, as mentioned before. "Free growth" deposition is a process in which the polypyrrole is continuously deposited onto the surface until the reactants are exhausted. This is in sharp contrast to the self-limiting behavior exhibited in the adsorption of pre-formed polyelectrolytes onto surfaces. That is, for typical polyelectrolytes, the deposition halts after monolayer coverage is achieved. Once a monolayer of the material covers the surface no more material deposits on the surface no matter how long the substrate is left in the dipping solution. This translates into a deposition versus time curve which shows a quick rise in the beginning but a flat plateau at longer times. Depending on the system, the plateau can be reached in 20 to 30 minutes.

Figure 2.7 above shows the behavior of the present in-situ polymerization process. It is clear that for surfaces fitted with negative charges (ionized sulfonated polystyrene groups), there is a linear correspondence between the dip time and the amount of polypyrrole

deposited onto the surface up to 60 minutes; that is, the rate of deposition of the newly formed polypyrrole is constant out to 60 minutes. This is in sharp contrast to the deposition onto the hydrophilic, hydrophobic, and positively charged surfaces. In these cases there is an apparent "induction period" of about 20 minutes during which time virtually no polypyrrole is deposited. After this induction period, the growth of polypyrrole onto these surfaces is nonlinear and exhibit a sharp rise in slope. The amount of polypyrrole deposited is still significantly less than that observed on the negatively charged surface and the type of deposition is also different; further evidence will be given below that suggests that self-assembly is occurring on the negatively charged surfaces whereas physisorption of microaggregates of polypyrrole is occurring on the other types of surfaces. The films produced with dip times of greater than 60 minutes are littered with visible aggregates of polypyrrole precipitate; therefore in all cases the absorbance versus time curves become superlinear, with this effect being least pronounced in the case of the negative surfaces. The fact that polypyrrole deposits in a very controlled manner on negatively charged surfaces makes it possible to use this process to fabricate single layer and multilayer thin films with well defined thicknesses. Further, it should be noted that the uniformity and adhesion of the films deposited on negatively charged substrates is exceptionally good while the films on the other surfaces are blotchy and can easily be rubbed off.

2.4.2 Selective Deposition

Since the chemistry of the surface of the substrate or, in the case of multilayer films, the chemistry of the "previous" layer strongly influences the deposition of polypyrrole, we were able to take advantage of these properties to selectively deposit polypyrrole onto certain areas of the surface of a substrate. That is, we can delineate a surface with adjacent electrically conducting and insulating regions by patterning a surface with positively and negatively charged regions. By keeping the dip times to less than 20 minutes each, the length of the "induction period" for the deposition onto the positively charged surface, we can deposit the polypyrrole selectively onto the negatively charged surface. The negative regions attract the p-doped conducting polymer while the positive regions "block" the deposition due to the effects of electrostatic repulsion. To date, we have used this approach to create with conducting and insulating regions on the surface of substrates with centimeter resolution.

Figure 2.8 shows a schematic representation of this process. A substrate with a negatively charged surface is dipped half-way into a solution containing the polycation, polyallylamine hydrochloride. The polycation is self-assembled onto the regions that were dipped in this manner. The resulting surface is then comprised of negative and positive regions. The entire substrate is then dipped into the polypyrrole active solution. The polypyrrole selectively deposits onto the areas with

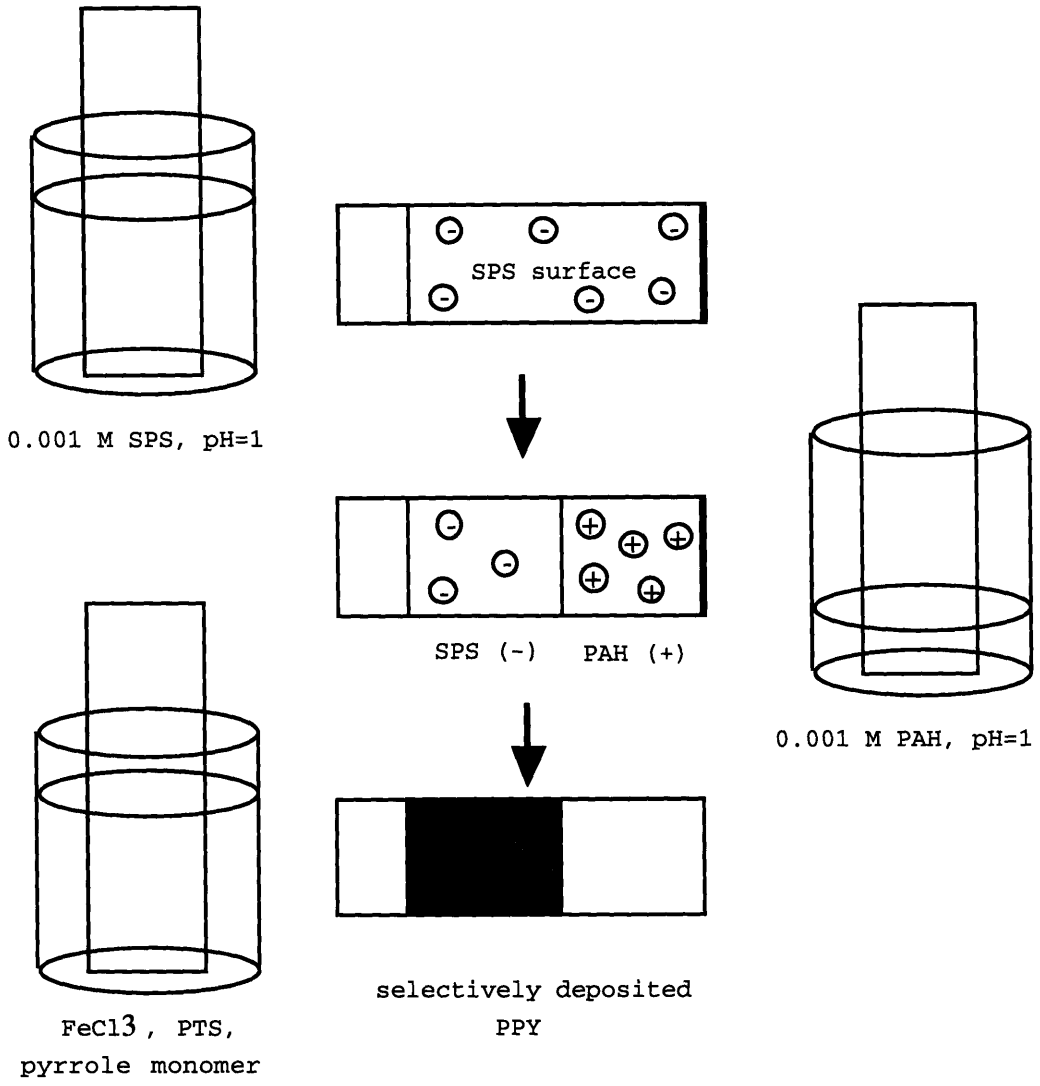

Figure 2.8 Selective Deposition of Polypyrrole

the negative sulfonated polystyrene and is selectively "blocked" in the regions with the positively charged polyallylamine hydrochloride. The substrate is then dipped entirely into a solution of sulfonated polystyrene to render the entire surface negative again. Then the steps of "blocking"

certain regions and selectively depositing the polypyrrole are repeated to build a multilayer film on the surface of a substrate. Chemolithographic techniques which can pattern a surface with positive and negative charges, when combined with self-assembly of conducting polymers, will make it possible to pattern a surface with adjacent conducting and insulating regions with micron resolution.

2.4.3 Self-Assembly versus Free Growth

As mentioned before, although the free growth process has been used with some degree of success in depositing films onto various surfaces, we desire control over the deposition process at the molecular level. Therefore we develop molecular self-assembly. Again, extremely dilute concentrations of reactants are used; this allows the active dipping solution to be used over a period of 2 to 3 hours before the gross precipitation of polypyrrole occurs. The dip times into this active solution are typically 5 to 10 minutes each. Between these dips, the substrate is dipped into the solution of sulfonated polystyrene. This alternate dipping self-assembly process ensures that the surface that is exposed to the active polypyrrole solution is covered with negative charges after each dip into the polyanionic solution. In this way, films of many layers can be built up, taking advantage of the linear deposition characteristic of polypyrrole onto negatively charged surfaces. Since the dip times are kept to less than 10 minutes each, the adsorbed layer is

nearly a true monolayer. Using a particular dip time, the thickness of this layer is determined by the solution chemistry. Due to the controlled deposition of polypyrrole onto negatively charged surfaces, a highly reproducible amount of polypyrrole is deposited with each dip. Figure 2.9 shows the overlaid absorption spectra of a multilayer film taken after each polypyrrole layer was deposited. The inset shows that the deposition is indeed linear as expected. Figure 2.10 shows that this linear characteristic holds for self-assembly carried out with other solution chemistries. Note that the term "bilayer" is used to represent one polypyrrole dip and one polyanion dip. Since the sulfonated polystyrene component of each bilayer is colorless and does not absorb in the wavelengths scanned by the absorbance measurements, the increase in absorbance only traces the deposition of the polypyrrole. The larger the slope of the lines in the figure, the greater the thickness per deposited layer of polypyrrole. For example, the addition of the reaction rate enhancer, p-toluene sulfonic acid to the active solution results in a slightly larger slope, indicating that in a given dip time, more polypyrrole is being deposited.

Further, although not shown here, the polyaniline system behaves similarly; that is, in-situ polymerized polyaniline also exhibits the linear deposition characteristic of the self-assembly procedure. For the conditions specified in the experimental section, the self-assembled films of polyaniline are extremely uniform, highly adherent, and blue.

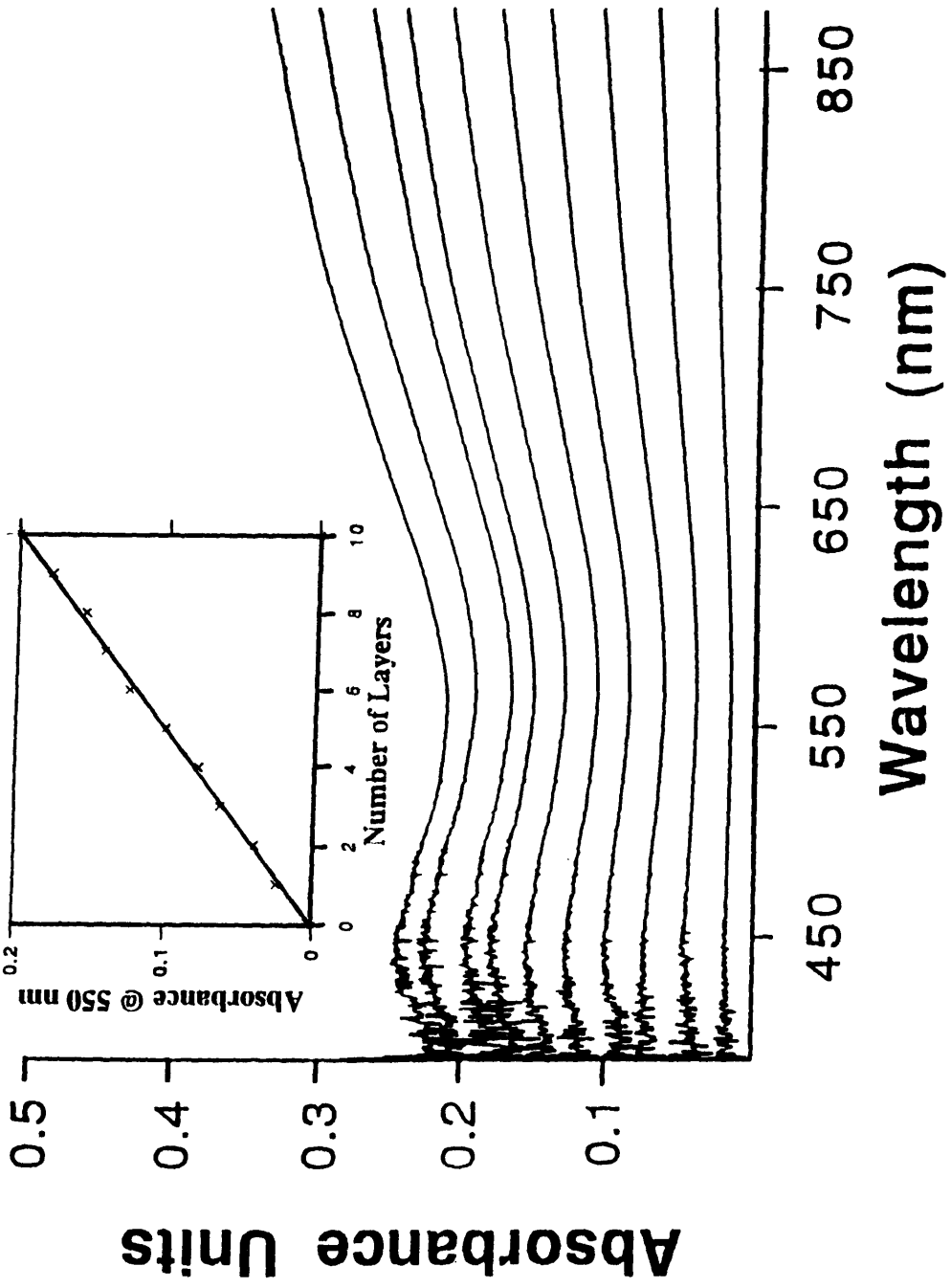

Figure 2.9 **Overlaid Absorbance Spectra of Polypyrrole with Inset of Linear Deposition**

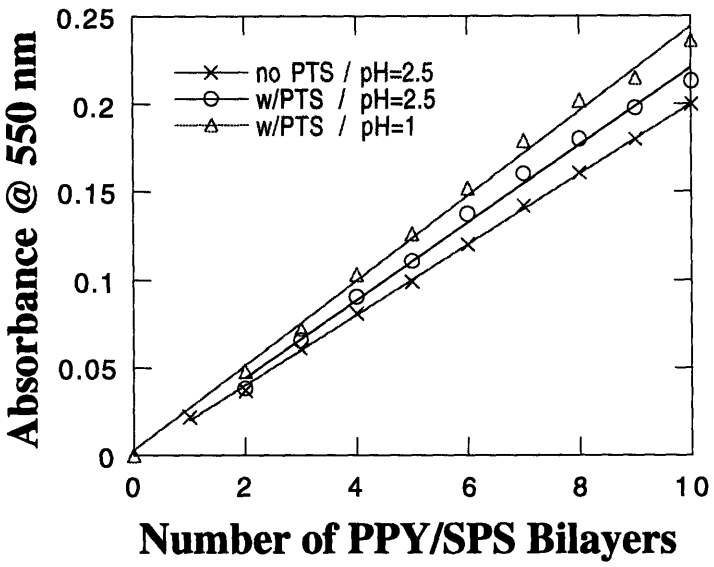

Figure 2.10 Linear Deposition of PPY

2.4.4 Conductivity Considerations

Now that we have characterized the deposition of polypyrrole either by free growth or by self-assembly, we will discuss the conductive properties of the films and the ability to control these properties through adjustments in the solution chemistry.

Table I summarizes the average conductivity and average per-bilayer thickness of representative polypyrrole sample films fabricated from dipping solutions with different reactant concentrations. All samples

contained ten bilayers of polypyrrole/sulfonated polystyrene made using five minute dips in the polypyrrole active solution and 10 minute dips in the SPS. The very low concentrations of reactants used in this study should

Table I: AVERAGE CONDUCTIVITY AND BILAYER THICKNESS OF SAMPLE FILMS

Cell Contents: conductivity (S/cm), bilayer thickness (+/- 5 Å)	**pH = 2.5**	**pH = 1.0**	**pH = 0**
no PTS **0.003 M $FeCl_3$**	0.003 S/cm, 26 Å	2 S/cm, 35 Å	1 S/cm, 35 Å
no PTS **0.006 M $FeCl_3$**	0.05 - 0.15 S/cm, 33 Å	5 - 9 S/cm, 39 Å	14 - 20 S/cm, 34 Å
0.026 M PTS **0.006 M $FeCl_3$**	12 S/cm, 44 Å	18 - 27 S/cm, 47 Å	34 S/cm, 36 Å
0.005 M ASA **0.006 M $FeCl_3$**	15 S/cm, 45 Å	35 - 80 S/cm, 43 Å	47 S/cm, 36 Å

NOTE: All samples consist of 10 bilayers of PPY/SPS (5 minute dips in PPY solution and 10 minute dips in SPS solution). Single conductivity points represent average values of less than 5 measurements. Conductivity ranges represent the range of values observed in greater than 10 samples.

be noted immediately. As mentioned earlier, the reason for using such low concentrations is that greater control over the deposition process and better uniformity of the resultant films is obtained with more dilute solutions. In general, there is a tradeoff between control of the

deposition process and achieving higher conductivities by using greater reactant concentrations; that is, when greater concentrations are used to achieve higher conductivities, precipitation occurs more quickly in the active solution and precise control over the layer thickness is compromised. However, despite the low concentrations used in these experiments, the ultrathin films exhibit conductivities comparable to bulk polypyrrole samples. Clearly, the solution chemistry determines the conductivity and thickness of the deposited polypyrrole.

The first two rows in this table show that increasing the ferric chloride (oxidizing agent) concentration enhances the conductivity but does not significantly alter the average thickness of the bilayer building block of this film (polypyrrole/sulfonated polystyrene); for the 5 minute dipping times utilized, it stays remarkably constant around 35 Å. The higher oxidizer concentration leads to greater oxidative doping of the polymer and thus results in higher observed conductivities. An enhancement of the conductivity can also be achieved by adjusting the pH to unity or lower with hydrochloric acid. In general, the addition of a sulfonic acid was found to enhance the rate of reaction, thus producing thicker layers for a given dip time and also a further increase the conductivity. An exception to this trend is seen in the films prepared from the pH = 0 solutions which deliver a thickness per bilayer that is independent of the presence of sulfonic acids. Consistent with the work of Kuhn and colleagues [2.7], the use of anthraquinone sulfonic acid

(ASA) as a conductivity enhancer results in higher conductivities than p-toluene sulfonic acid (PTS).

Various other processing conditions were also investigated in the attempt to achieve greater control over the deposition process or to enhance the conductivity of the deposited polypyrrole. For example, the temperature of the dipping solutions was lowered and held constant at 3 °C. This simply caused thinner layers of polypyrrole to be deposited per dip; the deposition remained linear, but with a reduced slope. No increase in conductivity was observed, despite previous findings for electropolymerized polypyrrole [2.8a]. This suggests that cooling the dipping solution does not result in films with more ordered polypyrrole chains; rather, only the kinetics of deposition are slowed by the lower temperatures. Second, annealing of the samples in a oven at 90 °C after deposition of the multilayer film was found to improve the room temperature conductivity by up to 50% initially, perhaps by removing excess water. Additional heating beyond two 15-minute "anneals," however, caused a slow decrease in the conductivity, attributable to the normal degradation of the polymer in room air at elevated temperatures. Thin films with significantly higher conductivities can be prepared by simply increasing the ferric chloride concentration to 0.06 M (10 g/L) and using the usual 0.005 M ASA and 0.02 M pyrrole concentrations. In this case, thin films could be readily prepared with conductivities over 300 S/cm. The higher oxidizer concentrations needed to produce these exceptionally high conductivities, however,

make it possible to deposit only a few controlled layers before precipitation occurs in the bath. Increasing the concentration of the sulfonic acid additive close to five-fold (to 0.025 M) did not significantly enhance the conductivity of the films.

One of the most significant observations from these conductivity studies was that "bulk" conductivities could be achieved with films as thin as 100 Å. For example, films of 3 self-assembled bilayers or 15 minutes free growth showed conductivities between 60-80 S/cm. Figure 2.11 shows the linear increase in thickness with dip time and the associated increase in the conductivity for the PPY-ASA system in free

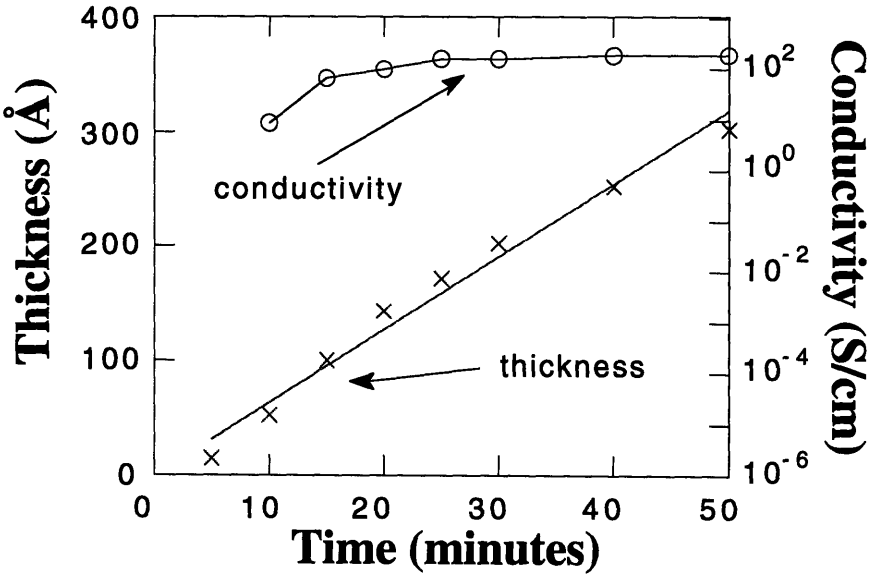

Figure 2.11 Conductivity and Thickness versus Time

growth mode. The graph shows that even though the thickness increases linearly, the conductivity quickly rises and reaches a plateau value at around 100 Å thickness. Multiple substrates were dipped into an active polypyrrole solution containing 0.006 M $FeCl_3$, 0.005 M ASA, 0.02 M pyrrole at pH=1.0; individual substrates were then removed after specific dip times. A substrate dipped for 5 minutes gives a film of around 20 Å, with an undetectable conductivity ($<10^{-6}$ S/cm). Therefore, no point is shown for the 5 minute (20 Å) film. It should be noted that although the deposition is subsequently linear, it is always observed that the first layer is thinner than the average layer thickness for the film; that is, the thickness of the film after the first 5 minutes is less than the thickness deposited during subsequent 5-minute intervals. Once the film reaches a thickness of about 60 Å the conductivity is already around 10 S/cm and by 100 Å, a conductivity close to the plateau value (about 100 S/cm) is achieved. These observations demonstrate that by around 100 Å total thickness, the film of polypyrrole becomes completely coherent on the microscopic level, with all "island" domains interconnected, thus leading to the observed "bulk" conductivity. This is significant as it represents the first clear demonstration of the minimum film thickness required to achieve maximum "bulk" conductivity in in-situ polymerized films of polypyrrole. Thus, it can be inferred that the two-dimensional percolation threshold has been reached by as little as 100 Å in these self-assembled films. The fact that bulk conductivity can be reached with

such ultrathin films speaks well of the microscopic quality of the films deposited by self-assembly.

Furthermore, it was found that the conductivity of sample films prepared via the layer-by-layer self-assembly method was the same as that of the films prepared by the free growth process when corrected to account for the SPS contribution to the thickness. For example, the conductivity of the above film after a single dip of 15 minutes was nearly identical to that of a film made with three 5-minute dips into the polypyrrole active solution (with 10 minute dips into the polyanion, SPS, in between each polypyrrole layer). The SPS remains an inert component in the self-assembled film accounting for about 15 Å of the average 45 Å thickness of each bilayer. These ultrathin films are at the same time extremely uniform optically and greater than 85% transparent, with a neutral gray tint. Currents of 1-10 mA are readily supported by these films, making them potential candidates to serve as one of the electrodes for organic light-emitting diodes.

2.4.5 Mechanism of Polypyrrole Deposition

The observations of the behavior of the deposition of polypyrrole in the free growth and self-assembly processes have allowed us to comment on the mechanism of the deposition process. In the free growth deposition process, it appears that the polypyrrole chains are

formed in solution and subsequently adsorbed onto the surface after achieving a critical molecular weight; the particular molecular weight necessary before deposition can occur depends on the nature of the substrate surface. For negatively charged surfaces, the ionic attractions developed between the growing polymer chains (positively charged due to delocalized bipolarons) and the substrate surface promote a uniform, continuous deposition process in which conducting polypyrrole chains are adsorbed onto the surface at an essentially constant rate. There is no evidence to support the notion that uncharged monomers are adsorbed to the surface before they are polymerized together. For hydrophobic, hydrophilic, and positively charged surfaces, adsorption onto the surface is driven primarily by the poor solubility of the oxidized polymer in water. In these cases, the polypyrrole chains, most likely in the form of larger sized aggregates, deposit onto the surface only after a relatively high molecular weight or aggregate size is achieved, resulting in a non-linear growth process and less uniform deposition. The induction period seen in the Figure 2.7 is attributed to the time required to achieve a critical aggregate size, after which the deposition occurs by physisorption of these aggregates onto the surfaces. Recall that the films deposited onto these surfaces tend to be blotchy and exhibit poor adhesion. Furthermore, the slopes of the curves for the non-negative surfaces rise sharply, consistent with the larger increase in absorbance due to the deposition of aggregates rather than a uniform film. Thus, for these surfaces, the polypyrrole is essentially forced out of the dipping solution and onto the surface by solubility effects.

The above hypothesis is supported by the following general observations. The longer induction period observed with the hydrophilic, hydrophobic, and positively charged surfaces as compared to the negatively charged surface suggests that the polypyrrole chains must grow to a larger size (or aggregate more) before they deposit onto the surface. Once this critical size is reached, the polypyrrole tends to deposit more rapidly and uncontrollably onto the surface. It was found, however, that constant filtering of the polypyrrole dipping solution with 0.45 micron syringe filters effectively eliminates deposition onto the "non-negative" surfaces for approximately the first 45 minutes of dipping. This indicates that the critical size of the aggregates for deposition onto these surfaces is greater than 0.45 microns. In sharp contrast, filtering has no effect on the linear deposition observed with negative surfaces, indicating that the polypyrrole chains are indeed attracted to the surface at earlier stages of formation; that is, the delocalized positive charges of the polarons and bipolarons of nascent p-doped polypyrrole chains are attracted to the negative charges on the surface. In this way, the surface chemistry is key to the deposition characteristics of the in-situ polymerized polypyrrole.

Optical micrographs show that without filtering, polypyrrole precipitates with sizes on the order of 1-5 microns will begin to attach and sparsely dot the surface of the film as the active solution ages [2.12]. The low density of these precipitates do not appreciably influence the

macroscopic deposition, uniformity, or conductivity of the ultrathin films, but may adversely affect the performance of ultrathin film devices such as light-emitting diodes. Thus filtering between each polypyrrole dip is thus highly desirable when the microscopic level and size of defects within the film are of concern, e.g. in thin film electronic devices. For the self-assembly procedure, constant filtering practically ensures the microscopic quality if the film and also prevents the deposition onto surfaces other than the negatively charged surface. Self-assembly can thus be said to produce "device quality" ultrathin films of conducting polymers.

Atomic force microscopy (AFM) studies show that the surface of the ultrathin films produced both by "free growth" onto a negatively charged substrate or via layer-by-layer self-assembly with sulfonated polystyrene is highly uniform and resembles a plane of "mushroom caps" closely packed together to give an average RMS surface roughness of 20-40 Å [2.13]. The "caps" themselves are roughly 100 Å in diameter. This surface morphology suggests a nucleation and growth mechanism for the deposition of in-situ polymerized polypyrrole. As the initial "layers" are deposited, "mushroom caps" stack on top of each other and form a coherent film, such that by 3 layers or 15 minutes free growth, a fully continuous film is formed, characterized by essentially "bulk" conductivity. More work is needed, however, to confirm the origin of this type of morphology and the nucleation and growth mechanism. In any event, it is clear that control over the deposition of

in-situ polymerized polypyrrole is best achieved with negatively charged surfaces; self-assembly which takes advantage of this deposition onto negatively charged surfaces thus provides molecular-level control and results in extremely uniform thin films.

2.5 Conclusions

Thus we have developed a new method for processing p-doped conducting polymers into ultrathin films with exceptional uniformity, optical quality, and adhesion. And it was demonstrated that molecular self-assembly provides the level of control over the deposition process necessary to create complex, multicomponent heterostructures.

2.6 Chapter 2 References

2.1 M.F. Rubner, "Conjugated Polymeric Conductors" in Molecular Electronics, J. Ashwell (Ed.), Research Studies Press Ltd., John Wiley & Sons, **1992**, p.65.

2.2 S.T. Wellinghoff, "Electrically Conducting Polymers for Electronic Applications" in Polymers for Electronic Applications, J.H. Lai (Ed.) CRC Press, Boca Raton, FL, **1989**, p.93.

2.3 J.C. Scott, P.Pfluger, M.T. Krounbi, G.B. Streek, *Phys. Rev. B.*, **1983**, (28), 1240.

2.4 A. Epstein, Hnadbook of Conducting Polymers, T.A. Skotheim (Ed.), Marcel Dekker, New York, **1986**, 1041.

2.5 a) I.G. Austen and N.F. Mott, *Adv. Phys.*, **1969**, 18, 41.

b) D.L.Ellis, PhD Thesis, Dept. of Chemistry, Harvard University, 1993.

c) R.Singh, R.P.Tandon, V.S.Panwar, S.Chandra, *J.Appl.Phys.*, **69** (4), 1991, p.2504

d) M. Ferreira, J.H. Cheung, M.F. Rubner, *SPE Proceedings*, New Orleans, LA, USA (1993).

e) J.H. Cheung, Sc.D. Thesis, Dept. Mat'l Sci. and Engr., MIT, June 1993. and references therein.

2.6 a) Gregory, R.V.; Kimbrell, W.C.; Kuhn, H.H. *Synthetic Metals*, **1989**, *28*, C823.

b) Gregory, R.V.; Kimbrell, W.C.; Kuhn, H.H. *Journal of Coated Fabrics*, **1991**, *20*.

2.7 a) Pron, A.; Fabianowski, W.; Budrowski, C. *Synthetic Metals*, **1987**, *18*, 49.

b) Dubitsky, Y.A.; Zhubanov, B.A. *Synthetic Metals*, **1993**, *53*, 303.

c) Pouzet, S.; Bolay, N.E.; Richard, A.; Jousse, F. *Synthetic Metals*, **1993**, *55-57*, 1079-1084.

2.8 a) Liang, W.; Lei, J.; Martin, C.R. *Synthetic Metals*, **1992**, *52*, 227-239, and references therein.

b) Martin, C.R. *Adv. Mater.*, **1991**, *3*, 457-459

c) Cai, Z. and Martin, C.R. *J. Amer. Chem. Soc.*, **1989**, *111*, 4138.

2.9 a) R.B. Rosner and M.F. Rubner *Chemistry of Materials* **1994**, *6*, 581-586.

b) Hong, K.; Rosner, R.B.; Rubner, M.F. *Chemistry of Materials* **1990**, *2*, 82-88.

c) Shimidzu, T.; Iyoda, T.; Ando, M.; Ohtani, A.; Kaneko, T.; Honda, K. *Thin Solid Films* **1988**, *160*, 67.

2.10 Shimidzu, T.; Iyoda, T.; Segawa, H.; Fujitsuka, M. *Polymer Preprints*, **1994**, *35*, 1, 236.

2.11 Dr. Hans Kuhn of Milliken Corporation is gratefully acknowledged for useful discussions regarding the use of ASA to enhance the conductivity of PPY.

2.12 Optical microscopy work done by Osamu Onitsuka.

2.13 Atomic force microscopy done by Bruce Carvalho.

Chapter 3

Self-Assembled Poly(p-phenylene vinylene)

3.1 Introduction

Recently, the activity in the area of organic light-emitting devices has increased to a frenzied pace. The design and successful synthesis of new materials coupled with new fabrication techniques and device architecture have brought organic thin film light-emitting devices to the verge of commercialization. Although environmental stability and operational efficiency still stand to be improved, the highly desirable properties of organic materials, such as the tunability of emission color across the entire visible spectrum and their abundance and relatively low cost make them especially attractive as alternatives or substitutes for traditional semiconductor materials in these applications. Further, due to the nature of most organic films used in these applications, especially the films based on organic polymeric materials, light-emitting diodes can be fabricated on flexible substrates, a feat not easily done with

traditional semiconductor materials. Although many types of organic materials, including small organic molecules, organic dyes, and polymeric macromolecules have been investigated for their solid state luminescence properties, of the polymeric class of these materials, none has been more widely studied than poly(p-phenylene vinylene) (PPV) and its derivatives. Improvements in the material itself and in device fabrication parameters have led to respectable device characteristics such as operating lifetime, light output intensity, and operational efficiency. The most common thin film fabrication technique for organic polymeric materials is spin-coating from organic solvents. Spin-coating may also be combined with other methods such as vacuum evaporation of organic small molecules to create multislab devices with enhanced properties. Indeed, organic thin film devices have been reported with high light output intensities of up to 100,000 Cd/m^2 [3.1], with respectable operational lifetimes of 1000 hours [3.2a,b] to 10,000 hours [3.2c], with high electron to photon conversion efficiencies [3.3], and with the whole spectrum of visible colors from the deepest reds to the darkest blues [3.4] to white light [3.5].

As these materials and device configurations are pushed to their limits during operation, new methods of processing and new device configurations are constantly being sought in order to further optimize the device parameters such as efficiency, lifetime, emission color, and others. Towards this end, we have employed self-assembly as the thin film processing technique which affords us control over the deposition

of materials at the molecular level. As seen in the previous chapters, this level of control, not easily achieved by other thin film techniques, will give us the ability to explore the influence of the architecture of the heterostructure thin films on the overall, macroscopic properties of the devices based on them. Recently there have been numerous reports of significant enhancements in the device efficiency or maximum light output in devices which employ two or more layers of different materials [3.5c] or employ films of multiple materials blended together [3.5d,e,f]. Our ability to manipulate a wide assortment of electroactive organic materials via self-assembly allows us to explore these novel interactions between layers of material or among the materials in blend films in a much more systematic way. In addition, self-assembly opens up an entirely new thicknesses regime, smaller than can be reliably achieved by spin-coating, for exploration (between 100 Å to 500 Å) and allows us to control the molecular environment of these materials simply by changing the layer-by-layer architecture of the thin film. Indeed, as will be seen shortly, the placement of single layers of material, on the order of 10 Å each, has measurable influence on the macroscopic properties of the thin film and device.

Before we delve into the use of self-assembled thin films of poly(p-phenylene vinylene) in electroluminescent devices, we will present the experimental conditions and parameters used in this study to deposit extremely uniform, device quality thin films via self-assembly. Then we will present the analysis of the properties of these films such as

absorbance, photoluminescence, and thickness. The results of these studies suggest that the self-assembled heterostructure films do indeed behave differently from spin-coated films of pure PPV, as used by other groups. The self-assembled films are subsequently built into a simple electroluminescent device configuration which consists of the organic thin film sandwiched between an indium tin oxide (ITO) electrode and aluminum electrode. The quality of the self-assembled films has allowed us to fabricate successful devices with films as thin as 80 Å; the ability to access this thickness regime, allows us to access higher electric fields (external voltage divided by the thickness of the film between the electrodes). Benefits include higher light output levels and lower turn-on voltages in some cases. Finally, as a demonstration of the power of self-assembly, it will be shown that novel architectures (sequence of layers self-assembled together) can be fabricated to controllably enhance the device efficiency and maximum light output of our thin film light-emitting devices (LEDs).

3.2 Self-Assembly of Poly(phenylene vinylene)

In this section, we describe first the deposition of PPV with the self-assembly technique and the solution conditions required to achieve self-assembly. Then we focus on the additional steps and handling techniques necessary to make working light-emitting devices based on

these ultrathin films. And finally we present a battery of characterization techniques used to analyze the devices.

3.2.1 Self-Assembly Conditions and Procedure

The molecular self-assembly of poly(p-phenylene vinylene) was accomplished with the following solutions. An aqueous solution of the diethylsulfonium precursor to poly(p-phenylene vinylene) was used as provided by Dr. Bing Hsieh of Xerox Corporation [3.6a]. Figure 3.1 shows the chemical structure of this PPV precursor and other polymers used in the self-assembly of PPV. The solution of PPV precursor is clear to slightly yellow depending on the particular synthesis batch. The yellow color in the solution is due to the partial conversion of the precursor to the highly-colored, conjugated PPV. It is well known that the sulfonium precursor to PPV is inherently unstable and will gradually convert to the conjugated form upon aging at room temperature and upon exposure to small amounts of UV radiation and oxygen [3.7]. The solution is viscous and the pH of the solution was measured to be 2.5. The sulfonium group of the PPV precursor is positively charged, making the water soluble polymer a cationic polyelectrolyte. Therefore, it must be self-assembled with suitable polyanions.

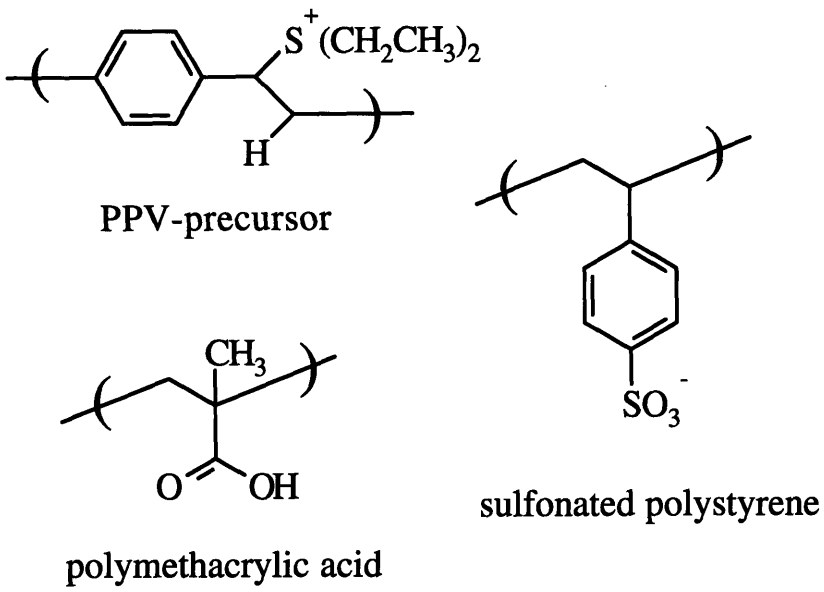

Figure 3.1 PPV-precursor and Counterpolymers

The solutions of polyanions used in the self-assembly of PPV are as follows. A solution of polyethyleneimine (PEI) was prepared by diluting a 30 vol% solution of PEI from Polysciences with ultrapure Millipore water. The final concentration was 0.1 vol% and the pH was 6.5. The solution of 0.01 M polymethacrylic acid (PMA) was prepared by dissolving the powder (50k molecular weight, 99% Aldrich) in Millipore water. The pH was adjusted to 4.5 by adding a few drops of hydrochloric acid. The solution of 0.01 M poly(styrene-4-sulfonate) (SPS) was prepared by dissolving the powder (75k molecular weight, 99.9% Aldrich) in Millipore water. The pH was adjusted to 4.5 by adding a few drops of hydrochloric acid. Sodium chloride was optionally added to adjust the ionic strength of both the PMA and SPS

solutions. It is generally known that increasing the ionic strength of the solutions of polymers results in thicker layers being deposited. The increased ionic strength allows the polyelectrolyte polymer to coil more tightly, giving a coiled configuration as opposed to an extended chain configuration. The addition of 1 M sodium chloride to the PMA solution results in a solution whose final pH is 3.5. The addition of 1 M sodium chloride to the SPS solution results in a pH of 3.9. No further adjustments were made to the solution parameters.

The solutions of other polyanions were 0.001 M poly(thiophene-3-acetic acid) (PTAA), 0.001 M sulfonated polyaniline (SPAn), 0.001 M poly(N,N'-bis(p,p'-oxydiphenylene)pyro-mellitimide) (PMDA-ODA), and 0.001 M sulfonated fullerenes (S-C_{60}) [3.8] in ultrapure Millipore water. The reported concentrations for all of the above polyions are based on the molecular weight of the repeat unit containing one charged functional group. These materials were used in the photoluminescence studies only, and have not been used in the fabrication of PPV devices.

The self-assembly of ultrathin films of PPV takes place as follows. PPV may be self-assembled onto glass microscope slides for optical measurements and thickness measurements and onto glass substrates patterned with 2 mm wide lines of indium tin oxide for measurements of the device characteristics.

The glass microscope slides are first cleaned by the following procedure. All are immersed in a 7:3 concentrated sulfuric acid/hydrogen peroxide solution for one hour and rinsed thoroughly with ultrapure Millipore water. Then they are immersed in a 1:1:5 ammonium hydroxide/hydrogen peroxide/water solution for one hour and rinsed with ultrapure water. This removes all organic impurities from the surface and renders the surface hydrophilic. These cleaned slides are typically stored under fresh, ultrapure water to preserve the hydrophilic nature of the surface. These slides may be used as is in the self-assembly procedure, but an additional step may be added to anchor charges onto the surface by silane chemistry.

The slides were subjected to the treatments with N-2-aminoethyl-3-aminopropyl-trimethoxysilane (Huls America, Inc.) in toluene for 12 hours. The details of this treatment were outlined in Section 2.2.1. A single layer of sulfonated polystyrene was added to the surface to render it negative. The positively charged PPV precursor could then be self-assembled directly onto the surface. Also, instead of this lengthy silanization procedure, another surface pre-treatment step may be used to condition the surface of the substrate prior to self-assembly of PPV. The glass slides are cleaned in a 7:3 concentrated sulfuric acid/hydrogen peroxide solution and 1:1:5 ammonium hydroxide/hydrogen peroxide/water solution for one hour each as above. Then they are dipped into the PEI solution for 15 minutes. Although no covalent bonds are formed with the surface, the PEI layer has been shown to

enhance the adhesion of the subsequent, self-assembled layers to the surface. In the case of self-assembled PPV layers, after thermal conversion, the ultrathin films are so adherent that they can only be removed from the surface by scraping with a razor blade. After the positively charged PEI layer, a layer of polyanion must be used before the PPV precursor can be deposited.

After either of these substrate pre-treatment steps, the substrate is ready to be used in the self-assembly of PPV. The substrate is dipped into the solution containing the positively charged sulfonium precursor of PPV for 10 minutes, vigorously rinsed with ultrapure Millipore water, and dried in a stream of filtered, compressed air. Then it is dipped into the solution containing the polyanion and rinsed and dried in the same manner. This sequence of alternating dips into the PPV-p and the polyanion is repeated until the desired number of bilayers (pair of polyanion and PPV-p layers) are built up. The sample is then dried overnight with fresh desiccant in a nitrogen atmosphere and then dried overnight under dynamic vacuum (100 mTorr). Then, without breaking vacuum, the thermal conversion of the PPV-p to the conjugated, light-emitting form of PPV is effected by heating the samples from room temperature to 180 °C, 210 °C, or 250 °C, holding the temperature at that plateau for 2, 4, or 11 hours, and then allowing the samples to cool back down to room temperature over another 4 hour period, all under dynamic vacuum [3.6b,c]. The different results obtained for the various combinations of conversion temperatures and times will be discussed

later. In general longer conversion times were rarely used since we have shown that higher photoluminescence intensities were not achieved in sample films on glass. However, the utility of longer conversion times will be discussed later with respect to the results of the device quality tests; longer conversion times seem to produce more stable devices with longer operational lifetimes. Also, higher temperatures were usually not used in order to prevent the unwanted side reactions which form carbonyl groups along the backbone of the PPV. There is mounting evidence that carbonyl groups quench the luminescence of PPV [3.9a,b]. A complete discussion of the significance and influence of the conversion process on the quality of the film and the device characteristics follows in the results and discussion section below. Once the films of PPV are converted to their final, light-emitting form on glass substrates, they can be tested in the absorbance, photoluminescence, and thickness experiments.

3.2.2 Automatic Dipper Film Fabrication

We have also recently employed an automated method of fabricating self-assembled films of PPV. Using a programmable slide stainer, we have fabricated thin films with large numbers of bilayers. The unit can be programmed to dip the substrates (glass or patterned ITO) into a series of up to twelve 1500 milliliter "bins" of solutions. In this way, simple as well as complex multilayer heterostructure films can

be fabricated. The films produced by the automatic dipper are of high quality and the characteristic linear deposition is present. By tracing the optical absorbance or the thickness of the converted PPV films as a function of the number of bilayers deposited, we can plot straight lines. This process is accomplished by placing ten or more substrates with the same surface treatments into the slide holder. These slides are then dipped into each bin according to the sequence of the program. Included in this sequence are bins of pure water in which the slides are dipped and agitated. These rinse bins take the place of the hand rinsing with a stream of ultrapure water. The water of the rinse bins are changed between runs; each run builds 5 - 6 complete bilayers of PPV film.

The solutions used in the automatic dipper are as follows. The viscous PPV solution must be diluted to 1% or 2% of the original concentration by adding it to the appropriate volume of Millipore water. It should be noted that the viscous PPV is added to the water rather than the water to the PPV, which tends to result in clumpy solutions, requiring long times of stirring to dissolve completely. The initial experiments also used diluted polymethacrylic acid (PMA) and sulfonated polystyrene (SPS) solutions. These were made simply by diluting the polyanion solutions, described above in the experimental section 3.2.1, to 10% of the original concentration by adding ultrapure water. The resulting concentrations were on the order of 0.001 M for both the SPS and PMA and the sodium chloride concentration was 0.1 M; the pH of both the PMA and SPS solutions was about 4.5. These

particular solutions produced PPV films whose thicknesses were markedly smaller than films self-assembled with solutions of the original concentration. Therefore, to build up thicker films, the higher, original concentrations were used instead. However, lowering the salt concentration to 0.1 M (rather than 1.0 M) proved to result in fewer instances of residue left on the surfaces of the films. The absence of the vigorous rinsing by hand and drying by air gun allowed droplets of solution to remain in the surface of the film; when these droplets evaporated upon standing in air, residue was seen on the films. The use of 0.1 M salt in the solutions resulted in only slightly smaller thicknesses per bilayer but virtually eliminated the problem of residue. Therefore, for all the automatically dipped samples, the concentration of the polyanion was 0.01 M and the salt concentration was 0.1 M.

The exact sequence of steps for the automatic dipper self-assembly included a 10 minute dip into the dilute PPV solution followed by 2 one minute agitated dips into 2 "rinse" bins of pure water and a 3 minute agitated dip into a "flow-through" rinse bin in which the water is constantly replaced with fresh water. Then the polyanion dip of 10 minutes is used, again followed by three rinse steps. By using these dilute solutions, a very linear deposition characteristic was achieved, indicating that a reproducible amount of material is being deposited with each dip. After a certain number of dips, typically after each run of 5 - 6 bilayers, individual substrates are removed from the slide holder, dried and labeled, and stored in ambient atmosphere under

aluminum foil. Aluminum foil was used to protect the samples from exposure to ultraviolet radiation which would serve to begin the conversion process. The other substrates are allowed to continue to dip and removed after a specified number of bilayers has been deposited. In this way, when the process is finished, there was a series of substrates, each with a different number of bilayers of PPV film. This series of substrates were then simultaneously subjected to the thermal conversion procedure. These were held in a glass coplin (staining dish) with regular glass slides as spacers to hold the sample slides in a vertical position such that neither of the faces touch any surface.

3.2.3 Fabrication of PPV Light-Emitting Devices

Having described the self-assembly of PPV with various polyanions onto simple glass substrates, it is now appropriate to describe the full fabrication of PPV ultrathin film, light-emitting devices.

The process begins with the cleaning of the substrates which are patterned with 2 millimeter wide and 2000 Å thick lines of indium tin oxide (ITO). We receive these substrates from TDK, Japan. The two point resistance of each ITO line is around 10 Ohms. It is important to check the line to line resistance as we have found that in certain pieces of substrate, there is incomplete etching between the lines. This leads to "cross talk" in the subsequent operation of the devices in which pixels

that are not addressed still light up. This will introduce errors into the current-voltage and light-voltage characteristics of the device. Therefore, only pieces of substrate which have large two-point resistances between the lines (greater than 100 MΩ) should be used. These substrates are scored with a diamond cutter and broken into pieces of appropriate size. Typically, each sample is 1 inch by 1 inch, with four ITO lines and room for four perpendicular aluminum lines. The samples must be cleaned before they can be used in the self-assembly procedure; however, the previous methods of strong acid and strong base cleaning are not applicable here as strong acids destroy and etch the ITO away. Therefore these samples (cut pieces of substrates) are cleaned in a staining dish (coplin) in a 1:3 Lysol® (generic household cleaner):Millipore water solution and ultrasounded for 30 minutes. Then the cleaning solution is changed and replaced with fresh, ultrapure water. The samples are then put into the ultrasound again with the fresh water. This pure water rinsing step is repeated two more times. And finally, the water is replaced with acetone. And again the samples are ultrasounded in the acetone. This renders the surface free from any organic impurities and thus hydrophilic. These substrates are used immediately or stored under ultrapure water to maintain the hydrophilicity of the surface.

The cleaned ITO samples are then pre-treated, as with the glass substrates, with a 15 minute dip into the polyethyleneimine (PEI) solution, rinsed with ultrapure water, and dried with an air gun. Then a

layer of polyanion is self-assembled onto the surface and the self-assembly of PPV continues as above. The choice of the polyanion depends on the heterostructure that is to be built. For example, if a film of PPV and PMA is to be built, the first polyanionic layer after the PEI would be PMA. The PPV films are built up to the desired number of layers and placed in the oven for drying. The thermal conversion of the PPV precursor takes place exactly as described above. The resultant PPV films are yellow in color and transparent.

It should be noted that the thermal conversion of PPV is critical in determining the resultant absorbance, photoluminescence, and device properties. It was found by other groups that high temperature conversion at around 300 °C would lead to significant carbonyl formation along the polymer backbone [3.9a,b] from the reaction of PPV with any available oxygen or water. The extent of this unwanted side reaction depended strongly on the atmosphere to which the samples are exposed during thermal conversion. It was found that a reducing atmosphere of forming gas (5 - 10 % hydrogen in nitrogen) resulted in the lowest concentration of carbonyls compared to inert atmospheres of nitrogen gas, argon gas, or high vacuum. These carbonyls not only break up the conjugation but also act as efficient luminescence quenchers [3.9a,b]. We have chosen a typical conversion temperature of 210 °C to lessen these problems. Although it takes significantly longer to achieve the conversion of the PPV, the results for our ultrathin self-assembled films are remarkable. We have found that by using different

conversion times, from as little as 2 hours at the plateau temperature to as much as 24 hours at the plateau, the absorbance and the photoluminescence characteristics of the PPV film do not change appreciably. However, there is a noticeable improvement in the quality of the devices upon using longer conversion times. It is currently thought that the extra "annealing" at the conversion plateau temperature contributes to densifying the film, driving out more of the impurities such as the eliminated sulfonium groups and gaseous hydrochloric acid, and further removing the water molecules that may be tenaciously bound in the film. These water molecules have been shown by others to lead to the undesirable carbonyl formation. Therefore, the reduction of the water content, especially from films made using the aqueous self-assembly process, is desirable. It is known however, that the thermal conversion conditions employed here do not result in full conversion of the PPV [3.9c]. Further discussions about the utility of the thermal conversion process and supporting data and graphs will be presented in the results and discussion sections to follow.

The samples are then taken out into the air to be prepared for the evaporation of aluminum top electrodes. The samples are placed into a flat holder of glass slides and a stainless steel mask with 2 mm wide lines cut into it is taped down such that the aluminum lines would be perpendicular to the ITO lines beneath the PPV film. The sample is then brought into the thermal aluminum evaporator. The chamber is evacuated until a pressure of 5×10^{-6} Torr is achieved. The aluminum

is evaporated at a rate of 200 Å per second onto the PPV films by holding the filament voltage at 110 V for 7 seconds. The resultant thickness of the aluminum lines is typically between 1500 Å and 2000 Å. It should be noted that our procedure of aluminization deposits the aluminum top electrodes at rates greater that 200 Å per second, in contrast to the techniques of other groups which deposit at rates around 1 - 5 Å per second. New methods for accomplishing the deposition of the aluminum electrodes are being investigated by our group to slow the rate of deposition. It is believed that slower deposition rates would lead to less damage to the polymer film and a smoother interface between the metal and the polymer. As will be seen shortly, the interface between the polymer and the electrodes is critical to the performance of the device. The samples are then removed from the evaporation chamber and placed under dynamic vacuum of 100 mTorr until they are ready to be tested.

3.3 Characterization of PPV Light-Emitting Devices

The thin film light-emitting devices described above are then characterized by a battery of techniques. In some cases, when only samples on ITO are available, the sequence of characterization tests must begin with the current-voltage curves, done in a nitrogen glove

box. After these tests are completed, the samples may be removed into room air and characterized optically by absorbance and photoluminescence. In the cases where duplicate samples are available on glass slides, the optical characterization can be done on the samples on glass while the ITO samples are being characterized electrically. The facility of the automated dipping procedure has allowed us to make larger number of samples than by hand and thus has given us the ability to fabricate duplicate samples on glass for all of the samples on ITO. Each of these characterization techniques is described in detail below.

3.3.1 Optical and Thickness Characterization

Once converted, the optical measurements were performed. After thermal conversion, the films are typically allowed to cool in the oven without breaking vacuum and then allowed to stay under vacuum overnight. Then, with as little exposure to air as possible, the photoluminescence is taken with the SPEX312 scanning fluorimeter. The excitation wavelength was chosen to be as close to the peak in the absorbance spectra as possible. As a compromise between the PPV/SPS films and the PPV/PMA films a single excitation wavelength of 360 nm was chosen. The spectra were scanned from 380 nm to 680 nm, with a 0.25 second integration time. A point was taken every two nanometers and the output was chosen to be signal/reference. The sample is loaded into the sample holder and the fluorescence is measured in "front face" mode. In this mode, the excitation beam strikes the sample nearly

perpendicular to the surface of the substrate. The resulting photoluminescence is collected by mirrors also placed at nearly perpendicular to the substrate. Since our excitation wavelength is 360 nm, the range of emission wavelengths that are scanned range from 380 nm to 680 nm. In this way, the reflection of the excitation beam and its doublet at around 720 nm are not collected in the emission spectra.

It is also important to note that, by exciting the PPV in ambient air, the luminescence of the area that is scanned is degraded even after the short time it takes to complete the scan. This is due to the reaction of the PPV vinyl bonds with the available oxygen in the air, catalyzed by the ultraviolet radiation. It is clearly visible that the area that was scanned has a diminished photoluminescence compared to the immediately adjacent areas that were not scanned. Therefore, if multiple scans are to be taken on one sample, the sample must be carefully repositioned after each scan such that a new area is exposed to the excitation beam with each scan. In this way, highly reproducible results were obtained for the various areas of the PPV sample film, attesting to the uniformity and quality of the film that was deposited using the self-assembly technique.

The slit settings on the fluorimeter were minimized in order to enhance the resolution of the spectra to reveal any structure in the photoluminescence peaks. The slits were typically set to 1.0 mm on all four slits, two for the source and two for the detector. For samples with

low fluorescence intensity, the slits are opened to 2.0 mm for the slits on the source and 3.0 mm for both slits of the detector. The larger slits will result in spectra with non-zero endpoints near 380 nm and near 680 nm due to the inclusion of the tails of the excitation peak and its doublet at 720 nm.

The absorbance of the film is measured next. In a similar manner to that used for the conducting polymer films, a circular area of one square centimeter is scanned. The absorbance spectra is the result of the signal minus the reference, with background correction. The spectra were scanned in integration mode with 16 integrations each. In the case of PPV films on patterned ITO substrates, a special "mask" was used. This mask consisted of a 2 x 2 mm square hole in the middle of a piece of black felt paper. This was placed in front of the aperture to the detector. The sample was aligned such that the PPV film on a ITO strip or on an area of glass was in front of this square hole. The reference was done by placing a patterned ITO substrate with no PPV film in the same position in front of the detector. In this way the absorbance of the PPV film on the glass or on the ITO portions of the substrate were determined. Finally, it should be noted that it is important that the absorbance be taken after the photoluminescence measurements. This order was chosen after it was shown that the UV-visible lamp used in the absorbance measurements degrades the PPV in air and thus the photoluminescence after only a relatively short exposure time.

Therefore, the photoluminescence spectra should be taken first to reduce the variability introduced by experimental conditions.

The thicknesses of the self-assembled PPV films were performed with a Sloan Dektak in the manner described above. The profilometer uses a pressure-sensitive stylus to determine the surface features of any substrate. The stylus is held at a constant pressure and drawn across a surface; it follows and records the contours of the surface. For the PPV films, as with other organic thin films, a razor blade is used to score the surface with lines. It should be noted that the films of PPV are dense, hard, and very adherent to the substrate, making scratching difficult. In the case of PPV, a roughly square area is scratched off and the profilometer is scanned across the four edges of the square to obtain a step height. The average of more than ten such points is used to calculate the thickness of the film. The converted PPV film deposited on the ITO lines has been observed to be even more adherent, such that even hard scratching only slowly removes the film.

It should be noted that the stylus pressure and the diameter of the stylus head are important parameters that need to be carefully controlled in order to get reproducible results in the measurement of thickness in ultrathin organic films. In other work by our group, it has been shown that there is an optimal stylus pressure with which the measurements should be taken. If the stylus pressure is too low, the signal to noise ratio is bad due to "floating" of the stylus. If the stylus

pressure is too high, the stylus scratches into the film causing anomalously low readings. Furthermore, the debris accumulated on the head of the stylus may drop off to create large anomalous "bumps" while scanning the surface. For the PPV films, since they are "hard" and dense relative to the other polymer films, a stylus pressure of 12 mg can be used to measure the surface of the film. Typically, pressures of 5 mg are used for the other self-assembled polymer thin films. Finally, the Dektak profilometer was used to measure films of greater than 200 Å with confidence. The sensitivity and signal to noise ratio for films of 100 Å or less is too low for the Dektak to measure reliably.

3.3.2 Current-Voltage and Light-Voltage Curves

The sample devices of PPV films sandwiched between ITO and aluminum electrodes are now ready to be tested. Each sample has four ITO lines and four aluminum lines, the intersections of which give 16 "pixels" or active devices that can be addressed individually by hooking up the appropriate leads to the power source.

Before the samples can be analyzed, they need to be mounted onto "L"-shaped mounts which allow gold wire leads to be secured to one of the ends of each electrode line. These gold wires are taped down in a square "S" shape to prevent slippage and are electrically contacted to the ITO or aluminum lines by standard silver paste. Alligator clips may

then be used to connect the power source to the appropriate leads to address the selected pixel. Once the sample is mounted, it is placed in a dark box which contains the silicon photodiode (Model 1830-C from Newport Instruments) and wire leads from the programmable constant voltage source (Model 636 from Keithley). The active cell is placed directly above the photodiode roughly 1 cm above the surface of the diode. The photodiode itself is masked off with black paper; a 3 mm by 3 mm hole was cut in the middle to allow the light from only the active cell to stimulate the photodiode. The wire leads from the power source are connected to the appropriate gold wire leads of the sample and the box is closed and sealed.

The current-voltage and light-voltage curves are taken automatically by a custom LabView program written specifically for this task. The program runs on a PowerMac and controls three instruments: 1) the Keithley programmable voltage source, 2) the Hewlett-Packard digital multimeter, and 3) the Newport Instruments 1830-C silicon photodiode optical power meter. In essence the LabView program sends a series of commands to ramp the voltage from zero to a designated maximum voltage and reads the current and light intensity from the multimeter and optical power meter, respectively. Figure 3.3 displays the user interface of this program. The user can input the maximum forward bias, the maximum reverse bias, the step voltage, the

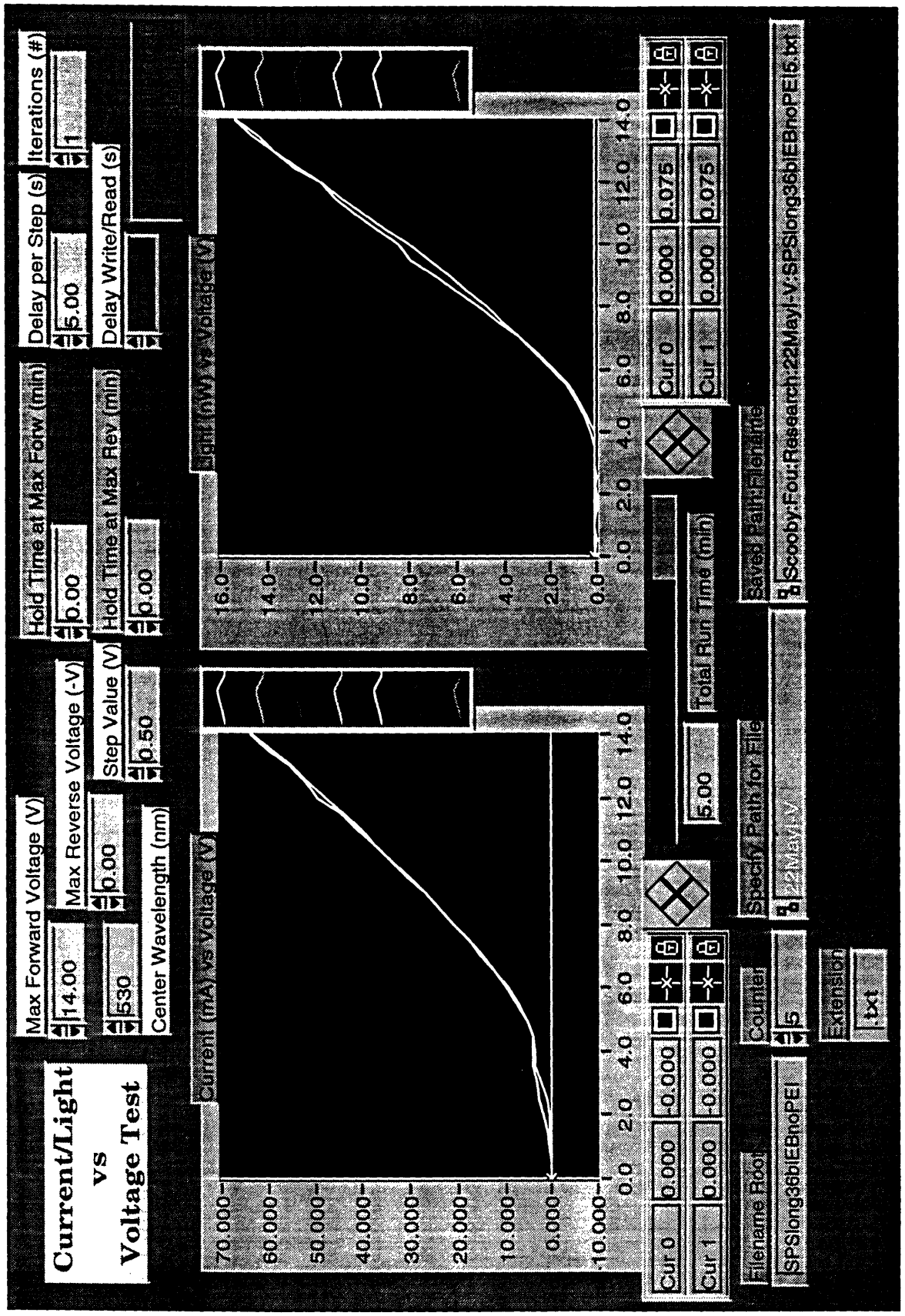

-V/Light Main Panel C.vi
)/22/95 2:53 PM

Figure 3.2 LabView Current/Light vs Voltage Interface

delay per step, the delay "write/read," and the center wavelength. The program begins by zeroing the optical power meter to account for any stray light, setting its center wavelength to the specified wavelength (this determines the wavelength range of sensitivity of the power meter), and addressing the two other instruments. Then the program ramps the voltage from zero up to the maximum forward bias in increments of the step voltage. The delay per step determines the time between each of these steps in voltage. And the "delay write/read" is the time between the command to change the voltage and the time when the current and light are read back to the computer. This was found to be useful since there is a finite amount of time required before the current and light intensity reach equilibrium values after a new voltage is set. Therefore, the new voltage is sent by the computer and the current and light are read back after the specified "delay write/read" interval. After the maximum forward bias has been reached, the user can specify a "hold time" at this maximum voltage. It has been found that there may be some annealing of the polymer film due to joule heating during the operation of the device. This annealing has been observed to improve the uniformity of the light emission and also slightly improve the intensity of the light, initially. However, if the device is held at this maximum voltage for longer times, the typical degradation in light and current commences, as evidenced by the "lifetime" tests, discussed below. After this "hold" time at maximum forward bias, if any, the computer ramps the voltage back down to zero with the same steps in voltage and delay per step. Then, if the user specifies a maximum

negative bias, the program proceeds to ramp the voltage down from zero to the maximum negative bias with the same voltage steps and delay per step. Again, there is the option to specify a "hold" time at maximum negative bias. After this, the program ramps the voltage back up to zero and one iteration is completed. If only the forward or only the reverse bias regimes are to be tested, the maximum reverse bias and the maximum forward bias are set to zero respectively.

The result of the program are two graphs shown on screen. The first is a current versus voltage plot and the second is a light intensity versus voltage plot. The current-voltage plot reports the currents in milliamps (mA). The conversion to current density simply requires dividing this number by 4 square millimeters, the area of each "pixel." The light intensity is reported in nanowatts (nW). The user can specify a filename root, a counter, an extension, and a path for saving the data. The counter is used when a series of iterations (or repetitions) are performed on the same active device. The counter is automatically incremented as each iteration is completed; the complete filename saved to disk consists of the filename root plus the counter and the extension. The data is saved as three columns of text separated by tabs. The first column is the voltage, the second is the current in mA, and the third is the light in nW. The data is saved after each iteration is run to completion; therefore, if any run is aborted before completion, the data is not saved. The data can still be recovered by moving the cursor of each graph on screen and reading off the points individually.

Each active pixel is scanned multiple times with the following protocol. The cell is scanned in forward bias only with an initial maximum forward bias set at a moderate number depending on the thickness of the particular sample, typically 6 volts for a 20 bilayer (≈ 300 Å) sample. Then the maximum voltage is increased with each iteration in the forward bias only. The voltage is increased until both the current and light curves show little hysteresis or until the cell "burns out." The mechanisms of "burn out" or breakdown are discussed below. When the device is first turned on, a hysteresis in the current and light curves may be seen in which the current and light values at each voltage value for the scan upward may not align with the values on the scan back down to zero. If the values of the light in the downward scan are greater than the values in the forward scan, then the device is thought to have been annealed and the light output improved. When this happens, we can go to a higher maximum voltage setting and scan the devices again. This process is repeated until a maximum voltage is reached at which the current and light versus voltage curves show little or no hysteresis in the upward and downward scans. At this voltage, several more iterations are taken so that they can be averaged together and presented as the representative current and light curves for the particular sample. After these iterations, if the device is still active, that is, not burned out, the maximum voltage is pushed to higher values in one volt increments. The device is scanned until a maximum voltage is reached that breaks down the device. This maximum voltage at which

the devices can be operated depends on the quality of the aluminum electrode and its thickness. It was found that thicker aluminum electrodes allow the device to be operated at higher voltages. This is due to the fact that one of the typical breakdown mechanism is the sparking and evaporation of the aluminum electrode at high voltages. Once the aluminum electrode is vaporized, no more current can flow through the device, rendering it useless.

After the forward bias scans, the same procedure is done for only the reverse bias on a new cell (pixel). Again, the cell is scanned until reproducible current and light plots with very little hysteresis are obtained. After the reproducible scans are obtained in both the forward and reverse bias regimes separately, a new cell is tested by scanning both the forward and reverse bias in each iteration. It was found that by scanning in this way, the cell is broken down sooner than it would be if the forward and reverse bias regimes were scanned separately. Furthermore, there are anomalous features in the current curves that are not present by scanning each regime separately.

3.3.3 Device Lifetime Testing

After the device current-voltage and light-voltage curves are obtained with the previous LabView program, additional information on the lifetime of these devices in a nitrogen environment are obtained

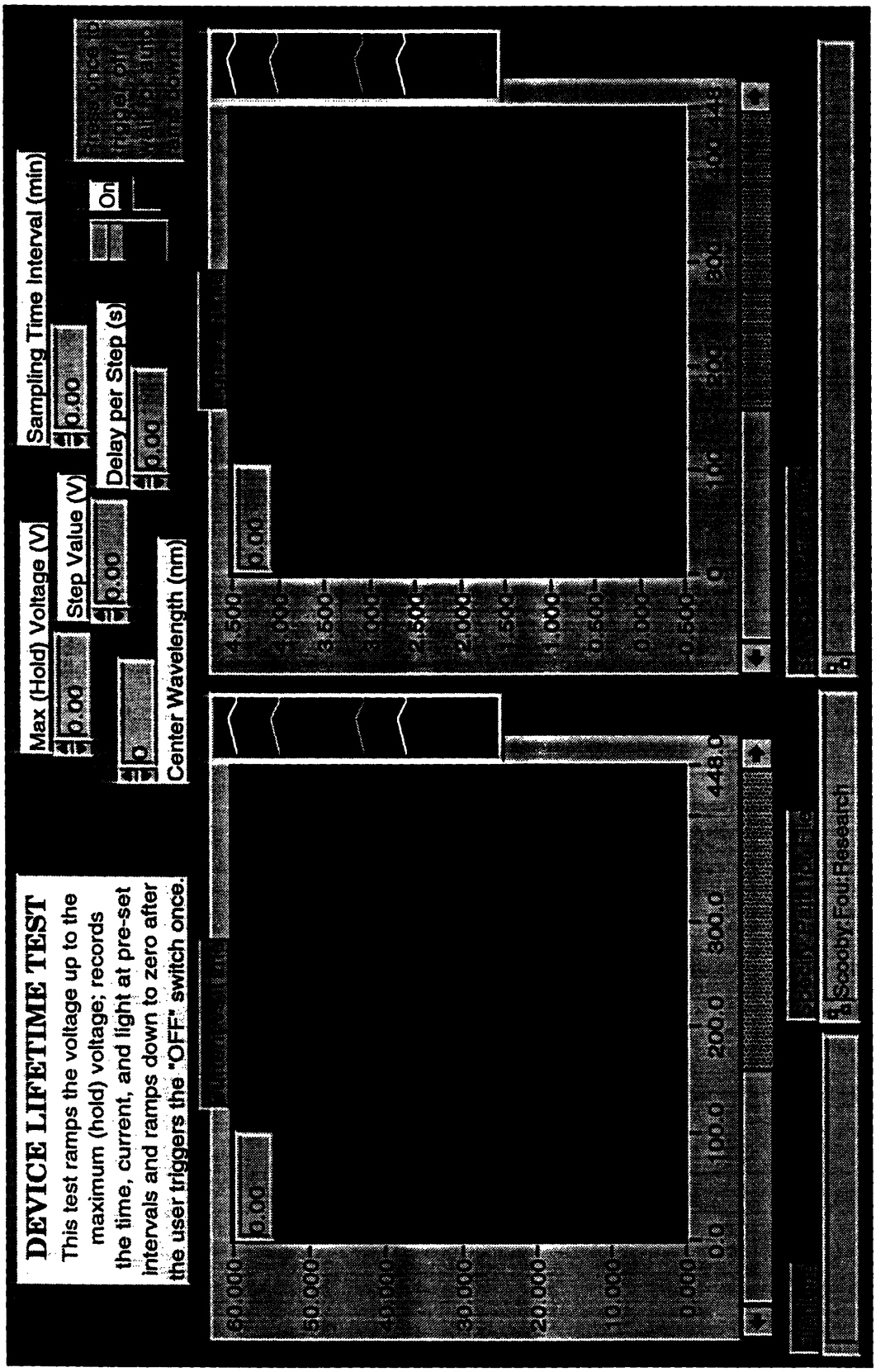

Figure 3.3 LabView Device Lifetime Testing Program

by running another custom LabView program. Again, the computer controls the three instruments: power source, optical power meter, and digital multimeter. The lifetime testing program provides the following features (see Figure 3.3). The user may enter the maximum (hold) voltage at which the device will be held during the lifetime test, the step value to be used during the ramp-up to the maximum voltage, and the delay per step. The center wavelength is also set in order to determine the sensitivity of the optical power meter to the electroluminescence wavelength of the device. Finally, the "sampling time interval" determines the period of time between each measurement of current and light. The data is saved after each point is taken and is saved as three columns of text separated by tabs. The first column is the time, in minutes, at which the current and light values are read. The second column is the value of the current, in milliamps, at the specified time. And the third column is the light intensity, in nanowatts.

3.3.4 Electroluminescence Spectra

The electroluminescence of the PPV samples was taken in ambient air with the Oriel Multispec. The following measurement procedure was used. A light-tight box was made by sealing the edges of a regular cardboard box. A fiber optic cable was inserted into the bottom of the box such that the aperture to the fiber optic cable was pointing up into the box and raised 0.75 inches from the bottom of the box. The sample

of PPV devices was positioned such that the active cell was directly on top of the aperture of the fiber optic cable. The sample was secured by tape onto mounts that were flush in height with the top of the fiber optic cable. Then the wire leads from the power source were inserted into the box and the openings sealed off with black electrical tape. The leads were connected to appropriately address the active cell. The box was closed and sealed with black electrical tape. A background was taken with the device off, to account for any stray light. The device was turned on to a moderate voltage and the light collected by a 30 to 60 second integration. The aperture of the Oriel detector was removed to allow the maximum amount of light into the detector. This was done with the knowledge that resolution in the spectra would be diminished. But since typical features of peaks in polymer absorbance spectra are broad, this method was deemed acceptable for determining the electroluminescence peak positions. The voltage was adjusted upward such that the device became successively brighter. The electroluminescence spectra were recorded for the highest possible voltage before breakdown of the device. These spectra gave the best signal to noise ratio.

3.3.5 Efficiency Calculations and Other Graphs

As the last section in this experimental procedures section, we present here comments on the calculations used in the analyses of the devices.

One important calculation is the efficiency of the self-assembled PPV devices. The efficiency of the devices was calculated without correction for losses and waveguiding due to the ITO and the glass substrate. The efficiency is therefore reported as the external, detectable yield of photons per electron. This calculation is simplistic but straightforward and no attempt was made to calculate or estimate the internal quantum efficiency other than using "correction factors" widely published in the literature for converting between external and internal quantum efficiencies [3.10]. The flux of photons (photons per second) was obtained by dividing the power (in Joules per second) with the average energy of the photons being emitted. This average energy was based on the center wavelength chosen for the maximum sensitivity of the optical power meter. Typically, this is 530 nm. Thus, assuming a symmetric distribution of photon energies around the energy of photons of this wavelength, we calculate the number of photons per second by dividing the raw light power output reading with the energy per photon. In a similar manner, we calculate the number of electrons per second by dividing the current (in coulombs per second) by the charge of each electron (in coulombs per electron). Once these two numbers are

obtained, we take the ratio of photon flux over electron flux to give photons per electron. This gives us a standard estimate of the efficiency of the device.

Other graphs that were generated include plots of light output versus current density. The linear characteristic in both forward and reverse bias indicate a constant efficiency at all levels of current measured; it should be noted however, that if the device is operated at high voltage levels the degradation of the device causes the light versus current curve to become sublinear. Furthermore, the difference in slopes between the forward and reverse bias curves qualitatively indicate a difference in the efficiency in the two regimes. The significance of this and the mechanisms responsible for this behavior will be discussed below, when models for the operation of thin film devices are proposed and supported by our experimental evidence.

Other figures of merit were used to characterize the films used in the thin film devices. For example, a figure of merit called absorbance per bilayer was calculated by taking the value of the absorbance at the maximum in the PPV absorbance spectra and dividing by the number of bilayers in that particular sample. This figure gives an indication of the amount of PPV present in the film, since most of the polyanions used, the SPS and PMA in particular, are colorless and do not absorb. The absorbance is due solely to the PPV incorporated into the film. The larger the absorbance per bilayer, the greater the amount of PPV

incorporated into the film per dip. Another figure of merit is the absorbance per thickness. This is calculated by dividing the absorbance by the thickness of the particular film. This figure provides a gauge of the fraction of PPV in a bilayer, again because the other components do not absorb. The larger the absorbance per thickness, the larger the fraction of PPV in each bilayer and the smaller the fraction of colorless polyanion. These two figures of merit taken together provide a relative measure of the PPV content in the thin films. The importance of this will become apparent later in the discussions of device performance as related to the film architecture and PPV content.

We can also use the photoluminescence per bilayer or photoluminescence per thickness in a similar manner. Finally, we define another figure of merit as the photoluminescence per absorbance. This is done by dividing the value of the intensity at the maximum of the photoluminescence peak by the value of the absorbance at the maximum of the absorbance peak. The units are meaningless. This figure gives an indication of the conversion efficiency. That is, as mentioned before, the conversion process is sensitive to parameters such as the temperature, length of time, and atmosphere. Since the unconverted PPV-precursor is colorless and the converted PPV is yellow in color, the intensity of the absorbance of the film after thermal conversion indicates the degree of conversion or the amount of converted, light-emitting PPV. However, the photoluminescence may or may not scale directly with the absorbance; that is, the photoluminescence may not increase linearly

with the absorbance which indicates the amount of converted PPV. The presence of quenching sites such as carbonyl groups will result in a lower photoluminescence for a given absorbance level. Therefore, although this number does not give an absolute measure of the amount of PPV in the film and the efficiency of the photoluminescence, it can be used in a relative comparison between different films. A larger photoluminescence per absorbance number indicates a film with less quenching sites and therefore a higher photoluminescence efficiency for a given amount of converted PPV.

3.4 Results and Discussion

3.4.1 Absorbance and Photoluminescence Studies

Before the very first devices were fabricated, the properties of the self-assembled poly(p-phenylene vinylene) films had to be studied. As mentioned above, the absorbance, photoluminescence, and thickness of the films of each of the self-assembled systems were measured. Of particular interest was the photoluminescence properties of the films. Figure 3.4 shows the characteristics of a series of self-assembled films made with the automatic dipper. The graph shows the overlaid

absorbance spectra for PPV self-assembled with the polyanion polymethacrylic acid (PMA). As can be clearly seen, the absorbance of the film increases with increasing number of bilayers deposited. In the smaller graph next to it, the maximum absorbance for each of the curves is plotted against the number of bilayers. There is a linear correspondence, as with all of our other self-assembly systems. In Figure 3.5, which shows the overlaid photoluminescence spectra for the same set of samples, the same trend exists. Finally, Figure 3.6 shows the linear build up of the thickness of the PPV/PMA film as measured by profilometry. It should be noted that each point represents a different sample, removed from the automatic dipping sequence after a specific number of bilayers were deposited. This is important because it clearly

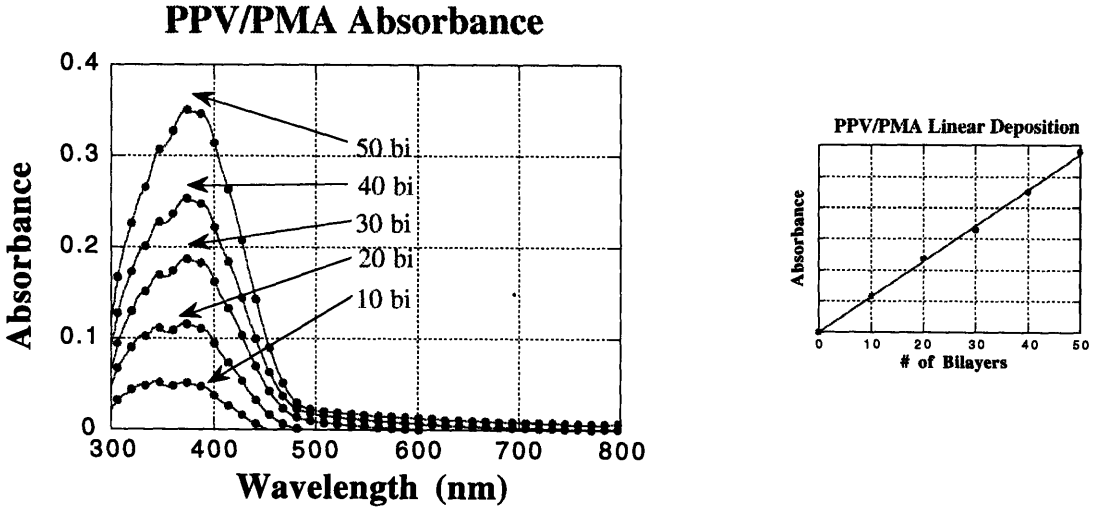

Figure 3.4 Overlaid Absorbance Spectra of PPV/PMA Films

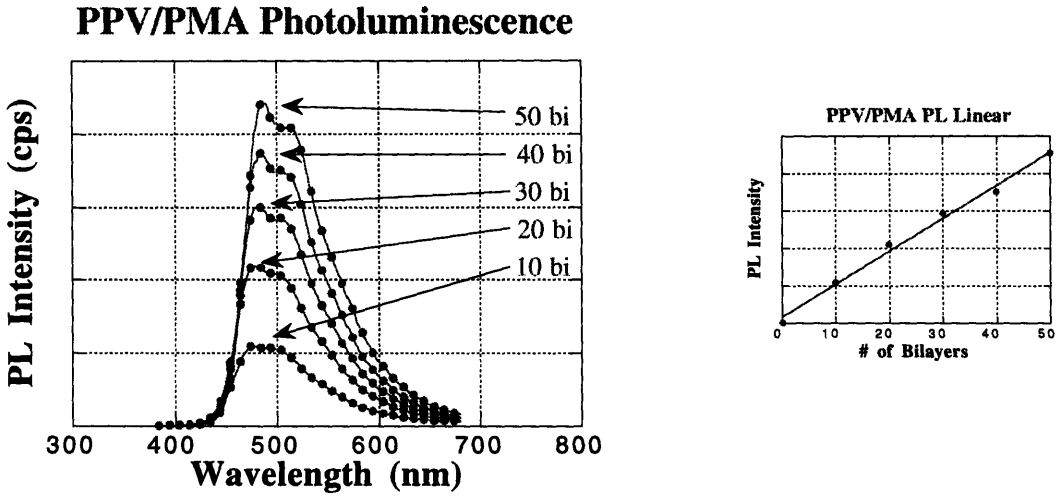

Figure 3.5 Overlaid Photoluminescence Spectra of PPV/PMA

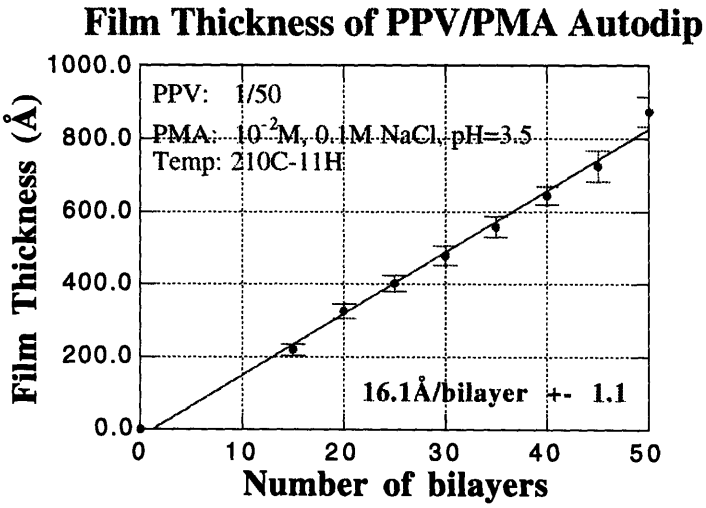

Figure 3.6 Dektak Profilometry of the Thickness of the PPV/PMA Series of Self-Assembled Films

demonstrates that self-assembly is remarkably reproducible and consistent. If the same solution conditions and dip times are used, the same amount of material will be deposited. In this case, the PPV/PMA self-assembled binary (two component) system gives a bilayer thickness of 16 Å. The 50 bilayer film is therefore 800 Å thick. A similar series of samples was made for the PPV/SPS binary system. Figure 3.7 shows the overlay of the absorbance spectra for the PPV/SPS samples; Figure 3.8 shows the corresponding photoluminescence spectra. And Figure 3.9 shows the linear build up of the film thickness as monitored by Dektak profilometry. For the solution conditions and automatic dipper sequence outlined above, the PPV/SPS system gave a bilayer thickness of 8 Å. The 50 bilayer film was thus 400 Å thick. What is interesting to note in the PPV/SPS system is that although the actual thickness of the film increases linearly with the number of bilayers (Figure 3.9), the absorbance of the film becomes sublinear at higher number of bilayers. This "bend over" effect is also seen in the photoluminescence graphs. It was carefully determined that this is not due to exhaustion of the dipping solutions; the amount of material dissolved in the dilute solutions is far greater than the minute quantities deposited onto the substrates as ultrathin films. The "bend over" effect in the absorbance and photoluminescence graphs is attributed to the incomplete conversion of the PPV in the presence of the SPS. This effect is seen reproducibly and most pronounced in the PPV/SPS binary system. As seen above, the PPV/PMA system exhibits extremely linear behavior. Although for the thermal conversion conditions used in this work, the PPV in all systems

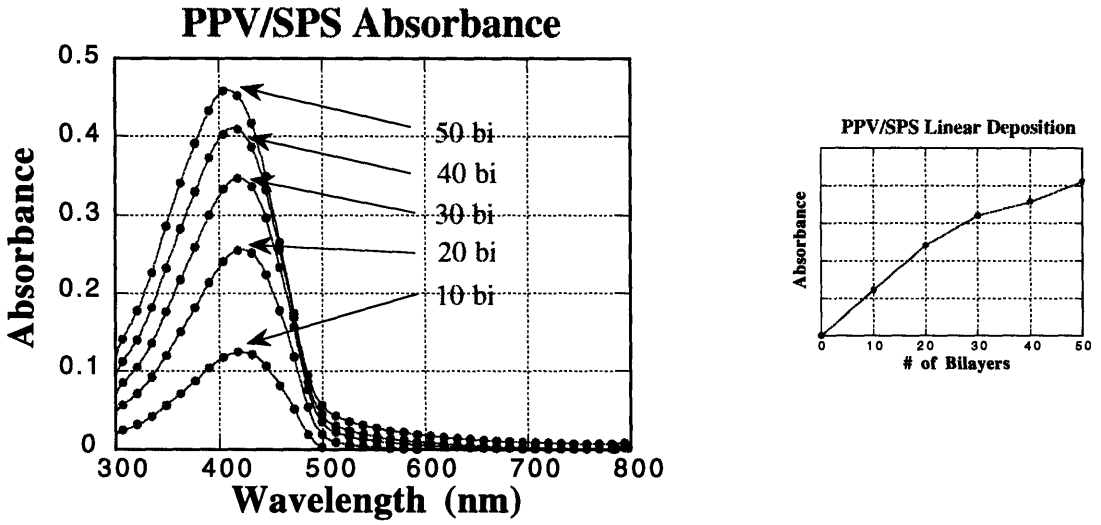

Figure 3.7 Overlaid Absorbance Spectra of PPV/SPS Films

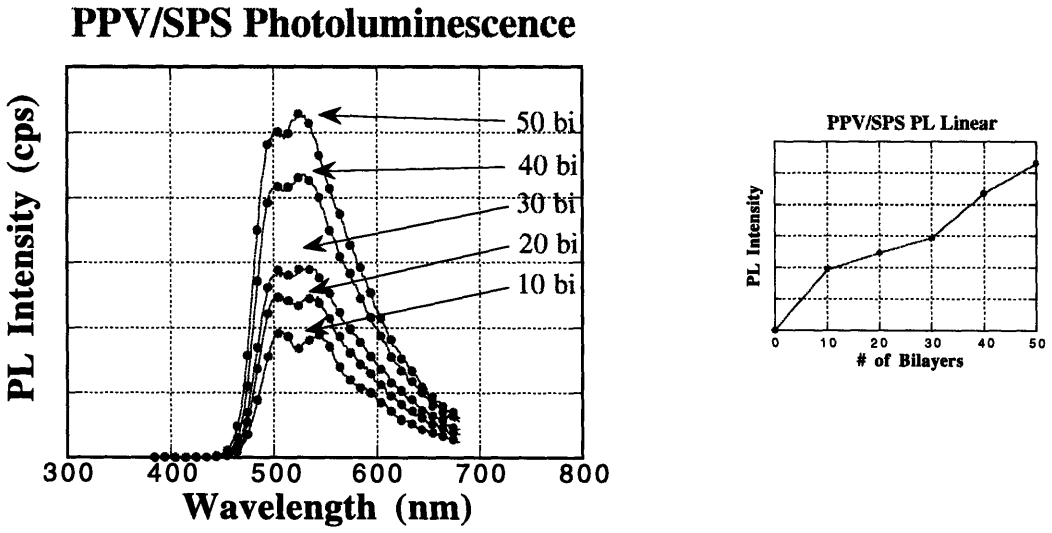

Figure 3.8 Overlaid Photoluminescence Spectra of PPV/SPS

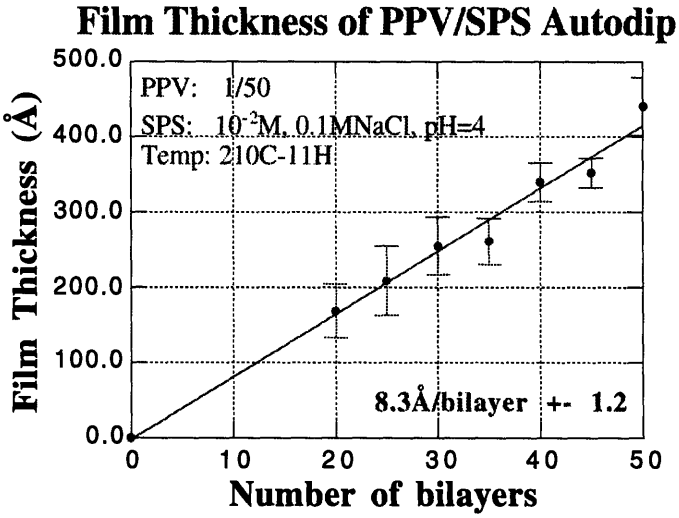

Figure 3.9 Dektak Profilometry of the Thickness of the PPV/SPS Series of Self-Assembled Films

is not brought to full conversion, in the thicker PPV/SPS samples, the extent of conversion is even less. It is possible that the diethyl sulfonium leaving groups and the evolved HCl molecules are bound more tenaciously in the PPV/SPS system, depending on their role in the partial doping of the PPV. In the thicker films, it is increasingly difficult to eliminate these species. These "impurities" may serve as non-radiative recombination sites; the larger numbers in the thicker films results in the sub-linear characteristic of the photoluminescence versus number of bilayers plots.

The successful self-assembly of PPV precursor with PMA or SPS was satisfying. But even more interesting was the fact that the photoluminescence of the films was dependent on the polyanion used as the counterpolymer to PPV in the self-assembly process. It was observed that not only was the intensity of the photoluminescence changed but the spectral shape and peak position were also strongly affected by the polyanion that was self-assembled with the PPV. From our arsenal of polyanions, it was found that when non-conjugated polymers such as polymethacrylic acid (PMA), polyacrylic acid (PAA), or sulfonated polystyrene (SPS) were self-assembled with PPV-precursor in a simple binary (two component) system, the films exhibited photoluminescence. However, when conjugated polyanions such as poly(thiophene-3-acetic acid) (PTAA), sulfonated polyaniline (SPAn), sulfonated fullerenes (S-C_{60}), or poly(N,N'-bis(p,p'-oxydiphenyl-ene)pyromellitimide) (PMDA-ODA) were used, the photoluminescence was completely quenched.

The PPV self-assembled successfully with all of the various polyanions mentioned above with the characteristic linear deposition. The absorbance curves of these binary systems exhibited differences in the positions of the absorbance maxima and peak shape. Figure 3.10 shows the absorbance spectra of PPV/PMA and PPV/SPS normalized to the same intensity for clarity. Figure 3.11 shows the corresponding photoluminescence spectra, also normalized for clarity. It is clearly seen that there is about a 40 nm shift in both the absorbance and the

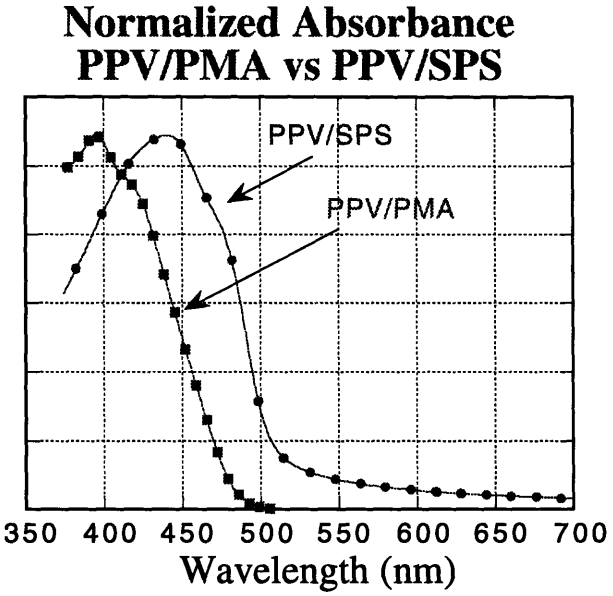

Figure 3.10 **Comparison of Absorbance Curves for PPV/PMA and PPV/SPS Binary Systems**

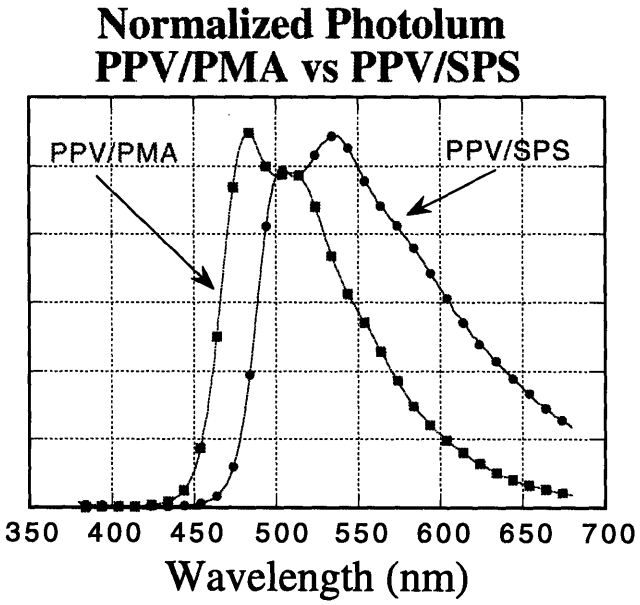

Figure 3.11 **Comparison of Photoluminescence Curves for PPV/PMA and PPV/SPS Binary Systems**

photoluminescence. Furthermore, while the absorbance of PPV/PMA is typically about one half that of the PPV/SPS, the intensity of its photoluminescence is always nearly an order of magnitude higher than the PPV/SPS system. The PPV/PMA peak is centered around 490 nm whereas the PPV/SPS peak is centered around 530 nm. This corresponds well with the color of the photoluminescence observed by the eye. The PPV/PMA appears bluish green while the PPV/SPS is yellow-green. These observations indeed point to the fact that by varying the molecular environment of the PPV, simply by self-assembling it with a different counterpolymer, we can tune its properties. And, as will be seen in the sections to come, molecular self-assembly will allow us to control the photoluminescent properties of the PPV by designing and fabricating different layer-by-layer supermolecular architectures.

The photoluminescence for the other binary systems such as the PPV/PTAA, the PPV/SPAn, and the PPV/C_{60} binary systems are not shown because on this scale, it is a flat line at zero intensity; the photoluminescence is completely quenched. In these binary systems in which the PPV is self-assembled with a conjugated polyanion, the photoluminescence quenching is attributed to charge transfer from the excited PPV to polyanion. For example in the case of the C_{60}, a well known strong electron acceptor, the excited carriers are transferred to the polyanion and then undergo non-radiative decay [3.12]. These studies by other groups have indicated that these interactions are not

ground state interactions; rather, the quenching effect is attributable to a photoinduced charge transfer between the PPV and the counterpolymer [3.12]. Since this quenching of the photoluminescence of PPV is observed when the PPV is self-assembled with conjugated polyanions, it is likely that the π-orbitals of both the PPV and the conjugated polyanion participate in the charge transfer interaction. For the π-orbitals of adjacent polymers molecules to interact, they must overlap; the degree of this overlap is dictated by the amount of bending, twisting, and coiling of the polymer chains as they are self-assembled together into a thin film and also during the thermal conversion process. Further, since the π-orbitals participate in modifying the photoluminescence characteristics of the film, it is possible to further tune this photoluminescence by modification of the π-orbitals of the counterpolymers by functionalization with electron withdrawing or electron donating groups. It should be noted that the electron withdrawing sulfonate groups on the rings of the sulfonated polystyrene may be responsible for a partial charge transfer from the PPV to the π-orbitals of the SPS, thus leading to the lower photoluminescence. Since the PPV only interacts with conjugated counterpolymers in the excited state, these systems create the unique opportunity for thin film photorectifying junction devices; these devices would exhibit rectifying characteristics only when the PPV is stimulated by photons and a photoinduced charge transfer interaction occurs. The investigation of these devices are not in the scope of this project and will be left to future work.

The intermolecular charge transfer interactions in the PPV/conjugated polymer binary systems are responsible for changing the intensity of the photoluminescence (quenching) but do not change the characteristics of the PPV itself, such as the conjugation length and thus the absorbance and photoluminescence color. However, the physical interaction between the PPV chains and the polyanion chains in adjacent layers do give rise to differences in conjugation length, as evidenced in the peak shifts in the absorbance and photoluminescence spectra of the PPV/PMA versus the PPV/SPS. Although more work is needed to deconvolute these effects from the effects of the thermal conversion process on the conjugation length of the PPV, it is clear and reproducible that for a given system of self-assembled PPV and a given thermal conversion profile, highly reproducible absorbance and photoluminescence characteristics are obtained. For example, the absorbance and photoluminescence of PPV/PMA is blue shifted by 40 nm relative to PPV/SPS; the absorbance of the PPV/PMA is half the intensity of the PPV/SPS; and the photoluminescence of the PPV/PMA is nearly an order of magnitude larger than that of the PPV/SPS.

Having seen that the molecular environment of the PPV (the neighboring polyanions self-assembled in the adjacent layers) influences the properties of the PPV, we went on to investigate deliberately changing this molecular environment to tune the overall characteristics of the PPV self-assembled film. Since self-assembly provided the

molecular level control necessary to manipulate and precisely place single layers of material (5 Å to 10 Å thick), we could build complex, layer-by-layer architectures to study intermolecular interactions at the molecular level. An example of using self-assembly to study intermolecular interactions is a series of experiments carried out in our group to re-establish the photoluminescence in binary PPV systems which exhibited quenched photoluminescence [3.11]. For the binary systems which showed quenched photoluminescence, such as PPV/C_{60} or PPV/PTAA, the luminescence intensity was deliberately and controllably re-established to an "un-quenched" intensity by separating the PPV layers from the polyanion layers that quench it. This was done by inserting a few inert "spacer" layers between the PPV and the quenching agent. Given the molecular level control of the self-assembly process, it was a relatively trivial task to insert single layers of material on the order of 5 Å to 10 Å each between the PPV and the polyanion. These spacer layers mediated and eliminated the quenching charge transfer interactions between the PPV and the counterpolymer. When the PPV was fully isolated from the quenching agent, the resulting photoluminescence intensity corresponded roughly to the intensity of a film of an unquenched binary system of similar thickness. The insertion of 3 - 5 "spacer" bilayers thus resulted in a heterostructure film with a completely un-quenched photoluminescence intensity. In the case of C_{60}, a strong electron acceptor, 7 "spacer" bilayers were necessary to re-establish the luminescence intensity back to the "un-quenched" levels while in the PPV/PTAA system only 5 "spacer" bilayers were needed.

From these experiments, it can be inferred that the distance of interaction for the charge transfer to occur between the PPV and the quenching polyanion is on the order of the thickness of the multiple spacer bilayers; the stronger electron accepting nature of the C_{60} in the PPV/C_{60} system meant the interaction could occur across greater distances than in the case of the PPV/PTAA. The results from this series of photoluminescence experiments is particularly significant for two reasons. First, it shows that the layer-by-layer architecture of the PPV self-assembled film remains intact even after the thermal conversion process; that is, the annealing at high temperature does not homogenize and intermix the layers, allowing us to observe the "un-quenching" effects. Second, this is a clear demonstration of the molecular level control of self-assembly which allows us to precisely insert layers of material between 5 Å to 10 Å each to mediate an intermolecular interaction at the molecular level. With such a powerful technique, more and more complex multilayer heterostructure architectures can be fabricated and explored for unique interactions that give rise to novel properties, which can be exploited in thin film devices.

In addition to the quenching caused by the counterpolymers self-assembled with the PPV, there is also evidence in the binary PPV systems of some degree of self-quenching between the PPV layers. This is borne out by the fact that when additional polyanion bilayers are inserted between each PPV/polyanion bilayer in the original binary system, the photoluminescence intensity increases incrementally. Self-

assembled films of around 100 Å have been shown to give equal or greater photoluminescence intensity than much thicker, spin-coated films of between 1000 Å and 2000 Å. The figures of merit, photoluminescence per absorbance and photoluminescence per thickness are higher for the PPV in the self-assembled films. This suggests that the isolation of PPV into individual layers of between 10 Å and 30 Å leads to less self-quenching and brighter photoluminescence. Other groups have also observed that when PPV is "diluted" in a matrix of polyvinylcarbazole, the probability of radiative transitions is enhanced [3.5e]. Finally, although there is interpenetration between layers in a PPV self-assembled film, it is clear from these quenching studies above that the layered structure and multilayer architecture is preserved even after the thermal conversion; the long conversion and annealing does not homogenize the components in the film. And it is quite remarkable that self-assembly provides such a simple means of manipulating electroactive polymers into multicomponent, multilayer films with complex supermolecular architectures.

3.4.2 Self-Assembled PPV Thin Film LEDs

With the knowledge of the solid state photoluminescence behavior of the self-assembled films, light-emitting devices (LEDs) based on the simple binary films of PPV/PMA and PPV/SPS were fabricated and characterized for their electroluminescence properties. In forward bias operation of these devices, holes are injected into the valence band of

the polymer from the ITO (anode) electrode and electrons are injected into the conduction band from the aluminum (cathode) electrode. These holes and electrons travel through the body of the polymer film under the influence of the applied field and undergo non-radiative or radiative transitions. They can recombine radiatively across the band-gap of the polymer, resulting in emission with a color characteristic of the band gap of the polymer. Although the mechanism of light-emission in these organic materials is relatively simple to understand, the mechanism of operation of the thin film devices based on organic thin films is still the subject of debate. It is the consensus, however, that an understanding of the role of the barriers at the interface between the polymer and both electrodes is critical to the understanding of what determines the shape of the current-voltage curves and the efficiency of the devices.

Towards that end, we began to fabricate light-emitting devices based on ultrathin self-assembled films of PPV. It is remarkable to note that films as thin as 80 Å could be successfully used as the active layers of the organic thin film light-emitting devices Although pinholes and defects have plagued other traditional thin film processing techniques in the fabrication of ultrathin films for such microelectronic devices, they are not problematic for the devices discussed here, even with the thinnest self-assembled films. This attests to the quality, uniformity, and density of the films produced by the self-assembly of PPV. Figure 3.12 shows a current-voltage curve for a PPV/PMA device based on a 580 Å self-assembled film, converted at 180 °C for 4 hours. (It should be

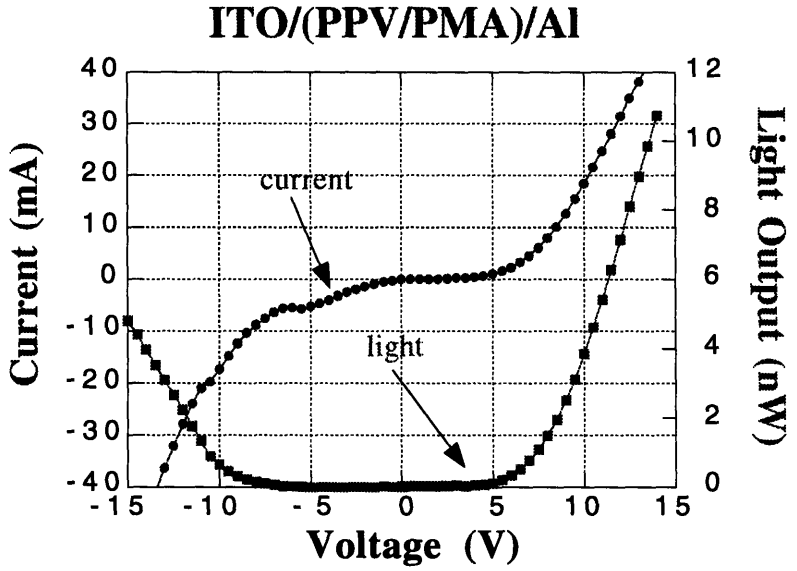

Figure 3.12 I-V Light Curve for PPV/PMA Self-Assembled Device (580 Å), 4 hours at 180 °C

noted that this plateau temperature is considered to be a low temperature for effecting the thermal conversion of PPV and the length of time is considered "short;" conversions at 210 °C an 11 hours will be discussed in the following sections.) The I-V characteristic is neither ohmic nor traditionally rectifying; rather, it is symmetric, with an exponential rise in current in both the forward and reverse bias regimes. Here we make a distinction between two terms that will be used in the subsequent sections in the discussion of the characteristics of the devices. The term "symmetric" is used to designate current-voltage curves which show current and light in both the forward and reverse biases. The label "symmetric and mirror image" refers to those current-

voltage curves which are symmetric and the rise in current occurs at exactly the same voltage. The curve is thus mirrored about the origin. This symmetric characteristic of the current-voltage plots is dependent on the thermal conversion conditions. In the samples which do show symmetry, the turn-on in the forward bias regime is usually lower than that in the reverse bias. And, although not yet attempted, AC operation of these symmetric devices may be possible.

The symmetric nature of the current and light versus voltage characteristics is thought to be due to the extremely small thicknesses of these self-assembled films, to interface effects between the metal electrodes and the self-assembled film, and to the partial electrochemical doping of the PPV in the presence of the acid groups of the counterpolymers and the abundant counterions left behind by the self-assembly process. Further study is needed, however, to clarify to role of these effects in producing the non-rectifying, symmetric I-V curves. In the PPV/SPS system, it is observed that the current-voltage curves are always symmetric and the current magnitudes larger by a factor of 5 to 10 than those of the PPV/PMA system. The presence of the strong sulfonic acid groups of the SPS suggests that doping of the PPV may indeed be occurring during the thermal conversion process or during operation of the device, similar to the results of other groups which deliberately dope PPV with various oxidizing agents, including SO_3 [3.14]. In addition, our absorbance studies of the PPV films on used device samples revealed bipolaron bands in some cases which are

indicative of doping in conjugated polymers. The much weaker carboxylic acid groups of the PMA can also dope the PPV but to a lesser extent. In general, however, the current carrying capacity of all of our self-assembled films is larger than that of films of small organic molecules built into similar ITO and aluminum device configurations.

More traditionally rectifying current-voltage characteristics have been widely published for PPV LEDs based on thicker spin-coated films [3.13]. We too have reproducibly generated rectifying I-V and light curves with spin-coated PPV films as shown in Figure 3.13. The PPV in this device was converted at 180 °C for 4 hours, similar to the self-assembled device shown above. Also, in some of our self-assembled

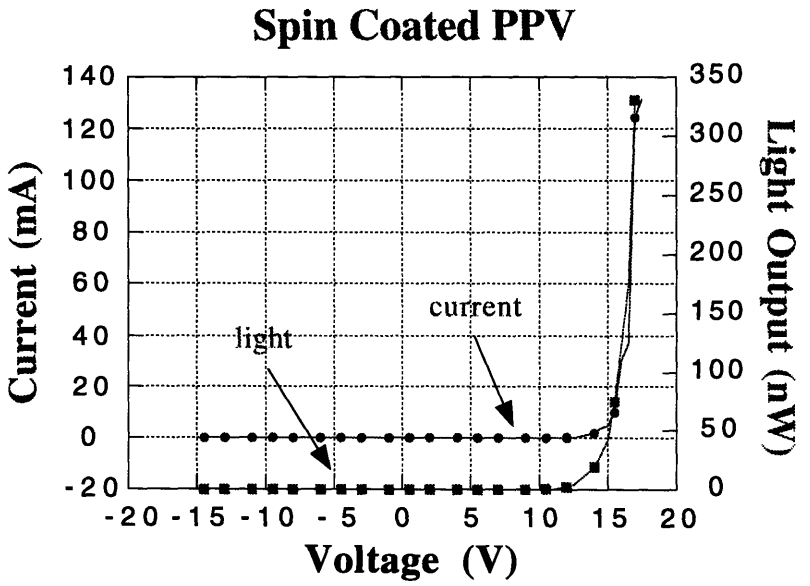

Figure 3.13 I-V and Light Curve for 940 Å Spin-Coated PPV Film Device, 4 hours at 180 °C

PPV/PMA films, longer conversion times of 11 hours at the plateau temperature of 210 °C have resulted in rectifying device characteristics. Although the role of doping of the PPV film in these devices is still not completely clear, the fact that the PPV/PMA films exhibit rectifying characteristics, lower current levels, and simultaneously higher light output while the PPV/SPS exhibits symmetric current-voltage curves, higher current levels, and low light output does indeed suggest that doping affects the device characteristics. In the case of the PPV/PMA binary system, at short conversion times, symmetric current-voltage curves are observed, while for long conversion times at higher temperatures, rectifying current-voltage curves are seen. The higher temperature and longer times used for the thermal conversion are believed to cause a more complete conversion of the PPV.

In all devices in forward and reverse bias operation, the light intensity maps out according to the current; in other words, there is a linear correspondence between the light intensity and the current. The plots of light intensity versus current will be extensively used in the sections to follow as a means to compare the relative efficiencies of devices. Since the efficiency is calculated as number of photons per electron, the slope of the light-current curves provides a qualitative measure of the efficiency. Another characteristic of the I-V plots is the "turn-on" voltage. The voltage at the beginning of the exponential rise in current and light is designated as the "turn-on" voltage since it

corresponds to the point at which the unaided eye can first see visible light emission from the device in a darkened room. The eye typically can detect intensities beginning around 1 nW. Finally, a more precise way to designate the turn-on voltage was implemented by taking the voltage (x-axis) intercept of the linear fit through the top 90% of the points on the current-voltage plots.

3.4.3 Device Thickness Study

Having demonstrated that we could successfully fabricate light-emitting devices based on our self-assembled films, we went on to do a series of experiments designed to give us further insight into the mechanism of operation of these devices. Previous work by I.D. Parker [3.15], showed that the external turn-on voltages of simple, spin-coated PPV devices varied directly with the thickness. That is, the turn-on voltage increased proportionally as thicker films were used as the active layer of the LEDs. This implied that there exists a singular electric field (external voltage divided by film thickness) at which the exponential rise in current ("turn-on") will occur; the value of this field is determined by the band-offsets between the polymer film and the electrode materials, ITO and aluminum in this case. The smaller offset determines the identity of the "majority" carrier in the film and the magnitude of the larger offset determines the efficiency of the device. The "majority" carrier in such polymer films is simply the more

abundant carrier. In polymer films, capacitance-voltage measurements have shown that there are extremely few free carriers, as evidenced by immediate depletion. Therefore all of the carriers must be injected during the operation of the device. A smaller barrier to injection means more carriers will be injected at a particular applied field. In the ITO/PPV/Al device configuration, the band offset between the ITO and the PPV is smaller than that of the Al and PPV. Therefore, during forward bias operation of the device, more holes are injected than electrons. Coupled with the fact that the mean free path and mobility are much greater for holes than for electrons in PPV, holes are the "majority" carriers in these films during operation. From further observations, Parker attributed the field-dependent and temperature-independent behavior of these spin-coated PPV devices (500 Å to 2000 Å thick) to a rigid band, tunneling model [3.15].

This model proposes that carriers tunnel from the electrodes into the polymer film when the device is sufficiently biased to create triangular barriers at the interface. The height of the barrier is given by the band offset between the polymer and the electrode material; and the width of the barrier is dependent on the amount of applied bias. The model assumes negligible band bending at the interface (due to insufficient numbers of intrinsic carriers in the polymer) and neglects interface effects such as surface smoothness and surface species. For spin-coated films, the surface of the polymer film is far from molecularly smooth. Furthermore, for the various techniques used to

deposit the top aluminum electrode, varying degrees of damage to the surface will occur from the bombardment of aluminum atoms. Also, the quantity and identity of surface species depends on the handling techniques of the devices. For example, if the PPV film is exposed to minute quantities of oxygen or water, surface species such as carbonyls or hydroxy groups will form. These will react with the aluminum during thermal evaporation of the electrode to form oxides at the interface. Although more work is needed to ascertain the influence of these surface species on the electronic states of the polymer at the interface and ultimately their influence on the external properties of the thin film devices, their presence introduces another variable which must be controlled and understood before a coherent and comprehensive model of the operation and microscopic mechanism of these devices can be put forth.

As a first step towards this understanding, self-assembly has allowed us accomplish an series of experiments with LEDs based on PPV films of various layer-by-layer architectures. First, in order to determine the applicability of the proposed rigid band model to our thinner self-assembled films (80 Å to 500Å), a series of single slab devices of different thicknesses were fabricated. The term "slab" is used to define a multiple bilayers of a certain binary combination of PPV such as PPV/PMA or PPV/SPS. This anticipates the sections to follow which describe our work with multi-slab devices in which "slabs" of PPV/PMA are stacked on top of PPV/SPS to form unique architectures.

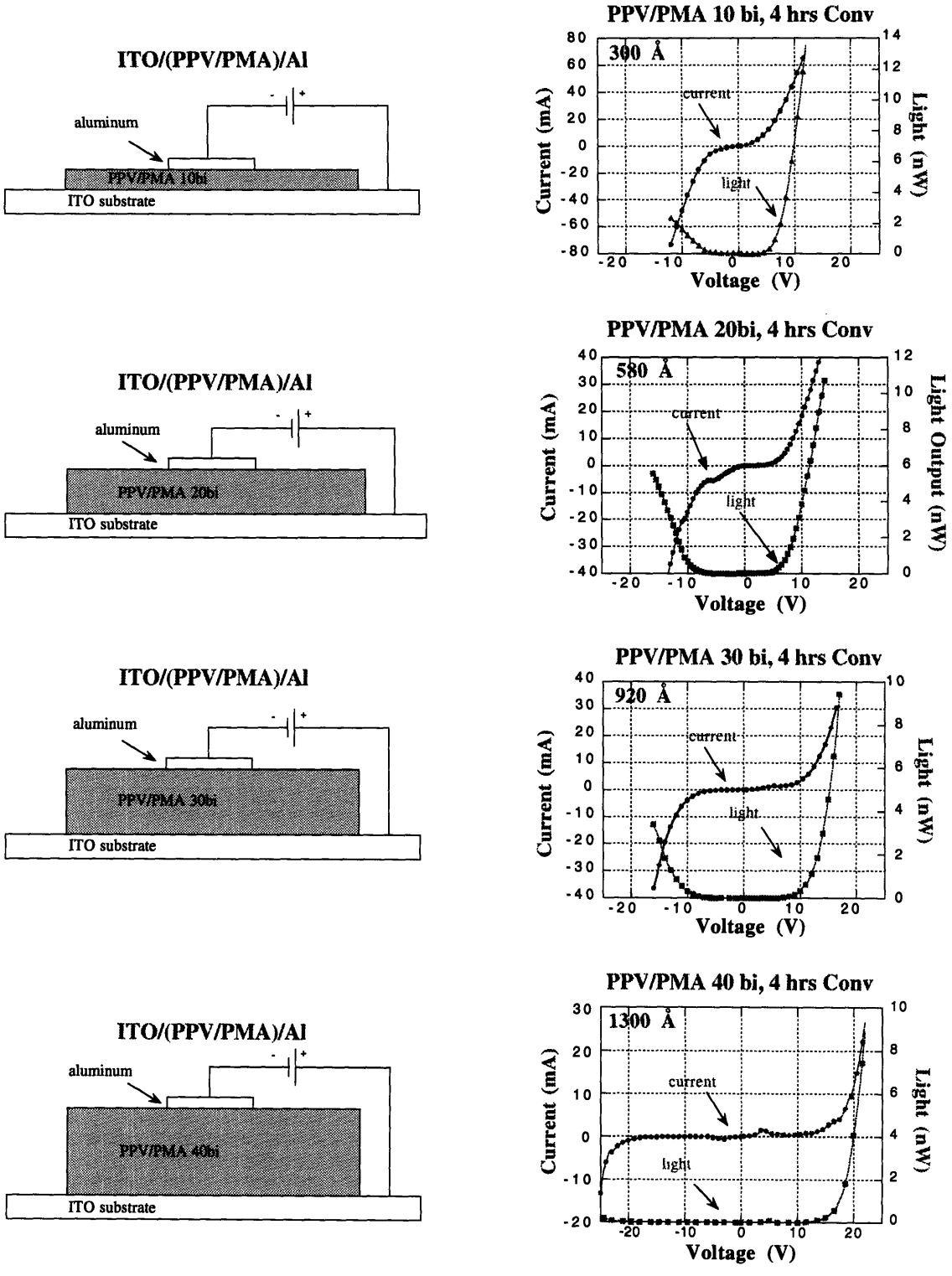

Figure 3.14 PPV/PMA Thickness Study, 4 hrs @ 180 °C

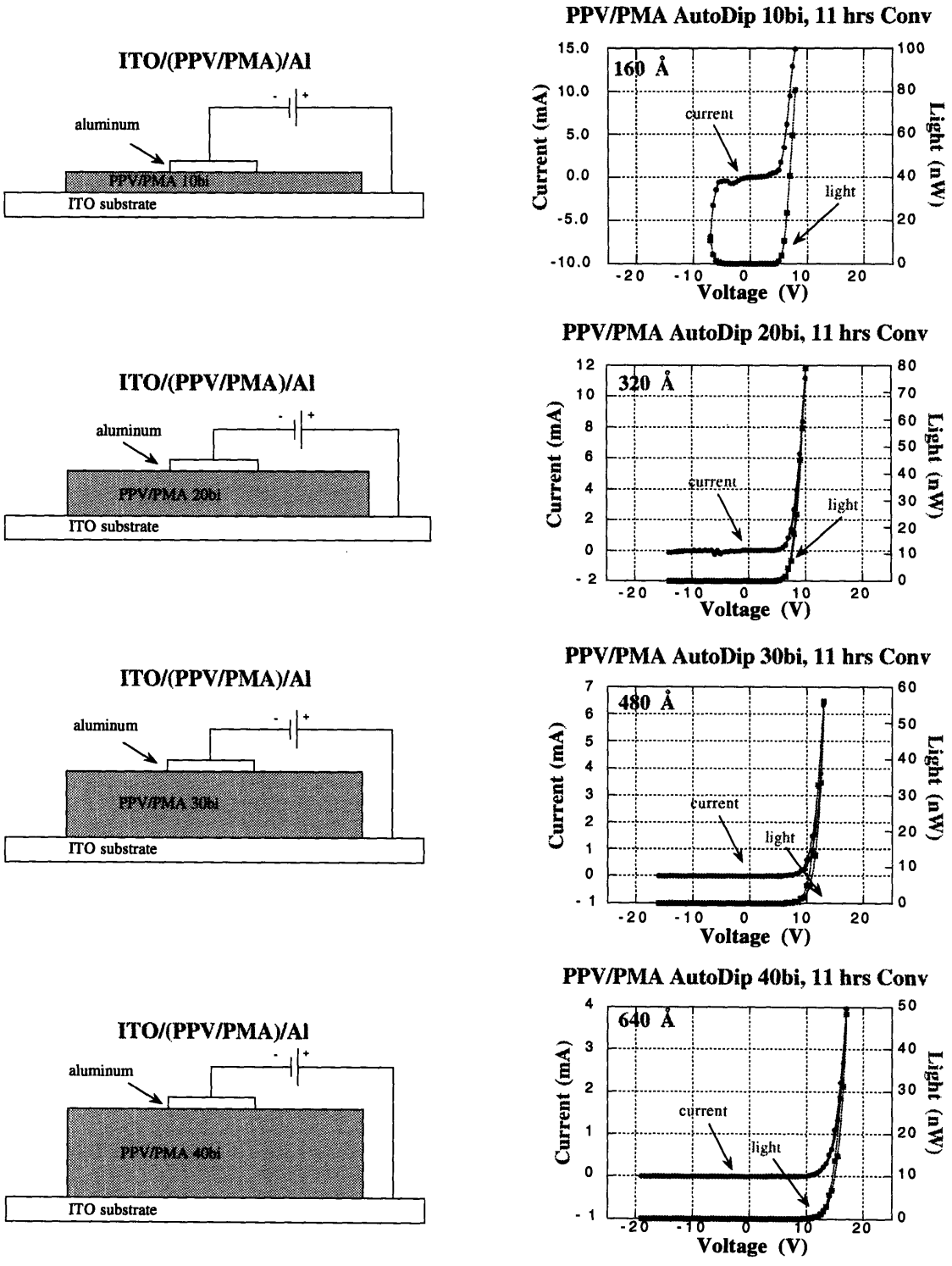

Figure 3.15 PPV/PMA Thickness Study, 11 hrs @ 210°C

The word "layer" is used here to define a single polymer layer of PPV or SPS or PMA; the word "bilayer" defines the basic building block of self-assembled films, for example a single PPV layer with a single SPS layer. Molecular self-assembly makes it a trivial matter to vary the thickness of these active layer films simply by stacking more bilayers on top of each other. Figure 3.14 shows schematic diagrams of simple PPV/PMA devices as a function of thickness and their corresponding current and light versus voltage graphs. The entire series of PPV/PMA films was converted at 180 °C for 4 hours. For comparison, Figure 3.15 shows another series of PPV/PMA films converted at 210 °C for 11 hours.

From both of these figures, it is clear that for the devices based on PPV/PMA self-assembled films, the turn-on voltage does indeed increase proportionally with thickness. This provides evidence supporting the proposed rigid band tunneling model. The increase in the turn-on voltage with increasing thickness also applies to the reverse bias. The differences between the two series of PPV/PMA samples converted with different thermal treatments include lower currents and higher light output for the more fully converted series of samples (210 °C for 11 hours). This is reasonable since the higher temperature will cause a greater fraction of the PPV-precursor to convert to the conjugated, light-emitting form of PPV; and the longer annealing serves to densify the film which would lower the incidence of defects in the film which allow current to "leak through" during operation. Although

the 20, 30, and 40 bilayer films of the second series of PPV/PMA films are rectifying, the thinnest sample of 10 bilayers (160 Å) shows symmetric current-voltage characteristics, similar to the samples of the less converted series. As was mentioned before, the symmetry in the current-voltage curves is likely due to the convolution of the effects of thermal treatment and the extremely small thicknesses of these devices.

In order to see the increase in turn-on voltage with thickness for these devices more clearly, the current-voltage plots of the long conversion series of samples from Figure 3.15 are overlaid in Figure 3.16. The next graph, Figure 3.17, shows an overlay of the current versus field plots; the value of the electric field is calculated by dividing the voltage by the thickness of the film.

Figure 3.17 shows that all of our PPV/PMA devices in the range of thicknesses under 500 Å turn on at an electric field strength of between 1.5 and 2 MV/cm. The curve for the 10 bilayer sample was omitted from this graph for clarity. It is remarkable that devices based on such thin films operate at all. Furthermore, the quality of the self-assembled films are good enough to allow continuous operation at such high electric fields. The lifetime of the device, however, depends on the conditions during fabrication and during operation. A more detailed discussion of the breakdown mechanisms responsible for device failure will be presented below.

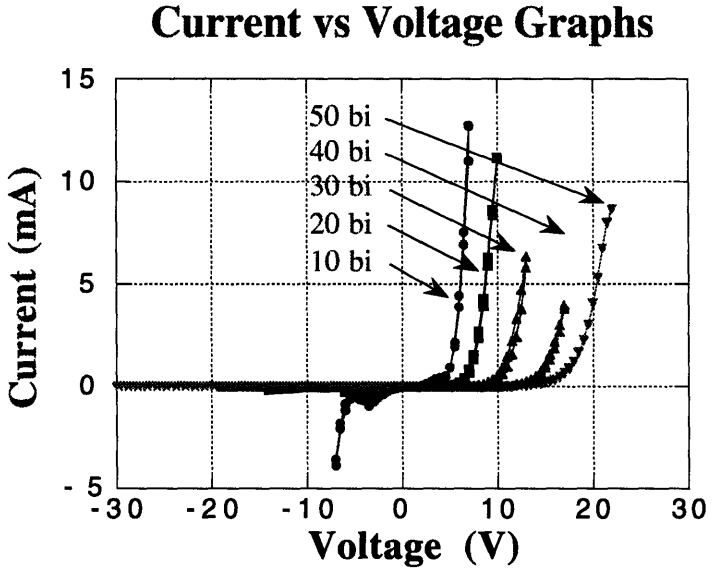

Figure 3.16 **Overlaid Current-Voltage Curves for PPV/PMA Thickness Study Samples**

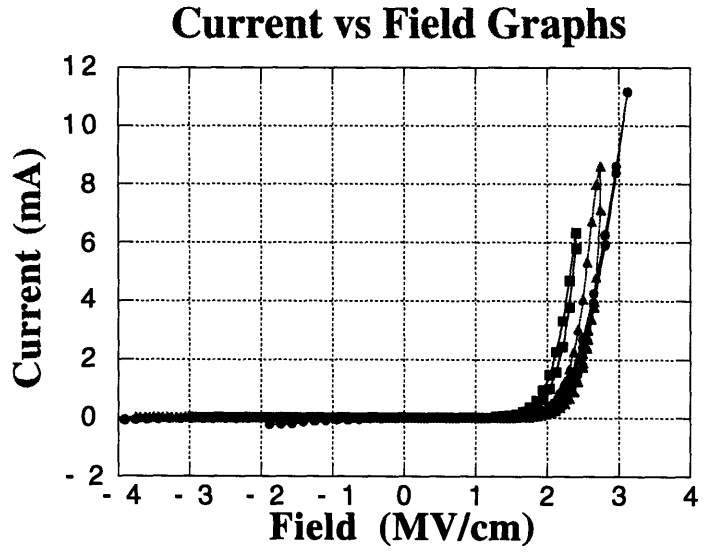

Figure 3.17 **Overlaid Current-Field Curves for PPV/PMA Thickness Study Samples**

In a similar thickness study for the PPV/SPS binary system, we show Figures 3.18 and 3.19 below. Figure 3.18 presents the current and light versus voltage curves for PPV/SPS films of between 100 Å and 400 Å. In this case, it is clear that the current-voltage curves for all of the thicknesses are symmetric. As mentioned above, the symmetry is characteristic of the devices based on the PPV/SPS heterostructure films. Another feature of the PPV/SPS system is its high current and low light output, compared to the PPV/PMA series above. The current reported in milliamps is the current driven through our device area of 4 square millimeters, which translates into a current density on the order of 1000 - 2000 mA/cm^2. Finally, it should be noted that the PPV/SPS system behaves differently from the PPV/PMA self-assembled system in that the turn-on voltage remains essentially constant at around 4 V for all thicknesses in the case of the PPV/SPS. There is only a slight increase in the turn-on voltage in both forward and reverse bias with increasing film thickness. Thus when the current is plotted versus the electric field in Figure 3.14, there is an inverse relationship in the turn-on field with increasing thickness. The turn-on field actually decreases when the thickness of the film is increased. The fact that the PPV/SPS exhibits much higher current magnitudes than the PPV/PMA, the symmetric current-voltage characteristics, and the non-linear scaling of the turn-on voltage with increasing thickness all indicate that a modified mechanism is operational in these devices. It is likely that the rigid band

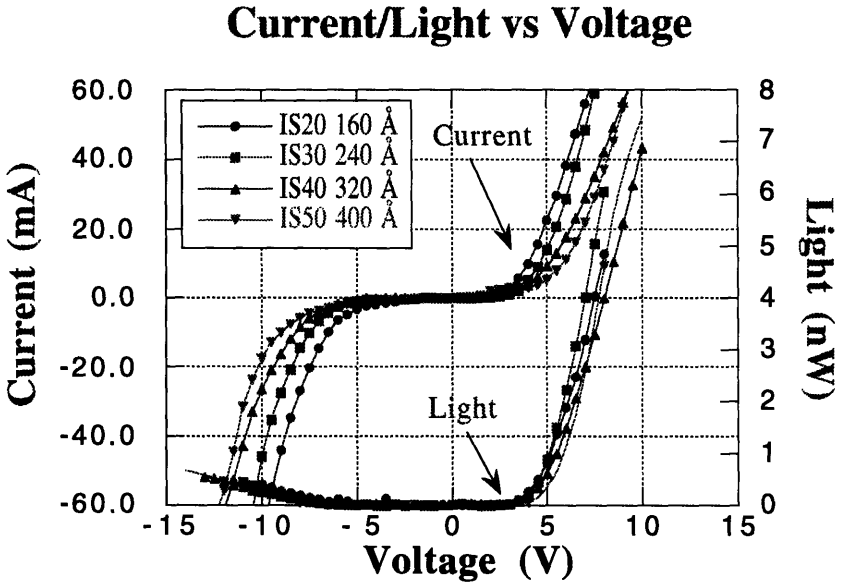

Figure 3.18 **Overlaid Current-Voltage and Light-Voltage Curves for PPV/SPS Thickness Study Samples**

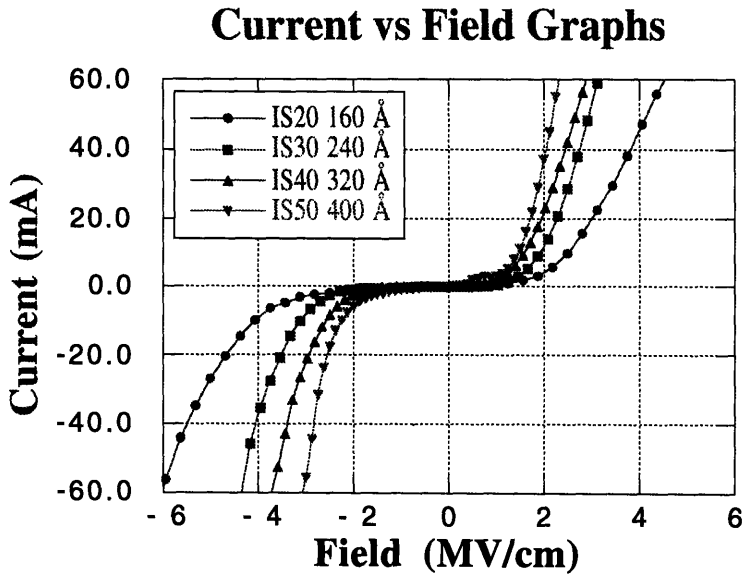

Figure 3.19 **Overlaid Current-Field Curves for PPV/SPS Thickness Study Samples**

model is an oversimplification in the PPV/SPS system in which doping of the PPV by the strong sulfonic acid groups in the presence of abundant counterions may impart higher conductivity to the film. It is known that doping of the PPV results in higher conductivity and lower luminescence, (electroluminescence in this case) [3.12g]. In addition, as mentioned before, the π-orbitals on the benzene ring of the polystyrene and the electron-withdrawing sulfonate groups on the ring may contribute to partial electron transfer from the PPV to the SPS. This too may account for the fact that the PPV/SPS shows lower photoluminescence and electroluminescence than the PPV/PMA. And, as will be addressed later, this partial charge transfer imparts a slight p-doped character to the PPV/SPS relative to the PPV/PMA.

As a visual aid to clarify the difference between the PPV/SPS and the PPV/PMA, we plot the light output versus current for corresponding devices of identical thickness in Figure 3.20. It should be noted first of all that in each case the light versus current is linear; that is, the light scales proportionally to the increase in current as the applied voltage is increased. And, since our measure of efficiency is photons per electron, the slope of these curves gives us a direct comparison of the relative efficiencies of the devices. The larger the slope (light per current) the more efficient the device. It is clear that PPV/PMA device, with the much larger slope, is more efficient than the PPV/SPS device of similar thickness. Finally, from the graph, the PPV/SPS device does give off light in the reverse bias so there are

points on the negative current side. The PPV/PMA device is rectifying so no points are seen in the reverse bias side. In an expanded scale (not shown here) the slope of the light versus current for the PPV/SPS in reverse bias is smaller than in forward bias, indicating a difference in efficiency in the two regimes. This is reasonable and consistent with the fact that in reverse bias operation, when holes are being injected from the aluminum electrode, the band offset (barrier to tunneling) is larger at the aluminum than that for injection of holes from the ITO electrode in forward bias operation. Since the ability to inject the "minority" carrier electrons into the device determines the overall efficiency of the

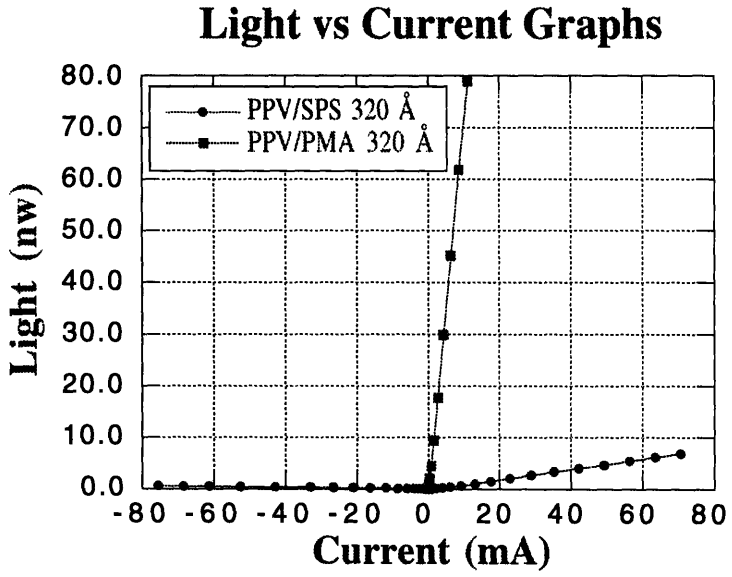

Figure 3.20 Comparison of Light-Current Graphs for PPV/PMA and PPV/SPS Self-Assembled Devices

device, forward bias operation is observed to be more efficient that reverse bias operation in all samples that show a symmetric current-voltage characteristic.

Another piece of evidence that can be gathered from the thickness studies of single slab devices is that fact that the efficiency increases incrementally as the thickness of the polymer film is increased. This can be seen in Figure 3.21 which shows the overlay of the light-current curves for the PPV/PMA series of samples and the PPV/SPS thickness series. The slopes of these curves increase as thicker active layers are used. There may be several factors involved in producing this enhancement effect. As thicker films are made, short-circuit defects that extend all the way through the film to allow carriers to "leak" through without recombining radiatively are "plugged" and their numbers reduced. Other pieces of evidence from our other experiments argue

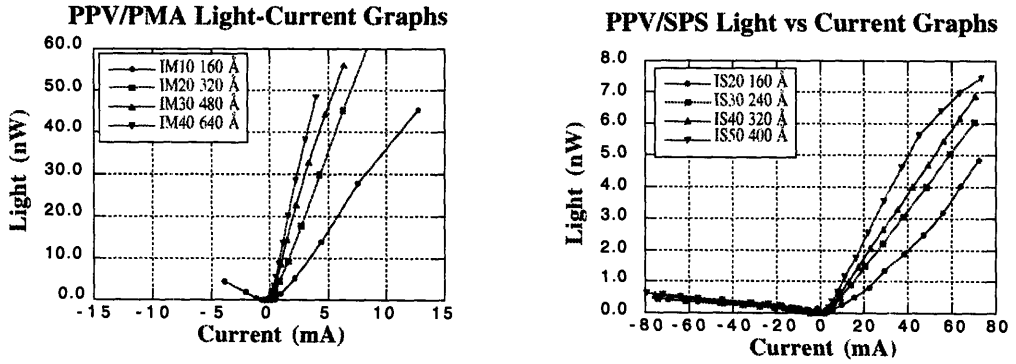

Figure 3.21 Overlay of Light-Current Graphs for PPV/PMA and PPV/SPS Thickness Series

that defects, such as pinholes, which render the device useless are not present in large numbers. The fact that self-assembled films of as little as 80 Å operate successfully as devices attests to the fact that the self-assembled films are not riddled with short circuit defects; rather, the films are dense and coherent, especially after the thermal conversion step which serves to densify the film. (Previous studies in our group have shown that the overall thickness of the film decreases after thermal conversion and the elimination of the sulfonium leaving group [3.11].) Furthermore, the successful operation of a large-area device of nearly 4 square centimeters (260 Å thick) suggests that the defect density of these films is sufficiently low. Therefore, to account for the increase in efficiency with increasing film thickness, it is more likely that there are simply more radiative recombination sites in the body of the film. A corollary to this statement is that in the thicknesses regime accessible to self-assembly, radiative recombination occurs throughout the body of the film and is not spatially localized to thin "zones" near the electrodes, as speculated by other groups. This does not imply, though, that simply by increasing the thickness of the devices indefinitely, more efficient devices will be achieved. First of all, the increases seen here are noticeable but small. And a point of diminishing returns is reached for thicker films due to the difference in the mean free path length and the mobility of holes versus electrons, as mentioned earlier. The mean free path of electrons is smaller than that of holes by a factor of 10 and the mobility smaller by a factor of 100. Thus for much thicker films, such as spin coated PPV films, the electrons will be lost to non-radiative

events and this kind of enhancement in efficiency with thickness is lost. The ability to control thicknesses down to the range of 100 Å to 500 Å by self-assembly has allowed us to elucidate these effects. However, even greater enhancements in the device efficiency and light output are sought. Therefore, we turn next to the manipulation of the layer-by-layer architecture of the heterostructure thin film.

3.4.4 Multislab Heterostructure Devices

As mentioned earlier, other groups have found that by introducing different materials in the form of multiple layers or blends, the efficiency and maximum light output of the light-emitting devices could be significantly enhanced [3.5]. In most cases, carrier transport layers were added to one or both sides of the emitter layer not only to improve injection efficiency, but also to limit the regions where recombination could take place. Based on the body of information on our single-slab, self-assembled PPV devices presented above, we designed and fabricated novel layer-by-layer architectures in the attempt to further improve our devices. From the photoluminescence studies, it was shown that the PPV/SPS was fundamentally different from the PPV/PMA as prepared by our technique. The longer conjugation length of the PPV/SPS gave it an green color corresponding to a slightly smaller band gap than the PPV/PMA, which was bluish. In conjunction with this, the device characteristics showed that the PPV/SPS system carried an order of magnitude more current than the PPV/PMA device

but emitted roughly an order of magnitude less light. In the spirit of the work of the other groups, we decided to use the PPV/SPS system as a current transport "slab" in a dual slab architecture with a PPV/PMA slab serving as the emitting layer. The slightly smaller band gap of the PPV/SPS system, its placement relative to the work function level of the ITO, and the fact that in all cases the turn-on voltage of the PPV/SPS was lower than that of the PPV/PMA of similar thickness all indicate a smaller barrier to the injection of holes from the ITO in forward bias. Therefore a "slab" of 5 bilayers of PPV/SPS was self-assembled next to the ITO to serve as a carrier transport layer and a "slab" of 15 bilayers of PPV/PMA stacked on top of it to serve as the emitter layer. This particular device was designated as ISM to stand for the ITO/(PPV/SPS)/(PPV/PMA)/aluminum device configuration. Figure 3.22 presents schematics of the device architecture and the corresponding current-voltage and light-voltage curves. It is clear from these graphs that the new dual-slab architecture has significantly increased the light output over the single slab PPV/PMA from 80 nW to 600 nW. As a rough estimate, 600 nW corresponds to about 100 Cd/m^2; this number reported for light-output does not take into account waveguiding and losses due to internal reflection in our device configuration. The success of this new architecture confirms the fact that self-assembled PPV/SPS differs from self-assembled PPV/PMA and that they serve their designated function in a dual-slab architecture. As before, when we plot the light-current graphs for comparison in Figure 3.23, we see that the slope of the curve for the ISM dual-slab device is

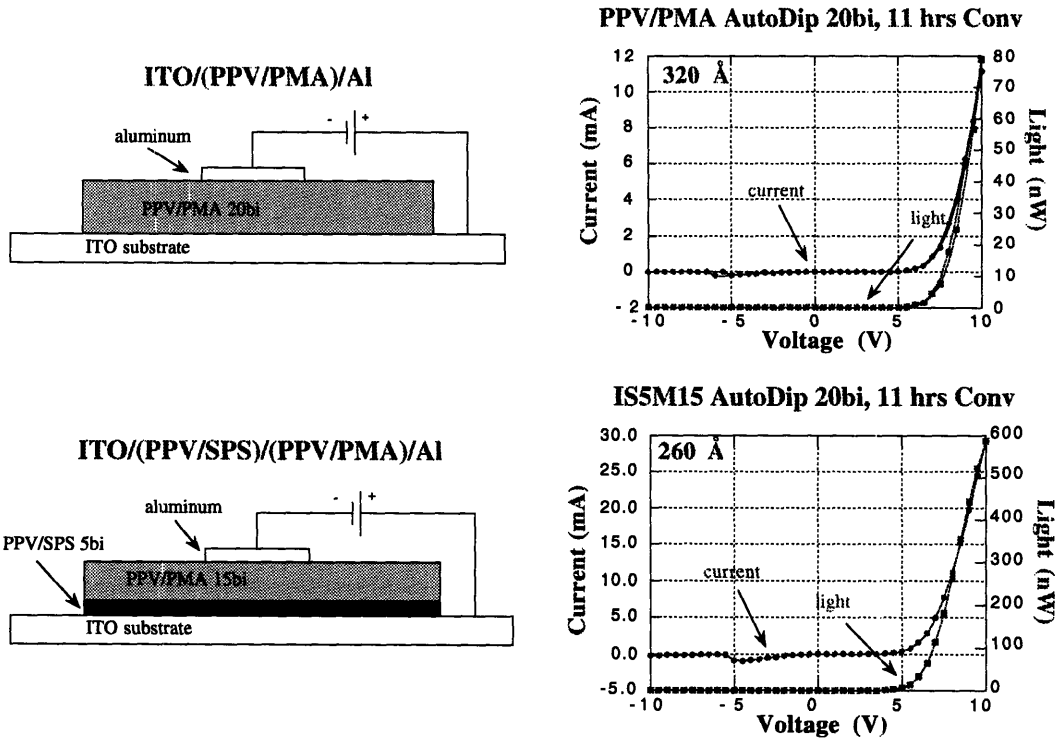

Figure 3.22 Comparison of Single Slab PPV/PMA Device with Dual Slab ISM Device

much steeper than that of the PPV/PMA device, indicating its greater efficiency. Based on our calculations, the external efficiency of the ISM device is estimated to be 0.001 % photons per electron. Also included in this figure is our own schematic flat-band diagram for the ISM device architecture. Reminiscent of Parker's rigid band model, the schematic diagrams shown here are acknowledged to be a simplified picture of the actual mechanisms of operation in these thin film polymeric light-emitting devices. However, despite its simplicity, it can qualitatively

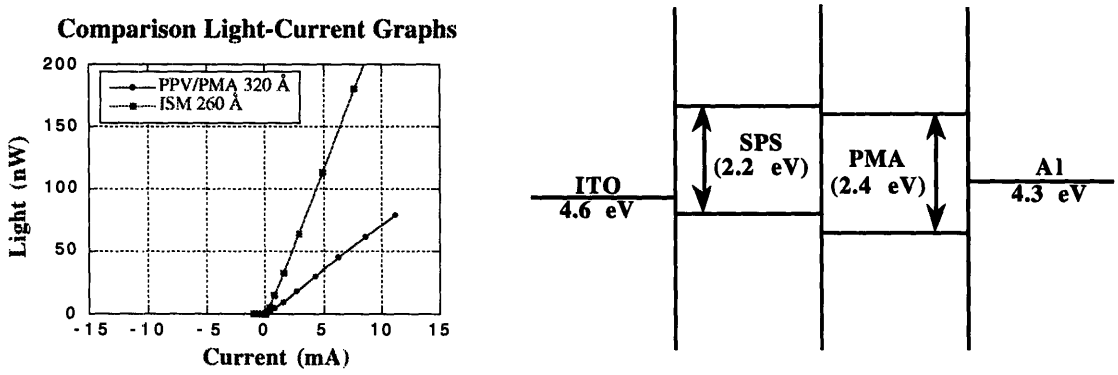

Figure 3.23 Light-Current Graphs for PPV/PMA 20 bi and ISM Device and Schematic Flat-Band Diagram of ISM Device

account for all of the major features of our single and dual slab devices. The details of the diagram are obtained as follows. The energy gap of the PPV/PMA is estimated to be 2.4 eV from the photoluminescence spectrum using the energy of the center of the peak FWHM line; similarly, the gap for the PPV/SPS is approximately 2.2 eV. Our choice of the offset of the Fermi levels of the PPV/PMA and PPV/SPS is based on the our previous observations that the SPS tends to accept electrons from the PPV, giving the PPV a slight relative, p-doped character. The PMA on the other hand does not accept electrons from the PPV due to its unconjugated nature and the lack of π-orbitals for overlap with the PPV. Therefore, when placed together, the alignment of the Fermi energies lowers the PPV/PMA slab relative to the PPV/SPS slab. The levels of the ITO and aluminum electrodes are taken from the literature; these values are assumed by many groups.

To re-iterate the original model by Parker, the tunneling current through a triangular barrier at the interface is governed by the applied electric field (slanting the rigid bands) and the height of the barrier at the polymer/electrode interface, as determined by the offsets of the bands of the polymer and the work function of the metal electrodes. In our devices, there always exists a smaller offset at the PPV/ITO interface than at the PPV/aluminum interface; therefore, in forward bias operation, holes are always the majority carrier. The other (larger) offset determines the rate of injection of the minority carrier electrons into the PPV. Since the light output and efficiency are determined by the radiative recombination of majority (holes) and minority (electrons) carriers, the rate of injection of minority carriers into the film is "limiting" and therefore determines the number of electrons available for radiative recombination and the efficiency of the device. In our single slab devices, the better band matching at the PPV/PMA to aluminum interface can account for the larger efficiency of the PPV/PMA compared to the PPV/SPS. On the other hand, the better band matching at the PPV/SPS to ITO interface accounts for the lower turn-on voltage and higher current of the PPV/SPS compared to the PPV/PMA. In our dual-slab system with the PPV/SPS slab next to the ITO and the PPV/PMA slab next to the aluminum, the injection efficiencies at both polymer/electrode interfaces are increased. As a result, a slightly lower turn-on voltage, a larger current magnitude, and

a much higher overall efficiency are all observed for the ISM device compared to the PPV/PMA device.

If the band matching at the electrode interfaces does indeed lead to these observed differences in the characteristics of the device, then the placement of the slabs of PPV/SPS and PPV/PMA must also be important. For example, if we switched the position of the slabs so that the PPV/PMA emitter slab is next to the ITO and the PPV/SPS transport layer is next to the aluminum, then we should see differences in the forward bias characteristics of the device. Figure 3.24 shows the overlaid light-current curves and the schematic flat band diagram for the new device architecture labeled as IMS, to represent the ITO/(PPV/PMA)/(PPV/SPS)/aluminum architecture. From the schematic diagram, it is seen that by reversing the placement of the slabs, the band offsets are increased at both the ITO interface and the aluminum interface. Therefore, it is reasonable to expect that in forward bias operation, the IMS device would be markedly less efficient than the ISM or even the PPV/PMA (single slab) device. Indeed, the light-current graph next to it shows that the slope of the light-current curve of the IMS device is much smaller than that of the ISM device. The samples shown here consist of a slab of 10 bilayers of PPV/SPS and a slab of 20 bilayers of PPV/PMA, giving a total thickness of 400 Å. For all of the other dual-slab combinations tested, the IMS architecture was always less efficient than the ISM architecture. The success of this simple model in explaining the qualitative differences between the single

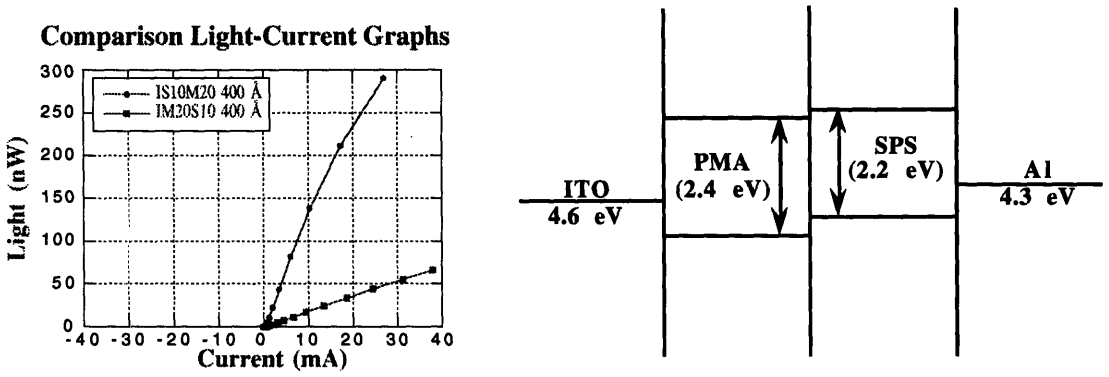

Figure 3.24 Light-Current Graphs for ISM Device and IMS Device and Schematic Flat-Band Diagram of IMS Device

slab, the ISM, and the IMS architectures further justifies our placement of the bands of the PPV/SPS and PPV/PMA relative to each other.

It should also be reiterated, however, that this is an oversimplification of the complex processes responsible for the behavior of these thin film devices. We have neglected any band bending that may occur at the interfaces due to the assumption of low levels of intrinsic carriers in the polymer material. We have also neglected the effects of surface species due to contamination by minute quantities of oxygen and water during any step of the fabrication process. Although it is beyond the scope of this work to perform elemental and electronic analysis of the species at the polymer/electrode interfaces, the work of other groups have shown that these surface species may alter the electronic states at the interface and cause slight

band-bending [3.16]. This band-bending is only noticeable at low applied biases when the magnitude of the applied bias is on the same order as the magnitude of the built-in voltage [3.16].

With self-assembly, we can however study the effects of thinner and thinner "slabs" of material on the overall performance of the devices. Even single layers or bilayers at the interface of the polymer film and the electrodes will be shown to affect the device properties in detectable ways. Towards this end we designed two series of experiments. The first consisted of reducing the number of bilayers in the PPV/SPS slab of the ISM device while holding the number of bilayers of the emitting PPV/PMA slab constant. The second series of experiments consisted of changing the single layer or bilayer in contact with each of the electrodes. As will be seen shortly, our results indicate remarkably that the placement of a single layer or bilayer of around 10 Å thick can indeed influence the performance of the self-assembled light-emitting device.

In the first set of experiments, we change the thickness of the PPV/SPS "slab" in the dual-slab architecture, while holding the PPV/PMA slab at constant thickness. The three architectures shown in Figure 3.25 are designated as IS20M20, IS10M20, and IS1M20. The first consists of a slab of 20 bilayers of PPV/SPS next to the ITO with a slab of 20 bilayers of PPV/PMA, hence IS20M20. The second has a 10 bilayer slab of PPV/SPS with a 20 bilayer slab of PPV/PMA. And the

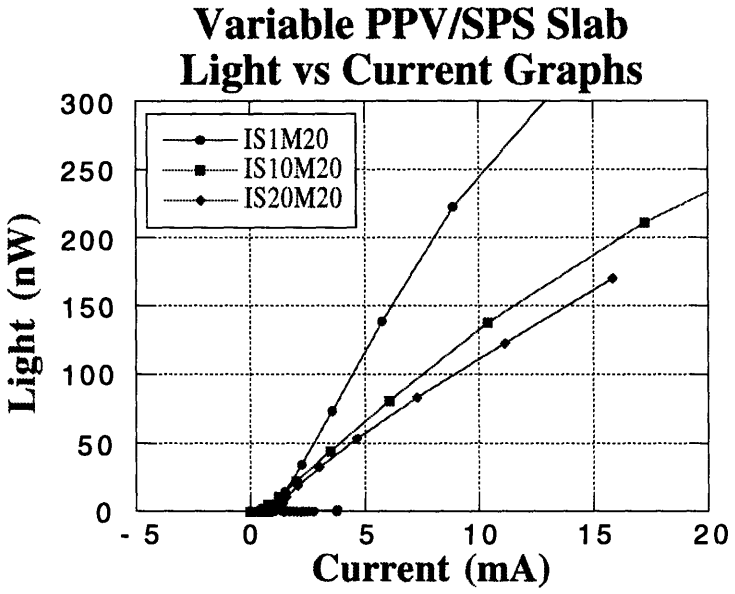

Figure 3.25 Overlay of Light-Current Curves for Various Modified ISM Device Architectures

third has only one single bilayer of PPV/SPS next to the ITO and a 20 bilayer slab of PPV/PMA. What is incredible is the fact that there exists a trend toward higher efficiency as we decrease the number of bilayers (or thickness) of the PPV/SPS slab. It is clear from the figure that the IS1M20 device has the greatest slope and is the most efficient. This means that a single bilayer of material, which has a thickness in this case of 8 Å, can significantly alter the device characteristics. Molecular self-assembly has thus uniquely allowed us to manipulate these electroactive polymers with the molecular level control necessary to fabricate these layer-by-layer device architectures. From the result of this series of experiments, we infer that the enhancement in the efficiency of the dual-

slab ISM devices over single-slab devices such as PPV/PMA is due to the changes at the interface between the polymer film and the ITO with the introduction of PPV/SPS material. And the enhancements are likely not due to the formation of an extra hetero-interface in the middle of the film between the PPV/SPS and PPV/PMA slabs, since 1 bilayer of PPV/SPS with an 8 Å thickness hardly suffices as a "slab." Therefore, although more work is needed to clarify the exact role of the PPV/SPS bilayer at the interface, it is speculated that the PPV/SPS bilayer helps to smooth the interface at the molecular level, the nature of the PPV/SPS changes the electronic states at the interface, or the higher conductivity of the PPV/SPS bilayer facilitates injection from the electrode into the rest of the polymer film.

Since the observation that a single bilayer had such a marked influence on the device properties, we had to re-examine the entire architecture of the self-assembled film layer by layer. For example, in our previous films, a bilayer of polyethyleneimine (PEI)/polyanion deposited onto the ITO before the actual deposition of the PPV/polyanion bilayers to promote the adhesion of the rest of the film. Since the PEI/polyanion bilayer combination was placed right next to the ITO electrode, we had to ascertain its influence on the properties of the overall device. Therefore, a series of samples were prepared with and without this bilayer on the ITO. The samples without this bilayer simply started with a PPV layer directly on the ITO. Samples of the

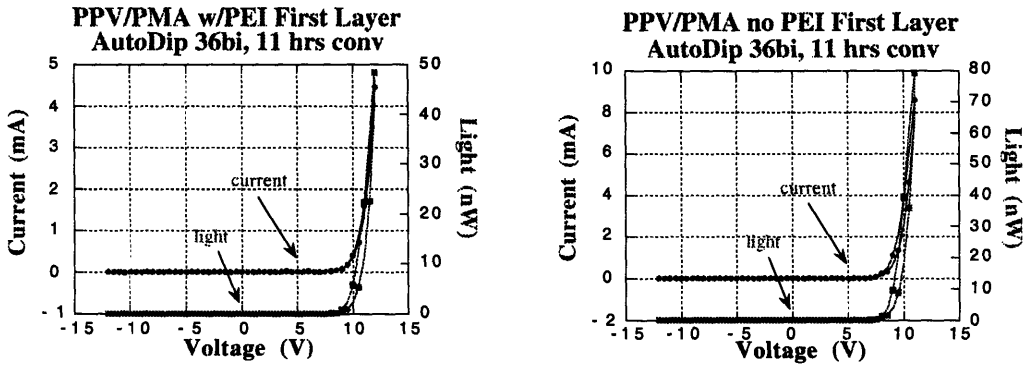

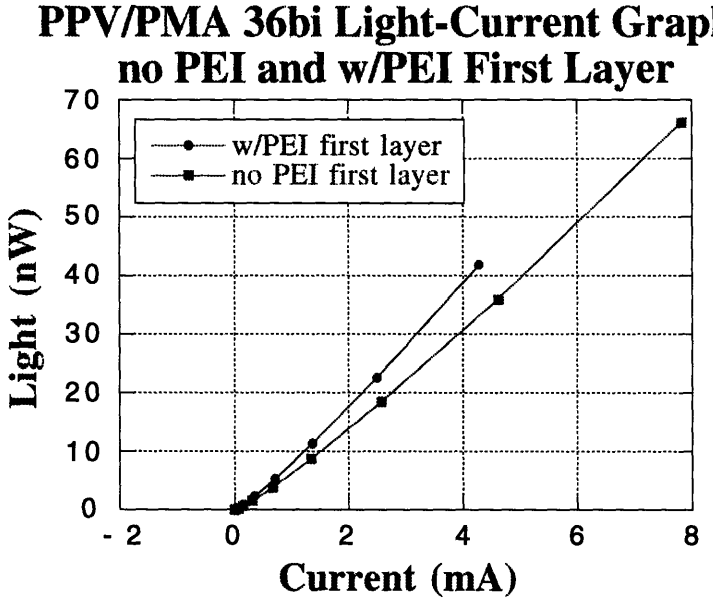

Figure 3.26 **Current-Voltage and Light-Voltage Curves for PPV/PMA Samples with and without PEI first layer; Overlay of Light-Current Curves**

same number of PPV/polyanion layers were fabricated and analyzed. Figure 3.26 shows the corresponding current-voltage and light voltage curves as well as an overlay of the light-current curves to show the small difference in the efficiency of the two devices. From the current-

voltage curves, it is seen that the turn-on voltage is slightly lower for the sample without the insulating PEI/PMA bilayer at the ITO interface. The presence of the PEI/PMA bilayer does affect the turn-on voltage because the ITO electrode in forward bias is responsible for the injection of the majority holes which determine the current-voltage characteristics of the device. But the effect of the PEI/PMA bilayer on the efficiency is small as seen in the light-current plot; this is reasonable since a change in number of overly abundant majority carriers in the body of the film would not significantly change the probability of radiative recombination events which are limited by the number of available minority carrier electrons. The fact that the sample with the PEI/PMA (insulating bilayer) has a slightly higher slope may indicate that it serves to block the electrons from exiting the film, thus slightly increasing the probability of a recombination event. Sundry other samples were made to confirm the observed effect of the PEI/polyanion bilayer. In each case, as expected, there was only a slight difference in the efficiency between the sample with the PEI/polyanion bilayer and the corresponding sample without the bilayer.

To complete the set of experiments regarding the role of single layers next to the electrodes, we turn next to the examination of the single layer next to the aluminum electrode. In our self-assembly process, we have the option to end the buildup of the multilayer film with a dip into the PPV or a dip into the polyanion. In our early work, all of the samples were made with a final dip into the polyanion.,

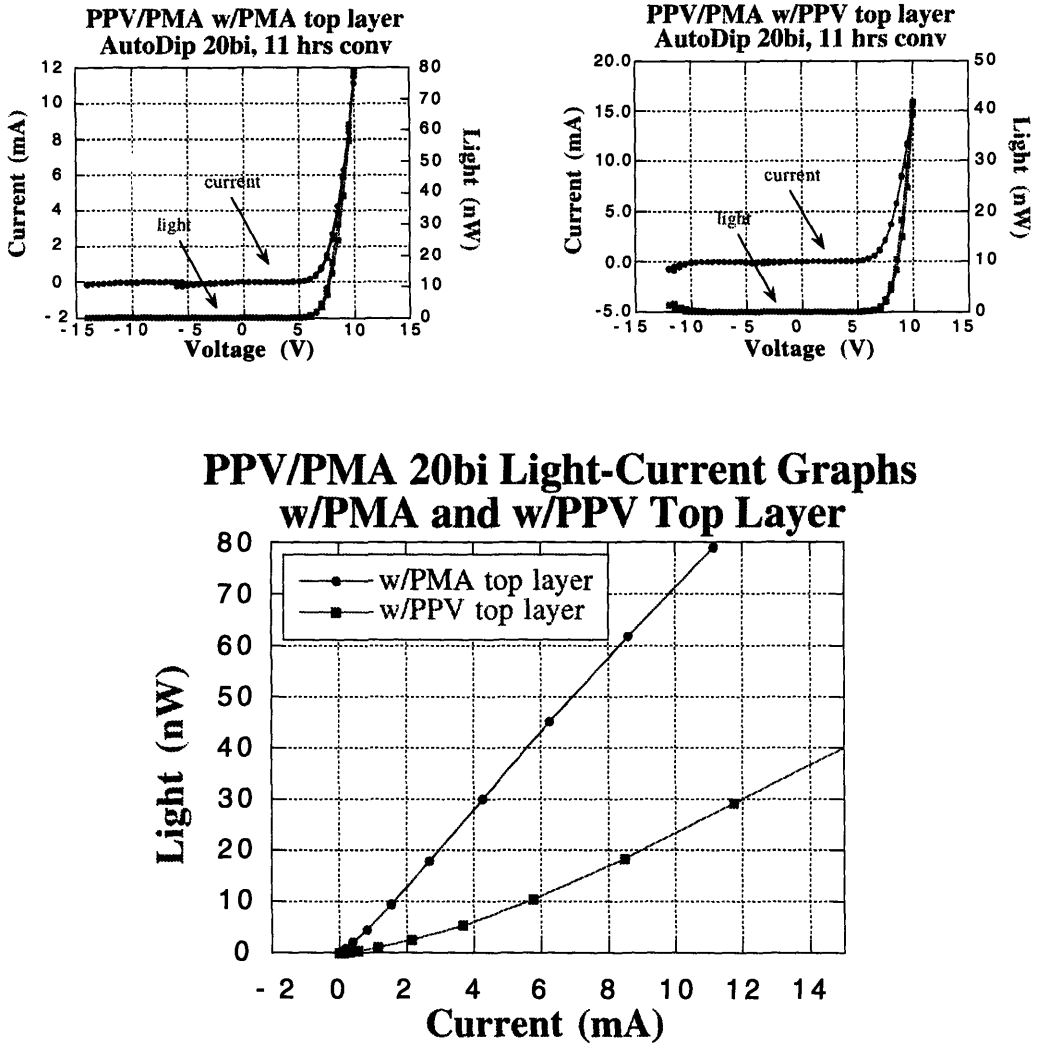

Figure 3.27 Current-Voltage and Light-Voltage Curves for PPV/PMA Samples with PMA top layer or PPV top layer; Overlay of Light-Current Curves

thought to enhance the storability of the samples before thermal conversion. But because of the non-conjugated (insulating) nature of the polyanions used, relative to that of the conjugated PPV, the question remained whether the single polyanion layer next to the aluminum

electrode would be detrimental to the injection of minority electrons in forward bias operation and therefore the efficiency. But as Figure 3.27 shows, the efficiency of the device is actually enhanced significantly by the presence of the single polyanion layer. The turn-on voltage in the current-voltage graphs does not change. This is reasonable since the interface at the ITO electrode is held constant in both samples; no PEI/polyanion bilayer was used. Furthermore, for every other sample architecture in a side-by-side comparison, the sample with a polyanion top layer was more efficient than its counterpart with the PPV top layer by a factor of 2 to 4. Further experiments are necessary to clarify the reasons for these observations.

3.4.5 Breakdown Mechanisms and Device Lifetime

Finally, we turn to addressing the question of the lifetimes of these ultrathin light-emitting devices based on self-assembled films. Some of the PPV devices exhibited respectable lifetimes in the range of several hours to over 250 hours under constant voltage operation in a nitrogen atmosphere. Figure 3.28 shows two lifetime tests performed on ISM samples. The devices were typically held at 0.5 V to 1.0 V above the turn on at a light emission level of at least 1 nW, visible to the unaided eye in a darkened room. The electroluminescence color was chalky green to the eye. In a well-performing device, the elapsed time before the light output decreased to one-half the original intensity was

30 minutes while the time for the intensity to drop to one-tenth of the original intensity was 125 hours. We could also hold the device at the maximum forward bias that could be supported. In the figure, the device was held at 10 V. When this is done, most of the devices exhibit a decay in the light to one tenth the original intensity in 15 - 30 minutes,

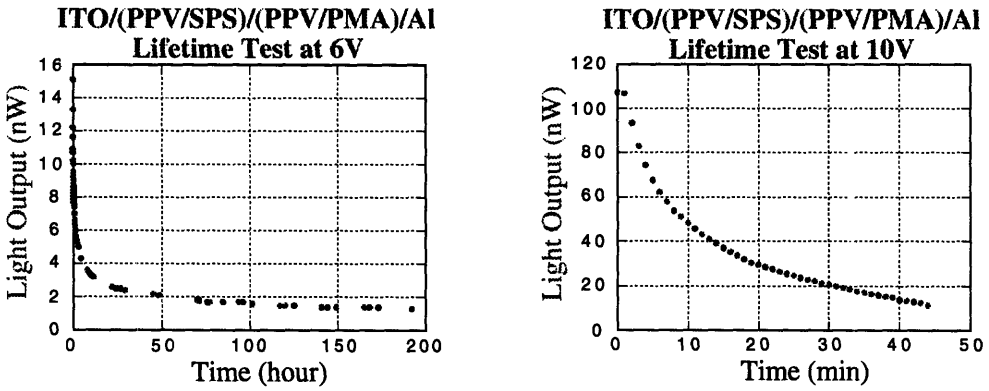

Figure 3.28 Lifetime Graphs for ISM Device operated at 6 V and maximum 10 V

under nitrogen. As mentioned in our previous study, two possible mechanisms may account for the burn-out that is typically observed. The first is labeled "punch-through," in which the current is observed to jump rapidly with a corresponding drop in light intensity. It is likely that short circuit channels are formed through the ultrathin film, perhaps by the electromigration of aluminum under the influence of the large fields (typically 1 - 5 MV/cm). It has also been observed that the sudden increase in the current may be followed by a decrease back to the original levels. According to other hypotheses, the joule heating

associated with this event may serve to anneal the film enough to close the short circuit channels thus returning the current level back to the original magnitude [3.17]. The second possible breakdown mechanism occurs when the aluminum electrodes spark and vaporize at high voltages (high fields), with the sudden loss of current. The use of thicker aluminum electrodes (around 1500 Å) has virtually eliminated the instances of this burn-out mechanism. In our lifetime studies, none of the devices were pushed to breakdown; rather the device was held at constant voltage while the current magnitude and the light intensity were recorded. The decrease in light intensity is attributed to the phenomenon of luminescence "fatigue" [3.18] in which non-radiative sites are generated and accumulated under the high fields of operation (typically from 0.5 to 5 MV/cm). As pointed out earlier, it is remarkable that these ultrathin films of as little as 80 Å can be used for hours under constant DC operation at such enormous electric fields. The quality of the self-assembled films makes this possible. Further, consistent with our earlier observations, it was found that although longer conversion times do not appreciably change the absorbance and photoluminescence characteristics of the PPV film, the extended time anneals and densifies the film and also removes more of the water or volatile impurities in the film. This leads to less hysteresis in the current and light curves as well as greater stability during device operation and longer lifetimes.

3.5 PPV Self-Assembly Conclusions

In conclusion, we have shown that we can modify the materials properties of the PPV by self-assembling it with different polyanions. This is borne out by the differences seen in the absorbance spectra and the photoluminescence spectra. Self-assembly was also used to study the intermolecular interactions between the component materials contained in the self-assembled heterostructure film. Then the first working light-emitting thin film devices based on self-assembled films of PPV were presented. Remarkably, devices as thin as 80 Å were operated and characterized, attesting to the high quality of the self-assembled films. Then using self-assembly we showed that a controlled modification of the layer-by-layer architecture of the film in a dual-slab device allowed us to increase the light output by nearly and order of magnitude. The results of these experiments allowed us to propose a simple rigid band model that accounts for the differences in the PPV/PMA and PPV/SPS binary systems and their influence on the properties of the light-emitting devices. Finally, self-assembly has uniquely provided us the ability to study the effects of single layers or single bilayers of material on the external, macroscopic properties of the device. In this way, self-assemble clearly presents unique advantages over other techniques in the fabrication and optimization of devices based on ultrathin organic films.

3.6 Chapter 3 References

3.1 Private Communication, Prof. M.F. Rubner.

3.2 a) N.C. Greenham, F. Cacialli, D.D.C. Bradley, R.H. Friend, et al, *MRS Fall 1993 Symp Q Proceedings*, p. 351

b) J.H. Burroughes, D.D.C. Bradley, A.R. Brown, R.N. Marks, K. Mackey, R. H. Friend, P.L. Burn, and A.B. Holmes, *Nature*, **347**, p. 539, (1990).

c) Y. Shirota, et al., *Appl. Phys Lett.*, **65**, p.807, (1994)

3.3 a) S.C. Moratti, D.D.C. Bradley, R.H. Friend, N.C. Greenham, A.B. Holmes, *MRS Fall 1993 Symp Q Proceedings*, p. 371

b) D.R. Baigent, F. Cacialli, R.H. Friend, N.C. Greenham, J. Gruner, A.B. Holmes, S.C. Moratti, *American Chemical Society 1995 Spring Meeting Proceedings*, p.452.

3.4 J.R. Reynolds, A.D. Child, J.P. Ruiz, J.L. Musfeldt, et al, *MRS Proceedings Symp Q Fall 1993*. p. 191. and references therein.

3.5 a) J. Kido, M. Kimura, K. Nagai, *Science*, Vol.267, 3 March 1995, 1332-1334.

b) J. Kido, K. Hongawa, K. Okuyama, K. Nagai, *Appl. Phys. Lett.* **64** (7), 14 Feb 1994, 815.

c) C.W. Tang and S.A. Van Slyke, *Appl. Phys. Lett.*, **51**, 913 (1987).

d) H. Nishino, G. Yu, A.J. Heeger, T. -A. Chen, R.D. Rieke, *Synthetic Metals*, **68**, (1995), 243-247.

e) C. Zhang, H. von Seggern, K. Pakbaz, B. Kraabel, H. -W. Schmidt, A.J. Heeger, *Synthetic Metals*, **62**, (1994), 35-40.

f) B. Hu, Z. Yang, F.E. Karasz, *J. Appl. Phys.* **76** (4), 15 Aug 1994, 2419-2422.

3.6 a) B.R. Hsieh, H. Antoniadis, M.A. Abkowitz, and M. Stolka, *Polymer Preprints*, **33** (2), p. 414, (1992), and references therein.

b) M. Kanbe, M. Okawara, *J. Polym. Sci. A-1*, (1968), **6**, 1058.

c) R.A. Wessling, R.G. Zimmerman, U.S. Patent 1968, 3,401,152

3.7 F. Papadimitrakopoulos, K. Konstadinidis, T.M. Miller, R. Opila, E.A. Chandross, M.E. Galvin, *Chem. Mater.* **6** 1563 (1994).

3.8 M. Ferreira, M.F. Rubner, B.R. Hseih, *MRS Proceedings, Symposium Q*, **328**, p.119, (1994) and references therein.

3.9 a) F. Papadimitrakopoulos, T.M. Miller, E.A. Chandross, M.E. Galvin, *Polymer Preprints*, Vol.35, No.1, March 1994, p. 215

b) F. Papadimitrakopoulos, R.C. Haddon, M. Yan, T.M. Miller, L.J. Rothberg, H.E. Katz, M.E. Galvin, *MRS Proceedings, Spring 1995 Meeting*, at press.

c) I. Murase, T. Ohnishi, T. Noguchi, M. Hirooka, *Polym. Comm*, Vol. 25, Nov 1984, p.327.

3.10 N.C. Greenham, R.H. Friend, D.D.C. Bradley, *Adv. Mater*, **1994**, Vol.6, No.6, p. 491. and references therein.

3.11 a) M.S. Ferreira, PhD Thesis, University of Sao Paolo, Brazil, 1994.

b) M. Ferreira, M.F. Rubner, B.R. Hseih, *MRS Proceedings, Symposium Q*, **328**, p.119, (1994) and references therein.

3.12 a) S. A. Jenekhe, J.A. Osaheni, *Science*, **1994**, 265, 765.

b) M.F. Roberts, S.A. Jenekhe, A. Cameron, M. McMillan, J. Perlstein, *Chem. Mater.*, **1994**, 6, 658.

c) J.A. Osaheni, S.A. Jenekhe, *Macromolecules*, **1994**, 27, 739.

d) J.A. Osaheni, S.A. Jenekhe, J. Perlstein, *Appl. Phys. Lett.*, **1994**, 64, 3112.

e) S.A. Jenekhe, J.A. Osaheni, *Chem. Mater.*, **1994**, in press.

f) C.J. Yang, S.A. Jenekhe, *Supramolecular Science,* in press.

g) K. Yoshino, X.H. Yin, K. Muro, S. Kiyomatsu, S. Morita, A.A. Zakhidov, T. Noguchi, T. Ohnishi, *Jpn, J. Appl. Phys.,* Vol. 32 (1993), p. 357-360.

3.13 a) J.H. Burroughes, D.D.C. Bradley, A.R. Brown, R.N. Marks, K. Mackey, R. H. Friend, P.L. Burn, and A.B. Holmes, *Nature*, **347**, p. 539, (1990).

b) R.H. Friend, D.D.C. Bradley, P.D. Townsend, *J. Phys. D: Appl. Phys.*, **20**, (1987), 1367-1384.

b) D. Braun and A.J. Heeger, *Appl. Phys. Lett.*, **58** (18), p. 1982, (1991).

3.14 a) I. Murase, T. Ohnishi, T. Noguchi, M. Hirooka, *Polym. Comm*, Vol. 25, Nov 1984, p.327.

b) I. Murase, T. Ohnishi, T. Noguchi, M. Hirooka, *Polym. Comm*, Vol. 26, Dec 1985, p.362.

c) I. Murase, T. Ohnishi, T. Noguchi, M. Hirooka, *Polym. Comm*, Vol. 28, Aug 1987, p.229.

3.15 I.D. Parker, *J. Appl. Phys.*, **75** (3), p. 1656-1666, 1 Feb 1994.

3.16 a) E. Ettedgui, H. Razafitrimo, Y. Gao, B.R. Hsieh, M.W. Ruckman, *Synthetic Metals*, submitted for publication June 1, 1995.

b) B.R. Hsieh, E. Ettedgui, K.T. Park, Y. Gao, *Mol. Cryst. Liq. Cryst.*, 1994, Vol. 256, pp. 71-78.

c) B.R. Hsieh, E. Ettedgui, K.T. Park, Y. Gao, *Synthetic Metals*, submitted for publication June 1, 1995.

d) Y. Gao, K.T. Park, B.R. Hsieh, *J. Appl. Phys.*, **73** (11), 1 Jun 1993, p.7894-7898.

e) H. Razafitrimo, K.T. Park, E. Ettedgui, Y. Gao, B.R. Hsieh, *Polymer International*, **36** (1995) p. 147-153.

f) E. Ettedgui, H. Razafitrimo, K.T. Park, Y. Gao, B.R. Hsieh, *Surface and Interface Analysis*, Vol. 23, p.89-98, (1995).

g) E. Ettedgui, H. Razafitrimo, Y. Gao, B.R. Hsieh, *Appl. Phys. Lett*, submitted for publication June 1, 1995.

h) E. Ettedgui, H. Razafitrimo, K.T. Park, Y. Gao, B.R. Hsieh, *J. Appl. Phys.*, **75** (11), 1 June 1994, p.7526-7530.

3.17 Private communication from Osamu Onitsuka

3.18 D.D.C.Bradley, R.H.Friend. *J.Phys. Condensed Matter*, **I**, (1989), 3671-3678

Chapter 4

Concluding Remarks

Thus, we come to the end of this scientific journey. In closing, let us recall the highlights. In the beginning, the promise of a new thin film processing technique was espoused. Molecular self-assembly was presented as a technique which allowed us to dictate the deposition of single layers of material with molecular-level control. It would also allow us to work with certain electroactive polymers, difficult to process by other techniques. And while providing this sophisticated level of control, it would remain simple to use, thereby providing a means to bridge the gap between remaining a useful laboratory technique and becoming a technologically useful fabrication process for making ever more complex devices based on ultrathin organic films.

Along the journey, we showed that molecular self-assembly allowed us not only to deposit extremely uniform and highly conducting thin films of the technologically important polypyrrole, but also to selectively deposit the polypyrrole onto certain areas of a substrate in a controlled manner. We also showed that the thin films were coherent and dense such that "bulk" conductivity was achieved with as little as 60

Å of material. With the ability to manipulate a variety of polymers, a novel device architecture sandwiching conducting polypyrrole with insulating poly(thiophene-3-acetic acid) was designed and fabricated. The anisotropy in the transverse versus in-plane conductivity of these films expected from the design were indeed obtained.

We then went on to use self-assembly to deposit device quality thin films of the widely studied poly(p-phenylene vinylene). The intimate layer-by-layer contact between the PPV and the polyanions self-assembled with it gave rise to modified materials characteristics in the PPV, as evidenced by the modified absorbance and photoluminescence properties of the film. Thus, manipulating the molecular environment of the PPV to tune the properties of the film became a simple matter of self-assembling different layers next to the PPV or by building novel supermolecular architectures. Indeed, we could systematically recover the quenched photoluminescence in certain binary PPV systems by inserting "spacer layers" between the PPV and the quenching agent to mediate the charge transfer interaction. In this way, a simple processing technique could be applied as a powerful molecular probe to study the intermolecular interactions among the components deliberately built into multilayer heterostructure thin films.

Then, in the area of thin film light-emitting devices, self-assembly proved uniquely useful in fabricating operational devices as thin as 80 Å, in studying devices in the thickness regime between 100 Å and 500

Å, and in creating "dual-slab" architectures which proved to be markedly more efficient that correponding single slab devices. In this way, a simple processing technique has allowed us to improve the characteristics of thin film light-emitting devices based on the widely studied PPV. Finally, molecular self-assembly has allowed us control the placement of single layers of material, between 5 Å and 15 Å thick, to elucidate their influence on the macroscopic properties of the thin film devices.

In this way, self-assembly has indeed been demonstrated to be a powerful and versatile thin film processing technique. It greatly expands the horizons of possibility in the arena of organic thin film devices. And for the novel applications which demand ever more complex heterostructures which can take advantage of unique intermolecular interactions, molecular self-assembly will prove to be a vital means of achieving the fabrication and optimization of all-organic, molecular-scale devices. Although having only touched the surface of possibilities for this powerful new technique, in this work, we have nevertheless successfully accomplished the "Design, Fabrication, and Characterization of Complex, Multilayer Heterostructures of Conjugated and Non-Conjugated Polymers via Molecular Self-Assembly."

Quid est demonstratum....